On Quantum Superpositions in an Optomechanical System

Igor Pikovski

Oktober 2008

Diplomarbeit

Fachbereich Physik

Freie Universität Berlin

Betreuer am Fachbereich: Prof. Dr. J. Bosse

Arbeit angefertigt unter Anleitung von Prof. Dr. D. Bouwmeester
an der University of California Santa Barbara und an der Universiteit Leiden

Acknowledgements

The research presented in this thesis was performed during a stay at the University of California Santa Barbara and at Leiden University, where it was conducted under the supervision of Prof. Dirk Bouwmeester and with the support of Prof. Jeroen van den Brink.

First and foremost, I would like to express my sincere gratitude to Dirk Bouwmeester for giving me the opportunity to work on this project. He has introduced me to a promising research field, and throughout my time at UCSB and in Leiden Dirk Bouwmeester's support and his guidance allowed the work under his supervision to be very motivating and rewarding. The friendly atmosphere in the group and during our discussions made the work on this thesis very pleasant.

I am also very thankful to Prof. Jeroen van den Brink for his guidance and his support. He helped me to see many aspects of my research from a new perspective and provided many insights during our discussions. His various suggestions and comments are very appreciated. I would also like to thank Prof. J. Bosse for his support and supervision of my work. His help in organizing the project has allowed me to conduct the research abroad. He has also been very supportive during my visits in Berlin and I acknowledge the many scientific discussions we had.

This work would not have been possible without the help and commitment of Luuk Ament. He has been a guidance and a dear friend throughout the year and I have learned a lot from his problem solving skills during the countless discussions we had. He would always find time to discuss results and calculations, and it has been a great pleasure to collaborate with him. I also thank him for reviewing this manuscript and for numerous useful suggestions.

I also thank Dustin Kleckner and Dr. Evan Jeffrey and greatly acknowledge the many discussions with them. I have gained a lot of physical insight from their deep and unorthodox understanding of physics. Discussions and collaborations with Dustin and Evan have always been enjoyable and allowed me to see scientific problems from a new perspective.

Finally, I would like to thank Dr. Christoph Simon, Prof. Roger Penrose and Prof. Lajos Diósi for many useful discussions and for helpful and clarifying comments. I am also thankful to the University of Leiden and the University of California Santa Barbara for their kind hospitality.

Contents

1 Introduction

The inability to observe a macroscopic object to behave quantum mechanically has puzzled scientists since the quantum theory has been properly formulated. In 1935, Schrödinger demonstrated an apparent absurdity of quantum mechanics if applied at a macroscopic scale by formulating his famous thought experiment, in which a cat would exist in a quantum superposition of being dead and alive [1]. Our everyday experience suggests that some sort of transition between the realm of quantum mechanics and our classical world must take place. Different viewpoints have been advocated about how this quantum-classical transition can be understood (see [2] for an excellent overview), but until today, the debate was mostly of theoretical nature, since no testable experimental verification or falsification of any of the various interpretations seemed possible or within reach.

Recent experimental advances have allowed to study and verify quantum effects in relatively large systems. In molecular quantum interferometry quantum superpositions of C_{60} molecules have been created [3]. In superconducting electrical systems, superpositions of different electrical current states have been achieved [4, 5]. Currently, optomechanical setups are being widely explored, since they potentially allow to observe quantum effects in mechanical systems. Proposals include cooling mechanical modes to their quantum ground state [6, 7, 8, 9, 10], observing discrete quantum jumps [11], entangling mechanical oscillators to each other [12, 13, 14] or to optical modes [15, 16], and many more [17, 18, 19, 20]. In this work, we analyse in detail the proposed experiment by Marshall et al. [21] which aims to create a quantum superposition state of a massive mirror attached to a cantilever, hence realizing a so-called "Schrödinger cat state" of an object consisting of approximately 10^{14} atoms with a mass of about 10^{-12}kg. Such large and massive objects have never before been observed in a quantum superposition. The experiment thus aims to provide a test of quantum mechanics at an entirely unexplored scale. It could therefore also shed light on the quantum-classical transition, in particular regarding a possible breakdown of the quantum mechanical formalism which might be induced by gravity [22].

The idea of the experiment is to use a quantum system, a single photon, to create and read out a superposition state of a much larger system, a tiny mirror attached to a micro-cantilever. The superposition state of the mirror on the cantilever is monitored indirectly, through the quantum interference effects of the photon. In practice, fabricating various neccessary parts and performing the experiment poses a significant challenge, but it is within the reach of current technology. The setup is currently in prepeartion, figure 1 shows a state of the art cantilever with a micro-mirror glued onto, which has been fabricated in 2005.

In this thesis we present a review and a thorough analysis of the proposed experiment. Our goal is to address some important theoretical aspects which have not been considered in detail previously [19, 21, 23]. We discuss here the effect of a finite temperature of the cantilever and show how it affects the experimental outcome and its interpretation. The degree of non-classicality is analysed in phase space and we provide an upper bound on the tolerable temperatures of the mirror, which is important for an unambiguous demonstration of quantum effects. We also investigate different sources of decoherence and their effect on the experiment. We consider dissipation from the cantilever into other modes or into the bulk to which it is attached, thermal fluctuations of those phononic modes and also an external scattering environment. The possibility of measuring a gravitationally induced wavefunction collapse is also discussed at the end of the thesis.

This work is structured in the following way: In chapter 2 we give an introduction to a

possible gravitationally induced quantum-classical transition, which serves as a motivation for the rest of the thesis. We then present a detailed quantum mechanical analysis of the proposed experiment and discuss its various aspects in chapter 3. In chapter 4 we analyse the experiment in phase space which provides a way to quantify the transition from a quantum to a classical description. We discuss the influence of the environment on the experiment in chapter 5, where we calculate the decoherence times due to dissipation, thermal fluctuations and scattering from surrounding particles. Then we discuss the prospects of measuring a gravitationally induced collapse of the wavefunction in chapter 6. Chapter 7 gives a summary of the results and provides an outlook to current related research topics. Some results presented in this thesis have been published in [24].

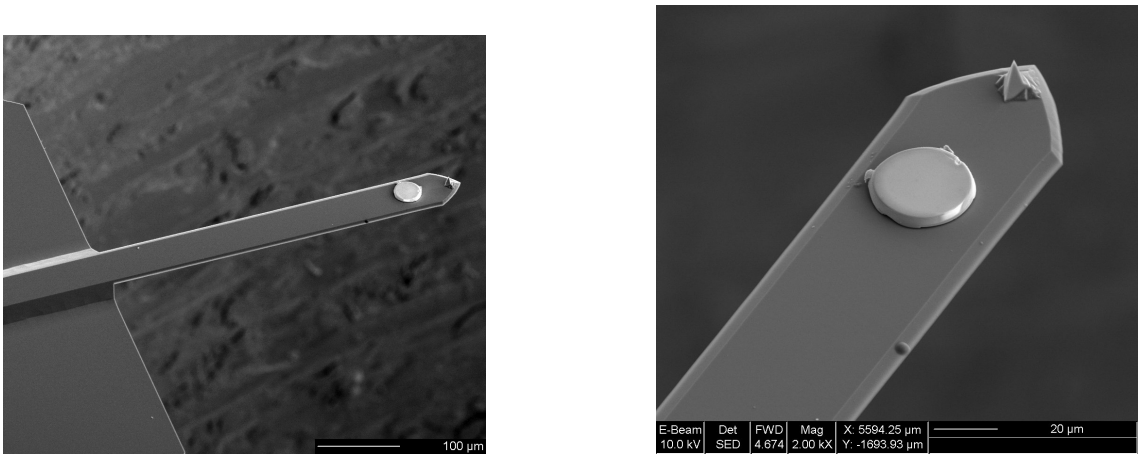

Figure 1: *The figures show a micro-fabricated tiny mirror attached to a silicon cantilever. It was used in [25] to demonstrate optical cooling of a mechanical mode. The mirror has the size of about 10 μm, and the cantilever's center of mass frequency is $\omega_c = 2\pi \times 1kHz$.*

2 Gravitationally Induced Wavefunction Collapse

The idea that gravity might play a role in the quantum-classical transition dates back to Feynman from his seminal lectures on gravity [26]. This idea has been taken up by F. Károlyházy [27] and further developed by L. Diósi [28, 29] and R. Penrose [22, 30, 31]. Penrose's approach was to study in detail the conflict between the underlying principles of quantum mechanics and Einstein's general theory of relativity, rather than proposing a dynamical mechanism that leads to a quantum state reduction. His conclusion is that the incompatibility between those two theories must lead to a transition from unitary quantum evolution to a non-unitary and more general description as the mass is increased. General relativistic effects will start to play a role as one increases the mass and according to Penrose this will result in a breakdown of quantum unitarity. Without knowing the exact theory, one would expect at least a decay of quantum superpositions which would provide a natural quantum-classical transition. In this section we briefly summarize Penrose's arguments [22, 31].

At the core of Einstein's theory of relativity lies the principle of covariance. It implies that all physical laws must be independent of the coordinates we use. In a more mathematical language, a space-time can be represented by a tensor field $g^{\mu\nu}$ on a manifold $\mathcal{M}$ and a coordinate transformation takes place through a diffeomorphism $\Phi\colon \mathcal{M} \to \mathcal{N}$, onto a new manifold $\mathcal{N}$. The covariance principle is simply a diffeomorphism invariance: Physical laws must not change if a diffeomorphism is applied, hence $\mathcal{M}$ and $\mathcal{N}$ are physically indistinguishable. This represents the gauge invariance of GR, the freedom to choose any coordinate labelling. For example, we can choose a specific metric $g^{\mu\nu}$ to describe the space-time manifold, but this corresponds to fixing the gauge. We are thus free to choose any other metric which is related by a diffeomorphism to $g^{\mu\nu}$, and it would describe the same space-time and lead to the same physical laws.

This implies that a diffeomorphism cannot relate two physically *different* manifolds, so we cannot identify two distinct space-times in a coordinate independent way. There is no way of "comparing" a space-time described by a metric $g^{\mu\nu}$ with a completely different space-time described by $\tilde{g}^{\mu\nu}$, since there cannot be any diffeomorphism relating those two metric tensors. Physical events can only occur in any of the two space-times individually, but one cannot describe an event in $g^{\mu\nu}$ in terms of the coordinates of $\tilde{g}^{\mu\nu}$, since it refers to a completely different manifold. That is to say, no *pointwise identification* is possible between two different space-times.

Now let us consider a quantum system which is evolving according to Schrödinger's equation. Usually in quantum mechanics, one assumes a background space-time on which the physical events take place. The full description including the space-time itself would require an understanding of quantum gravity, and we are not concerned about the details of such a theory. However, let us assume the simple case where the object under investigation is a massive particle. If we want to include all properties of the particle in something like a wavefunction $|\,\Psi\rangle$, we need to include its gravitational field in such a description as well, independent on how the exact theory would look like.

The idea is to consider what happens in principle once a massive particle is put into a spatial superposition, of being, say, in position A and position B (with respect to some reference frame, as the earth for example). In quantum mechanics, the wavefunction of the particle simply describes a superposition of the two possible states. Including the gravitational field of the particle, this implies that it is in a superposition of being in position A with a gravitational field due to its mass, and in position B with the same gravitational field that is simply displaced in the same way. Such a superposition evolves according to the same Schrödinger equation as

each of the states seperately, with the same energy eigenvalue. However, if the particle is massive enough, the notion of a gravitational field needs to be replaced by the more correct notion of a space-time stucture. In these terms, one has to think of a superposition of the particle to be in position A with a space-time structure given by $g_A^{\mu\nu}$, and being in position B with a *different* space-time structure given by $g_B^{\mu\nu}$ which describes a different manifold. Of course, the only difference between those two, naively, is just a spatial translation.

The question is, if a description in terms of two different space-times is in conflict with the laws of quantum mechanics. Indeed, quantum mechanics assumes a single background time-structure on which the laws are formulated. It assumes a single time-translation symmetry, which leads to the time evolution operator $\hat{T} = \partial/\partial t$. But now we are speaking of two distinct time-structures, and so we are also speaking of two fundamentally different time evolution operators $\hat{T}_A$ and $\hat{T}_B$ that correspond to different space-time manifolds. Of course, one could argue that the difference is minute, if present at all, since we are simply speaking of a spatial translation. But the point is that there is a fundamental problem of somehow identifying or comparing $\hat{T}_A$ with $\hat{T}_B$. Without doing so, there would be an ambiguity as to which time evolution operator to use for the Schrödinger evolution of the superposition state. But we have noted previously that comparing two different space-time structures is impossible in the general theory of relativity. Diffeomorphism invariance forbids to comletely identify one space-time manifold with another, unless they are equivalent. Therefore, Penrose argues that since no complete pointwise identification between the two space-times in a superposition is possible, there cannot in principle be any way to identify a single natural time evolution operator for the unitary quantum evolution of such a superposition (however, we note that an asymptotic identification is usually assumed in related problems and an asymptotic time translation operator can be found, but in Penrose's view a local notion should be required). This leads to the assumption that a quantum unitary evolution of massive superposition states should breakdown because it requires to identify a single time structure, which is at odds with the principle of general covariance.

The viewpoint Penrose takes is that since any time evolution operator "$\partial/\partial t$" for an evolution of a superposition of different space-times will have some intrinsic error, such a superpostion won't be stationary and will decay. The decay rate he estimates by suggesting a minimal error one would make when trying to identify the two space-times, by comparing the geodesics in the two space-times. This yields an energy uncertainty ΔE, which is the gravitational self-energy of the massive particle (see section 6). The decay rate of a quantum superposition is then suggested by an order of magnitude estimate $\tau \approx \hbar/\Delta E$.

3 A Detailed Analysis of the Proposed Experiment

The experiment as proposed by Marshall et al. [21] aims to create a quantum superposition of a massive object and the ultimate goal is to test Penrose's ideas. The object under investigation is a micro-sized mirror which is attached onto a movable cantilever, henceforth refered to simply as "cantilever".

In this chapter, we discuss in detail the proposed setup and show how a quantum superposition can be unambiguously created and verified.

3.1 A Qualitative Description of the Setup

The experiment is based on the simple principle of a Michelson-Interferometer, with only a single photon as the input beam. The photon is brought into a superposition of being in either of the two arms by a beam splitter. Both arms contain resonant cavities which store the photon for a longer period. However, one end of a cavity in one arm of the interferometer is actually a tiny mirror attached to a cantilever, which is movable and can be displaced by the photon pressure of the single photon. The photon field acts as a constant force on the cantilever which makes it oscillate in arm A. This optomechanical coupling entangles the photon with the cantilever and it thus creates a superposition of the combined photon-cantilever state, with the cantilever being displaced when the photon is in arm A and being not displaced otherwise.

After some time the photon leaks out of the cavity. It combines with the light field from the other arm and produces an interference pattern. If no displacement of the cantilever took place then the interference is perfectly visible. If, however, the cantilever was displaced into a state distinguishable from the non-displaced state, then the cantilever has effectively measured which path the photon took (since only one arm has a movable cantilever) and thus no interference can arise. In this way, the cantilever makes the setup to a which-path-interferometer. Figure 2 shows a diagram of the experimental realization.

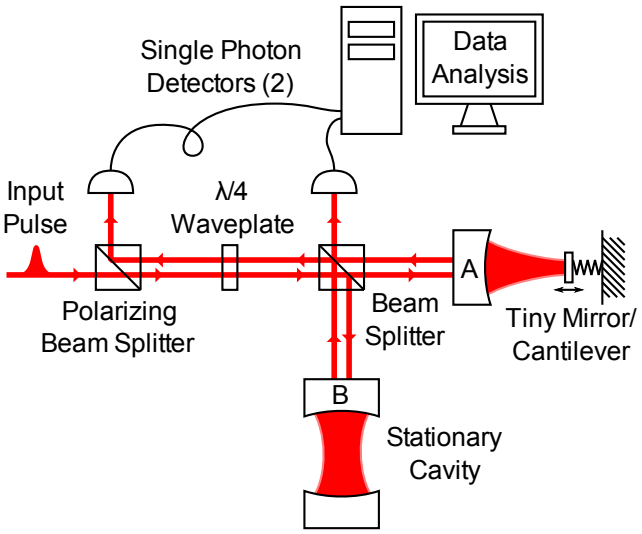

Figure 2: *A schematic diagram of the experimental setup.*

The interference visibility of the photon in fact depends on the time when the photon leaves the cavity. The photon pressure displaces the equilibrium position of the cantilever and makes it oscillate, but after a full mechanical oscillation the cantilever will be back where it was originally, when no photon was present. Thus if the photon leaves the setup exactly after a full mechanical oscillation, full photon interference can be obtained. Therefore the visibility of interference shows a periodic behaviour, with full visibility after each mechanical roundtrip and minimum interference visibility at every half mechanical roundtrip, when the cantilever has the greatest displacement.

We mention a few notes on the experimental realisation, but which do not alter the interpretation of the experiment. In practice, the quantity that can be measured is only the interferometeric visibility, and not an interference pattern at each run. This implies that one has to perform many runs of the experiment to get a single data point, and we will discuss the visibility in more detail in subsequent sections. Also, the light source used produces beam impulses with more than one photon on average, but the detectors are used to post-select onto light states with only one single photon on average. Finally, the finite reflectivity of the cavity allows for a photon to leak out with a certain probability and it is in this way that a time-dependent investigation of the visibility can be obtained. Therefore, data points for short times will be much more frequent than those for long times.

3.2 The Hamiltonian of the System

We start our quantum mechanical description with the Hamiltonian for the optomechanical system [32]. The coupling between the single mode photon field and the mirror is linear. This approximation holds when the displacement of the mirror is small compared to the length of the cavity and to the wavelength of the photon field. Since we use only a single photon from a coherent light source, these assumptions are easily satisfied. The Hamiltonian then reads:

$$\hat{H} = \hbar\omega_a(\hat{a}^\dagger\hat{a} + \hat{b}^\dagger\hat{b}) + \hbar\omega_c\,\hat{c}^\dagger\hat{c} - \kappa\,\hbar\omega_c\,\hat{a}^\dagger\hat{a}(\hat{c} + \hat{c}^\dagger) \tag{1}$$

Here the operators $\hat{a}$, $\hat{b}$ and $\hat{c}$ refer to the photon in arm A, the photon in arm B and the cantilever's center of mass mode, respectively. ω_a is the photon frequency, ω_c the cantilever frequency and κ is the optomechanical coupling constant. It is given in terms of the system parameters as (see appendix A.2)

$$\kappa = \frac{\omega_a}{\omega_c}\frac{1}{L}\sqrt{\frac{\hbar}{2m\omega_c}} \tag{2}$$

where L is the length of the optical cavity and $\sqrt{\hbar/2m\omega_c}$ the ground state wavepacket of the cantilever. This coupling is responsible for optomechanical entanglement and needs to be of order unity for this experiment, as we will show. Obtaining such a value of κ indeed poses the greatest experimental challenge, since it requires to fabricate a tiny mirror with a very high finesse.

For better readability a short note on notation: Unless otherwise stated, in the rest of this thesis we will mostly omit the operators acting in arm B, $\hat{b}$ and $\hat{b}^\dagger$, since we have just a trivial time evolution in that arm and those operators commute with all other ones. We also use the convention that in a product state the first state always refers to the photon and the second state to the cantilever.

3.3 Time Evolution Operator

To understand the full time evolution of the system we need to compute the unitary evolution operator $\hat{U}(t)$. We know that $\hat{U}(t) = e^{-i\hat{H}t/\hbar}$, but we can obtain it in a more convenient form as in Bose et al. [19]. The calculational details are presented in the appendix A.3, the result is (omitting the phase factor $e^{-i\omega_a \hat{b}^\dagger \hat{b} t}$ for the photon in arm B):

$$\hat{U}(t) = e^{-i\omega_a \hat{a}^\dagger \hat{a} t} e^{i\kappa^2 \left(\hat{a}^\dagger \hat{a}\right)^2 (\omega_c t - \sin\omega_c t)} e^{\kappa \hat{a}^\dagger \hat{a}\left[\hat{c}^\dagger\left(1-e^{-i\omega_c t}\right) - \hat{c}\left(1-e^{i\omega_c t}\right)\right]} e^{-i\omega_c \hat{c}^\dagger \hat{c} t} \tag{3}$$

With this time evolution operator we act on an arbitrary system state $|\, n\rangle |\, \beta\rangle$. Here we use a photon number state and a coherent state of the cantilever with amplitude β. The relations in appendix A.1 help us to write the time evolved state in a convenient form. Acting with $\hat{U}(t)$ on $|\, n\rangle |\, \beta\rangle$ we get:

$$\begin{aligned}
\hat{U}|\, n\rangle |\, \beta\rangle &= e^{-i\omega_a \hat{a}^\dagger \hat{a} t} e^{i\kappa^2 \left(\hat{a}^\dagger \hat{a}\right)^2 (\omega_c t - \sin\omega_c t)} e^{\kappa \hat{a}^\dagger \hat{a}\left[\hat{c}^\dagger\left(1-e^{-i\omega_c t}\right) - \hat{c}\left(1-e^{i\omega_c t}\right)\right]} e^{-i\omega_c \hat{c}^\dagger \hat{c} t} |\, n\rangle |\, \beta\rangle \\
&= e^{-in\omega_a t} e^{i\kappa^2 n^2 (\omega_c t - \sin\omega_c t)} e^{\kappa n\left[\hat{c}^\dagger\left(1-e^{-i\omega_c t}\right) - \hat{c}\left(1-e^{i\omega_c t}\right)\right]} |\, n\rangle |\, \beta e^{-i\omega_c t}\rangle \\
&= e^{-in\omega_a t} e^{i\kappa^2 n^2 (\omega_c t - \sin\omega_c t)} \hat{D}\left(\kappa n\left(1-e^{-i\omega_c t}\right)\right) \hat{D}\left(\beta e^{-i\omega_c t}\right) |\, n\rangle |\, 0\rangle \\
&= e^{-in\omega_a t} e^{i\kappa^2 n^2 (\omega_c t - \sin\omega_c t)} e^{i\kappa n \mathrm{Im}[\beta^* e^{i\omega_c t}(1-e^{-i\omega_c t})]} \hat{D}\left(\beta e^{-i\omega_c t} + \kappa n(1-e^{-i\omega_c t})\right) |\, n\rangle |\, 0\rangle
\end{aligned} \tag{4}$$

So the final result for the time evolved state is

$$\hat{U}|\, n\rangle |\, \beta\rangle = e^{-in\omega_a t} e^{i\kappa^2 n^2 (\omega_c t - \sin\omega_c t)} e^{i\kappa n \mathrm{Im}[\beta(1-e^{-i\omega_c t})]} |\, n\rangle |\, \beta e^{-i\omega_c t} + \kappa n(1-e^{-i\omega_c t})\rangle \tag{5}$$

For a photon number state, an initial coherent cantilever state thus stays a coherent state in time but changes its amplitude. Note that after each full mechanical oscillation, the cantilever is back in the same state as it was originally.

The choice of a coherent cantilever state is convenient, but it is also the most natural choice for an oscillator. Any weak damping will effectively act as a continuous measurement on the system and will eventually produce a minimum uncertainty state. Coherent states are shown to be the most robust states under such weak measurements [33]. We also note that the ground state is also a coherent state which will be relevant in the subsequent discussion (also, the introduction of finite temperatures will require an averaging, which can be conveniently performed over initial coherent states. This will be discussed in section 3.10).

3.4 System Wavefunction for Initially Pure States

We are now able to compute the time evolution of our system under investigation. The initial photon state is a superposition of the photon being in arm A and in arm B, and we take the initial mirror state to be a coherent state with amplitude β. Thus

$$|\, \Psi(0)\rangle = \frac{1}{\sqrt{2}} \left(|\, 0,1\rangle_{a,b} + |\, 1,0\rangle_{a,b}\right) \otimes |\, \beta\rangle_c \tag{6}$$

The subscripts a, b and c denote the interferometric arms A, B and the cantilever, respectively. We will omit the subscripts in the subsequent discussion.

This initial state evolves in time according to eq. (5) and becomes

$$|\, \Psi(t)\rangle = \frac{e^{-i\omega_a t}}{\sqrt{2}} \Big(|\, 0,1\rangle |\, \beta e^{-i\omega_c t}\rangle + e^{i\kappa^2 (\omega_c t - \sin\omega_c t) + i\kappa \mathrm{Im}[\beta(1-e^{-\omega_c t})]} |\, 1,0\rangle |\, \beta e^{-i\omega_c t} + \kappa(1-e^{-i\omega_c t})\rangle \Big) \tag{7}$$

which can be written for convenience as

$$|\,\Psi(t)\rangle = \frac{1}{\sqrt{2}} e^{-i\omega_a t}\Big(|\,0,1\rangle|\,\Phi_0(t)\rangle + e^{i\varphi(t)}|\,1,0\rangle|\,\Phi_1(t)\rangle\Big) \tag{8}$$

with the coherent state amplitudes and the relative phase

$$\begin{aligned} \Phi_0(t) &= \beta e^{-i\omega_c t} \\ \Phi_1(t) &= \beta e^{-i\omega_c t} + \kappa(1 - e^{-i\omega_c t}) \\ \varphi(t) &= \kappa^2\,(\omega_c t - \sin\omega_c t) + \kappa \mathrm{Im}[\beta(1 - e^{-i\omega_c t})] \\ &= \varphi_0(t) + \varphi_\beta(t) \end{aligned} \tag{9}$$

It is apparent that the photon and the cantilever states become entangled since the cantilever is only displaced into the coherent state $\Phi_1(t)$ if the photon is in arm A. Thus, it is now the combined system that is in a superposition and not just the photon part as in eq. (6).

The overlap between the two possible cantilever states is given by

$$|\langle\Phi_0(t)\,|\,\Phi_1(t)\rangle| = e^{-\kappa^2(1-cos\omega_c t)} \tag{10}$$

After a full mechanical oscillation the two states Φ_0 and Φ_1 become the same and they completely overlap. Thus after each mechanical oscillation photon and cantilever become completely disentangled, as is the case for the initial state. However, after half a mechanical roundtrip, $t = \pi/\omega_c$, the overlap between the two cantilever states is minimal, given by $|\langle\Phi_0(\pi/\omega_c)\,|\,\Phi_1(\pi/\omega_c)\rangle| = e^{-2\kappa^2}$. For a proper demonstration of a superposition, we require the overlap at that time to be sufficiently small, implying the condition for the optomechanical coupling

$$\kappa \gtrsim 1/\sqrt{2} \tag{11}$$

This is equivalent to stipulating that, in principle, a measurement of the cantilever state alone would be sufficient to determine which path the photon took. The spatial seperation of the two mirror states can also easily be computed by noting that the coherent states are eigenstates of the annihilation operator. Taking the real part of the difference between the two coherent states yields

$$\Delta x = \sqrt{\frac{8\hbar}{m\omega_c}}\kappa \tag{12}$$

and so the condition for the optomechanical coupling, eqn. (11), implies that the mirror should be displaced by about twice its ground state wavepacket size. Such a condition is rather arbitary, but the order of magnitude should be clear. We also note that obtaining this large a value of κ poses the most significant barrier to experimental realization.

3.5 The Interferometric Visibility

To probe the superposition, the actual quantity measured is the interferometric visibility as seen by the two single photon detectors. The visibility is a measure of the photon to exhibit quantum mechanical interference, and it can be computed by taking twice the absolute value of the off-diagonal elements of the reduced photon density matrix. This definition for the visibility is plausible: the detectors gain information only on the photon which implies that the rest of the wavefunction (in this case the cantilever states) must be integrated out. Also, quantum interference is caused by the off-diagonal elements of the density matrix. The exact relationship

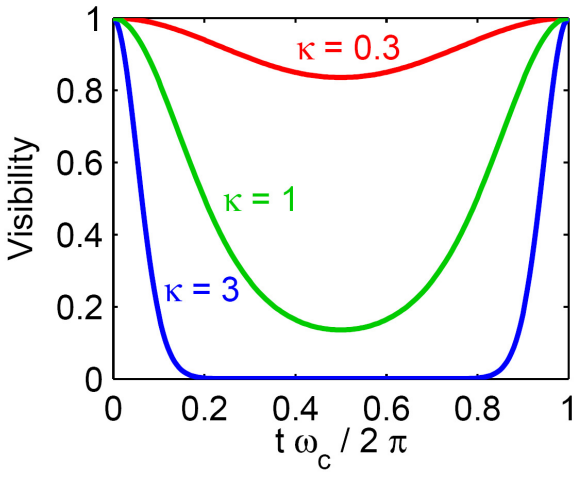

Figure 3: *The interferometric visibility for different optomechanical coupling constants κ. The visibility is reduced after the photon enters the cavity, and lost entirely for a large κ . However, full visibility is completely recovered after exactly one oscillation of the cantilever since the cantilever position at this time is the same as initially, regardless of the presence of the photon.*

between visibility and the detection probabilities at the single photon detectors is discussed in more detail in section 3.8.

We now compute the visibility, starting with the full density matrix of the system:

$$\begin{aligned}\hat{\rho}(t) &= |\,\Psi(t)\rangle\langle\Psi(t)\,| \\ &= \frac{1}{2}\Big(|\,0,1\rangle|\,\Phi_0\rangle + e^{i\varphi(t)}|\,1,0\rangle|\,\Phi_1(t)\rangle\Big)\Big(\langle 0,1\,|\langle\Phi_0(t)\,| + e^{-i\varphi(t)}\langle 1,0\,|\langle\Phi_1(t)\,|\Big) \\ &= \frac{1}{2}\Big(|\,0,1\rangle\langle 0,1\,|\otimes|\,\Phi_0\rangle\langle\Phi_0\,| + |\,1,0\rangle\langle 1,0\,|\otimes|\,\Phi_1\rangle\langle\Phi_1\,| + \\ &\quad + e^{i\varphi(t)}|\,1,0\rangle\langle 0,1\,|\otimes|\,\Phi_1\rangle\langle\Phi_0\,| + e^{-i\varphi(t)}|\,0,1\rangle\langle 1,0\,|\otimes|\,\Phi_0\rangle\langle\Phi_1\,|\Big)\end{aligned} \tag{13}$$

The cantilever states need to be traced out. Note that for any states $|\,\alpha\rangle$ and $|\,\beta\rangle$ we have

$$\mathrm{Tr}[|\,\alpha\rangle\langle\beta\,|] = \sum_n \langle n\,|\,\alpha\rangle\langle\beta\,|\,n\rangle = \sum_n \langle\beta\,|\,n\rangle\langle n\,|\,\alpha\rangle = \langle\beta\,|\,\alpha\rangle \tag{14}$$

Thus the reduced photon density matrix is

$$\begin{aligned}\hat{\rho}(t)^{(Ph)} = \mathrm{Tr}_c[\hat{\rho}(t)] = \frac{1}{2}\Big(&|\,0,1\rangle\langle 0,1\,| + |\,1,0\rangle\langle 1,0\,| + \\ &+ e^{i\varphi(t)}\langle\Phi_0\,|\,\Phi_1\rangle|\,1,0\rangle\langle 0,1\,| + e^{-i\varphi(t)}\langle\Phi_1\,|\,\Phi_0\rangle|\,0,1\rangle\langle 1,0\,|\Big)\end{aligned} \tag{15}$$

where Tr_c denotes a trace over the cantilever states. From the off-diagonal elements of the above photon density matrix, and eqn. (10) for the overlap, we finally obtain the visibility:

$$v(t) = 2|\rho(t)_{01}^{(Ph)}| = e^{-\kappa^2(1-\cos\omega_c t)} \tag{16}$$

This function is plotted in figure 3 for different κ. It exhibits a periodic behaviour characterized by a suppression of the interference visibility after half a mechanical roundtrip and a

revival to perfect visibility after a full period. As we noted before, the reduction of visibility is due to the fact that the displaced cantilever has information about which path the photon took, and the revival shows that the cantilever indeed behaves quantum mechanically since it can become periodically entangled. In section 3.9 we show explicitly that such a visibility pattern is a direct proof that the photon was entangled with the cantilever and thus that the cantilever was in a superposition.

3.6 Cantilever States after a Photon Detection

In this section we calculate the state of the cantilever after a measurement on the photon has been performed. The detectors at the output ports measure the photon states in a specific basis. The corresponding basis states determine into which state the mirror is projected after photon detection. These basis states can be computed for any given setup and depend on the phase difference between the two arms due to a phase changer (which is equivalent to a path length difference). For the setup at hand, we have computed the photon states at the two detector ports in appendix A.4. The result shows that the two output ports detect a photon in the basis spanned by :

$$\begin{aligned} |+\rangle &= \frac{1}{\sqrt{2}}\Big(|0,1\rangle + e^{i\theta}|1,0\rangle\Big) \\ |-\rangle &= \frac{1}{\sqrt{2}}\Big(|0,1\rangle - e^{i\theta}|1,0\rangle\Big) \end{aligned} \tag{17}$$

The relative phase θ accounts for a path length difference between the two arms and can be varied experimentally by the use of an optical phase modulator. In general it will also be time dependent if the two cavities have not exactly the same size, and will thus yield a running phase difference of the light in the two arms.

The entangled state of photon and cantilever can be expressed in terms of the above basis states. From eqn. (8) we have:

$$\begin{aligned} |\Psi(t)\rangle &= \frac{e^{-i\omega_a t}}{\sqrt{2}}\Big(|0,1\rangle \otimes |\Phi_0(t)\rangle + e^{i\varphi(t)}|1,0\rangle \otimes |\Phi_1(t)\rangle\Big) \\ &= \frac{1}{2}\frac{e^{-i\omega_a t}}{\sqrt{2}}\Big(|0,1\rangle + e^{i\theta}|1,0\rangle\Big) \otimes \Big(|\Phi_0(t)\rangle + e^{i\varphi(t)-i\theta}|\Phi_1(t)\rangle\Big) + \\ &\quad + \frac{1}{2}\frac{e^{-i\omega_a t}}{\sqrt{2}}\Big(|0,1\rangle - e^{i\theta}|1,0\rangle\Big) \otimes \Big(|\Phi_0(t)\rangle - e^{i\varphi(t)-i\theta}|\Phi_1(t)\rangle\Big) \end{aligned} \tag{18}$$

We can thus express the total state as

$$|\Psi(t)\rangle = \mathcal{N}_+|+\rangle|\Phi_+\rangle + \mathcal{N}_-|-\rangle|\Phi_-\rangle \tag{19}$$

with

$$|\pm\rangle = \frac{1}{\sqrt{2}}\Big(|0,1\rangle \pm e^{i\theta}|1,0\rangle\Big) \tag{20}$$

$$|\Phi_\pm\rangle = \frac{e^{-i\omega_a t}}{2\mathcal{N}_\pm}\Big(|\Phi_0(t)\rangle \pm e^{i\varphi(t)-i\theta}|\Phi_1(t)\rangle\Big) \tag{21}$$

being the photon and the mirror states, respectively. The factor $\mathcal{N}_\pm$ ensures a proper normalization of the above cantilever states and incorporates the probability of finding a photon in

one of the corresponding photon states, as we will show in the next section. It's absolute value is found by setting $\langle \Phi_\pm \,|\, \Phi_\pm \rangle = 1$ and is given by

$$|\mathcal{N}_\pm|^2 = \frac{1}{4}\left(2 \pm e^{-i\varphi(t)+i\theta}\langle \Phi_1 \,|\, \Phi_0\rangle \pm e^{i\varphi(t)-i\theta}\langle \Phi_0 \,|\, \Phi_1\rangle\right) \tag{22}$$

It is now a trivial task to see into which state the mirror is projected once a photon state has been detected at one of the output ports. Since the detectors measure the photon state $|+\rangle$ or $|-\rangle$, depending on what port the photon arrives at, the mirror will be projected into the state $\mathcal{N}_+|\,\Phi_+\rangle$ or $\mathcal{N}_-|\,\Phi_-\rangle$, respectively. Thus the cantilever will be indeed in a superposition state.

3.7 Detection Probabilities

We now determine the photon detection probabilities at the two detector ports. We will show that they are directly related to the interfermetric visibility.

To find the photon detection probabilities, we have to consider the total system at the time of detection and trace out all possible cantilever states. By performing the calculation in terms of the state written in the form (19) we get

$$\begin{aligned}\hat{\rho}(t)^{(Ph)} &= \mathrm{Tr}_c\big\{|\,\Psi(t)\rangle\langle\Psi(t)\,|\big\} = \\ &= |\mathcal{N}_+|^2|+\rangle\langle+| + |\mathcal{N}_-|^2|-\rangle\langle-| + \\ &\quad + \mathcal{N}_+\mathcal{N}_-^*\langle\Phi_-\,|\,\Phi_+\rangle\,|+\rangle\langle-| + \mathcal{N}_-\mathcal{N}_+^*\langle\Phi_+\,|\,\Phi_-\rangle\,|-\rangle\langle+|\end{aligned} \tag{23}$$

Choosing the arbitary convention that the detector outputs A and B measure the photon states $|+\rangle$ and $|-\rangle$, respectively, we obtain the detection probabilities

$$\begin{aligned}p(A) &= \langle+|\,\hat{\rho}(t)^{(Ph)}|+\rangle = |\mathcal{N}_+|^2 \\ p(B) &= \langle-|\,\hat{\rho}(t)^{(Ph)}|-\rangle = |\mathcal{N}_-|^2\end{aligned} \tag{24}$$

Note that the total probability to measure the photon is $p(A)+p(B)=1$, as can be seen from eq. (22).

These probabilities are the main experimental data we can get in the setup. In practice we are intersted in the interferometric visibility which is extracted from the difference of the probabilities, $p(A)-p(B)$. If the cantilever is initially cooled to the ground state we have $\beta = 0$ and $\langle \Phi_1 \,|\, \Phi_0\rangle = e^{-\kappa^2(1-cos\omega_c t)}$ in eq. (22), so that:

$$p(A) - p(B) = \cos\left(\theta - \varphi_0(t)\right) e^{-\kappa^2(1-cos\omega_c t)} \tag{25}$$

with $\varphi_0(t) = \kappa^2\left(\omega_c t - \sin\omega_c t\right)$. This expression consists of two factors: The first is an oscillatory factor which depends on the relative arm length difference induced by the photon pressure and on the phase θ from the phase modulater in the setup. The second factor is the envelope which represents only the ability of the system to show interference due to optomechanical entanglement, and which we define to be the interferometric visibility $v(t)$. Thus in practice, only the envelope will be of interest. A possible data curve is shown in figure 4, which includes a length difference in the two cavities and has thus a time-dependent relative phase.

For the more general case of initial coherent mirror states, we obtain the same result but with a different induced phaseshift:

$$p(A) - p(B) = \cos\left(\theta - \tilde{\varphi}(t)\right) e^{-\kappa^2(1-cos\omega_c t)} \tag{26}$$

with $\tilde{\varphi}(t,\beta) = \kappa^2(\omega_c t - \sin\omega_c t) + 2\kappa\mathrm{Im}[\beta(1-e^{-i\omega_c t})]$.

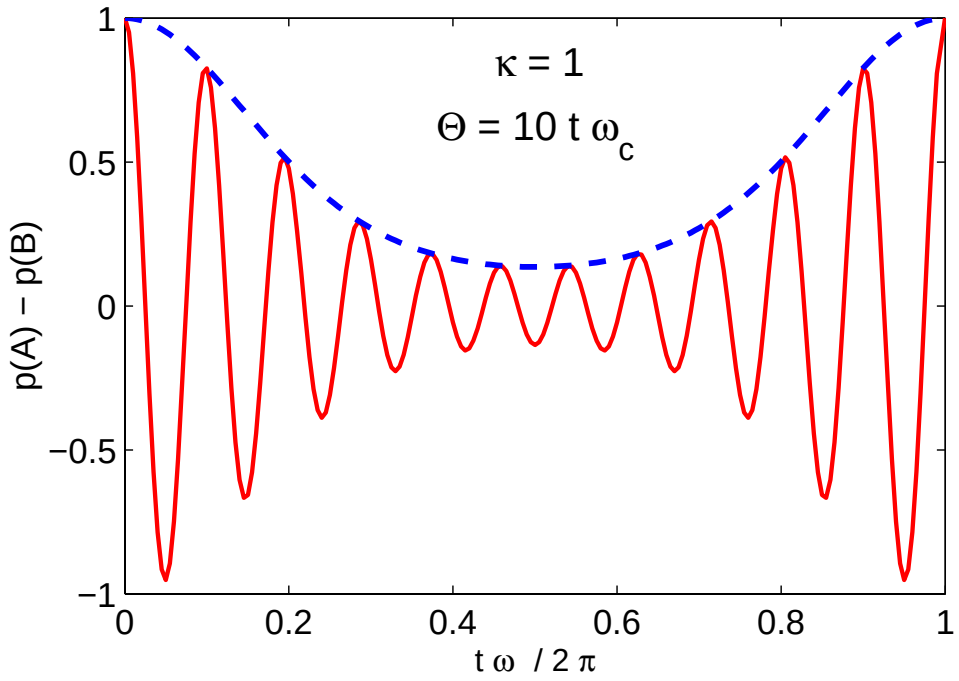

Figure 4: *Photon detection probability difference for the two detectors in the setup (solid red line), for $\beta = 0$. This curve is close to what an actual data curve might look like. The envelope (dashed blue line) is the interferometric visibility. The time dependent phase θ is due to a slight difference in the length of the two cavities in arms A and B and a finite input light pulse duration. It yields a highly oscillating curve which allows the construction of the envelope.*

3.8 Visibility and Detection Probabilities

In the previous section we have defined the visibility to be the envelope of $p(A) - p(B)$. Here we will show that it is consistent with the previous definition of $v(t)$ which we used in section 3.5:

$$v(t) = 2|\rho(t)^{(Ph)}_{01}| \tag{27}$$

Rewriting the photon density matrix (23) in terms of the Fock basis states (omitting labelling the photon in arm B, since it is always conjugate to the photon state in arm A) we get

$$\begin{aligned}\rho(t)^{(Ph)} = \frac{1}{2}\Big\{ &|\,0\rangle\langle 0\,|\Big(|\mathcal{N}_+|^2 + |\mathcal{N}_-|^2 + \mathcal{N}_+\mathcal{N}_-^*\langle\Phi_-\,|\,\Phi_+\rangle + \mathcal{N}_-\mathcal{N}_+^*\langle\Phi_+\,|\,\Phi_-\rangle\Big) + \\ &+|\,1\rangle\langle 1\,|\Big(|\mathcal{N}_+|^2 + |\mathcal{N}_-|^2 - \mathcal{N}_+\mathcal{N}_-^*\langle\Phi_-\,|\,\Phi_+\rangle - \mathcal{N}_-\mathcal{N}_+^*\langle\Phi_+\,|\,\Phi_-\rangle\Big) + \\ &+|\,0\rangle\langle 1\,|e^{-i\theta}\Big(|\mathcal{N}_+|^2 - |\mathcal{N}_-|^2 - \mathcal{N}_+\mathcal{N}_-^*\langle\Phi_-\,|\,\Phi_+\rangle + \mathcal{N}_-\mathcal{N}_+^*\langle\Phi_+\,|\,\Phi_-\rangle\Big) + \\ &+|\,1\rangle\langle 0\,|e^{i\theta}\Big(|\mathcal{N}_+|^2 - |\mathcal{N}_-|^2 + \mathcal{N}_+\mathcal{N}_-^*\langle\Phi_-\,|\,\Phi_+\rangle - \mathcal{N}_-\mathcal{N}_+^*\langle\Phi_+\,|\,\Phi_-\rangle\Big)\Big\}\end{aligned} \tag{28}$$

Note that the mirror states $|\,\Phi_\pm\rangle$ are not orthogonal. Their inner product is given by

$$\mathcal{N}_\mp\mathcal{N}_\pm^*\langle\Phi_\pm\,|\,\Phi_\mp\rangle = \frac{1}{4}\big(\pm e^{-i\varphi(t)+i\theta}\langle\Phi_1\,|\,\Phi_0\rangle \mp e^{i\varphi(t)-i\theta}\langle\Phi_0\,|\,\Phi_1\rangle\big) \tag{29}$$

so that we have

$$\mathcal{N}_-\mathcal{N}_+^*\langle\Phi_+\,|\,\Phi_-\rangle + \mathcal{N}_+\mathcal{N}_-^*\langle\Phi_-\,|\,\Phi_+\rangle = 0 \tag{30}$$

$$\mathcal{N}_-\mathcal{N}_+^*\langle\Phi_+\,|\,\Phi_-\rangle - \mathcal{N}_+\mathcal{N}_-^*\langle\Phi_-\,|\,\Phi_+\rangle = \frac{1}{2}\big(e^{i\varphi(t)-i\theta}\langle\Phi_0\,|\,\Phi_1\rangle - e^{-i\varphi(t)+i\theta}\langle\Phi_1\,|\,\Phi_0\rangle\big) \tag{31}$$

and

$$|\mathcal{N}_+|^2 - |\mathcal{N}_-|^2 = \frac{1}{2}\big(e^{i\varphi(t)-i\theta}\langle\Phi_0\,|\,\Phi_1\rangle + e^{-i\varphi(t)+i\theta}\langle\Phi_1\,|\,\Phi_0\rangle\big) \tag{32}$$

We have already shown that we can also write $|\mathcal{N}_+|^2 = p(A)$ and $|\mathcal{N}_-|^2 = p(B)$. Thus we have

$$\begin{aligned} v(t) = 2|\rho(t)_{01}^{(Ph)}| &= \left||\mathcal{N}_+|^2 - |\mathcal{N}_-|^2 + \frac{1}{2}\big(e^{i\varphi(t)-i\theta}\langle\Phi_0\,|\,\Phi_1\rangle - e^{-i\varphi(t)+i\theta}\langle\Phi_1\,|\,\Phi_0\rangle\big)\right| \\ &= \left|(p(A)-p(B))\left(1 + \frac{e^{i\varphi(t)-i\theta}\langle\Phi_0\,|\,\Phi_1\rangle - e^{-i\varphi(t)+i\theta}\langle\Phi_1\,|\,\Phi_0\rangle}{e^{i\varphi(t)-i\theta}\langle\Phi_0\,|\,\Phi_1\rangle + e^{-i\varphi(t)+i\theta}\langle\Phi_1\,|\,\Phi_0\rangle}\right)\right| \\ &= (p\,(A) - p\,(B))\,\frac{\left|2e^{i\varphi(t)-i\theta}\langle\Phi_0\,|\,\Phi_1\rangle\right|}{e^{i\varphi(t)-i\theta}\langle\Phi_0\,|\,\Phi_1\rangle + e^{-i\varphi(t)+i\theta}\langle\Phi_1\,|\,\Phi_0\rangle} \\ &= (p(A)-p(B))\,\frac{1}{\cos\left(\theta-\tilde{\varphi}(t)\right)} \end{aligned} \tag{33}$$

with, as above, $\tilde{\varphi}(t,\beta) = \kappa^2(\omega_c t - \sin\omega_c t) + 2\kappa\mathrm{Im}[\beta(1-e^{-i\omega_c t})]$. We can thus see that the visibility as previously defined is indeed just the envelope of the detection probability differences,

$$p(A) - p(B) = \cos\left(\theta - \tilde{\varphi}(t)\right)\cdot v(t) \tag{34}$$

3.9 Visibility as a Measure of Entanglement

The loss and a subsequent revival of the visibility, as discussed in section 3.5, is in fact proof of a macroscopic quantum superposition. It is direct evidence of the periodic entanglement between the photon and the mirror. The displacement of the cantilever destroys the quantum intereference of the photon, since it is evidence on what path the photon took. The amount of suppression of the visibility shows how distinguishable the two mirror states in superposition are. Only for fully distinguishable states will the visibility drop to zero, since in this case there is absolute certainty about the path of the photon. But for any optomechanical coupling κ the entanglement between photon and mirror is lost after exactly a full mechanical oscillation, and so the visibility completely returns.

More quantitatively, the visibility can be mapped to the Von Neumann entropy of the system. It is defined as [34]

$$S(t) = -\mathrm{Tr}\big[\hat{\rho}(t)^{(Ph)}\cdot\log_2[\hat{\rho}(t)^{(Ph)}]\big] \tag{35}$$

Due to the cyclic trace property, we can conveniently calculate $S(t)$ by using a diagonalized form of $\hat{\rho}(t)^{(Ph)}$, with the eigenvalues as its diagonal entries. Calling the eigenvalues λ_i we thus get

$$S(t) = -\sum_i \lambda_i\cdot\log_2\lambda_i \tag{36}$$

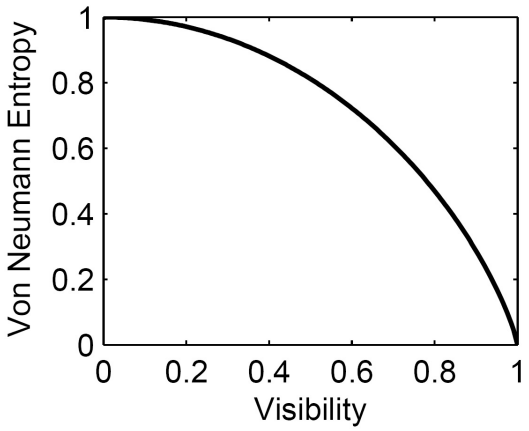

Figure 5: *The entropy $S(t)$ as a function of visibility, $v(t)$. High entropy corresponds to strong entanglement between the two subsystems of a pure bipartite state, whereas no entropy means no entanglement is present. Thus the visibility is a direct measure of entanglement between the photon and the cantilever.*

To compute the eigenvalues, we use the reduced photon density matrix, eq. (15). In the fock-state basis it is written as

$$\rho(t)^{(Ph)} = \frac{1}{2}\begin{pmatrix} 1 & v(t)\, e^{i\varphi(t)} \\ v(t)\, e^{-i\varphi(t)} & 1 \end{pmatrix} \tag{37}$$

where we wrote the off-diagonal elements in terms of the visibility $v(t)$. The eigenvalues are then easily found to be

$$\lambda_{1/2} = \frac{1}{2}(1 \pm v(t)) \tag{38}$$

Hence the Von Neumann entropy can be written in terms of the visibility as

$$\begin{aligned} S(t) &= -\sum_i \lambda_i \cdot \log_2 \lambda_i \\ &= -\frac{1}{2}(1+v(t)) \log_2 \left(\frac{1}{2}\,(1+v(t))\right) - \frac{1}{2}(1-v(t)) \log_2 \left(\frac{1}{2}\,(1-v(t))\right) \\ &= -\frac{1}{2}\log_2 \left(\frac{1}{4}\,(1+v(t))\,(1+v(t))\right) - \frac{1}{2} v(t) \log_2 \left(\frac{1+v(t)}{1-v(t)}\right) \\ &= 1 + \frac{1}{2} v(t) \log_2 \left(\frac{1-v(t)}{1+v(t)}\right) - \frac{1}{2}\log_2 \left(1-v(t)^2\right) \end{aligned} \tag{39}$$

The entropy as a function of the visibility is plotted in figure 5. We see that there is a one-to-one correspondence between the two quantities. Thus the visibility as obtained experimentally is a direct measure of the Von Neumann entropy of the photon-cantilever system.

For a pure bipartite system the Von Neumann entropy can also be interpreted as a measure of entanglement between the two subsystems [35]. A high Von Neumann entropy of one subsystem corresponds to high entanglement between the two subsystems. We thus conclude that when the initial state is pure (as is the case when the cantilever is in a known coherent state) the visibility alone is a direct measure of entanglement and thus a good measure for the non-classical behaviour of the cantilever.

3.10 Effects of Finite Cantilever Temperatures

Until now we have considered the cantilever to be in a known coherent state. In practice, determining the exact state of the cantilever is hardly possible (the theoretically predicted ground state cooling could provide a way [6, 7, 8, 9, 10]). When working at finite temperatures, we do not know enough details about the exact initial state of the cantilever, so the state has instead to be described by a thermal density matrix:

$$\hat{\rho}_c(0) = \frac{\sum_n e^{-E_n/k_BT} |\, n\rangle\langle n\,|}{\sum_n e^{-E_n/k_BT}} \tag{40}$$

This is the analogue of a classical statistical Boltzman distribution for the cantilever states. It is expressed in terms of energy eigenkets $|\, n\rangle$. However, it is convenient to rewrite the above density matrix in terms of coherent states $|\, \beta\rangle$ which can easily be done using the overcompletness of the coherent state basis (eqn. (153)):

$$\hat{\rho}_c(0) = \frac{1}{\pi\bar{n}} \int d^2\beta\, e^{-|\beta|^2/\bar{n}} |\, \beta\rangle\langle\beta\,| \tag{41}$$

where $\bar{n} = 1/(e^{\hbar\omega_c/k_BT} - 1)$ is the average thermal occupation number of the cantilever's center of mass mode. Note that here we only consider the effects of a thermally excited initial state, i.e. for a cantilever with no dissipation (mechanical quality factor $Q \to \infty$). The effects of dissipation and the resulting decoherence are discussed chapter 5.

We now compute the evolution of the full system with the initial cantilever state being eqn. (41). The analogue of the Schrödinger equation for the time evolution of density matrices is the Von-Neumann equation [34]:

$$\frac{d\hat{\rho}(t)}{dt} = -\frac{i}{\hbar}\Big[\hat{H}, \hat{\rho}(t)\Big] \tag{42}$$

For a time-independent Hamiltonian, the time evolved density matrix can thus be expressed as

$$\hat{\rho}(t) = e^{-i\hat{H}t/\hbar}\hat{\rho}(0)e^{i\hat{H}t/\hbar} = \hat{U}(t)\hat{\rho}(0)\hat{U}^\dagger(t) \tag{43}$$

In our case, the initial state of the system is given by the product of the thermal state of the cantilever and the superposition state of the photon:

$$\hat{\rho}(0) = \frac{1}{2\pi\bar{n}} \int d^2\beta\, e^{-|\beta|^2/\bar{n}} \Big(|\, 0,1\rangle + |\, 1,0\rangle\Big)\Big(\langle 0,1\,| + \langle 1,0\,|\Big) \otimes |\, \beta\rangle\langle\beta\,| \tag{44}$$

The time evolved, temperature dependent density matrix $\hat{\bar{\rho}}(\bar{n}, t)$ (in the following, we shall denote all thermally averaged quantities with a bar) becomes

$$\begin{aligned}
\hat{\bar{\rho}}(\bar{n}, t) &= \frac{1}{2\pi\bar{n}} \int d^2\beta\, e^{-|\beta|^2/\bar{n}} \hat{U}(t)\Big(|\, 0,1\rangle + |\, 1,0\rangle\Big) |\, \beta\rangle\langle\beta\,| \Big(\langle 0,1\,| + \langle 1,0\,|\Big)\hat{U}^\dagger(t) \\
&= \frac{1}{\pi\bar{n}} \int d^2\beta\, e^{-|\beta|^2/\bar{n}}\, |\, \psi(t)\rangle\langle\psi(t)\,| \\
&= \frac{1}{\pi\bar{n}} \int d^2\beta\, e^{-|\beta|^2/\bar{n}}\, \hat{\rho}(\beta, t)
\end{aligned} \tag{45}$$

Thus we can use the time evolution of an initial pure cantilever, given in eq. (13), and simply average over all coherent states with the Gaussian weight $e^{-|\beta|^2/\bar{n}}$ to obtain the time evolved

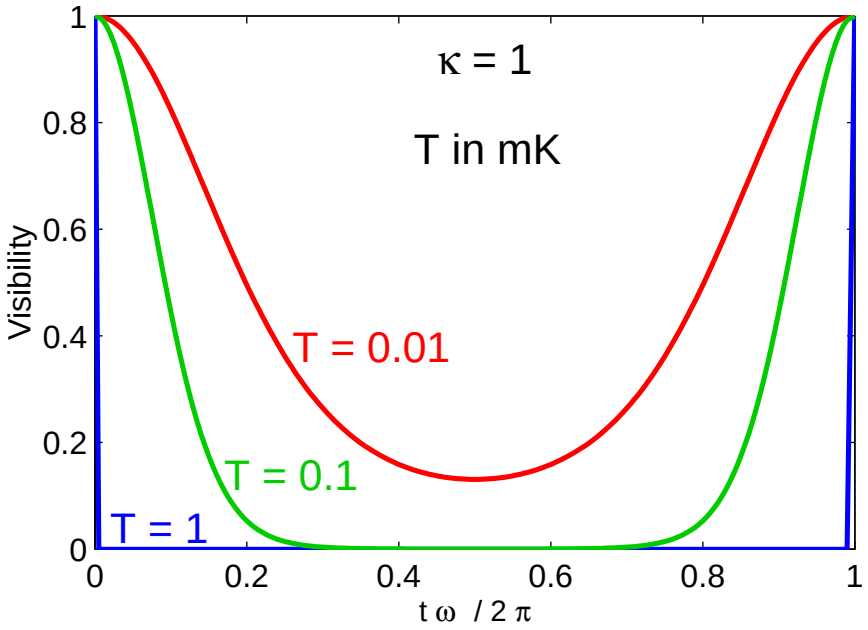

Figure 6: *The effect of finite temperatures on the interferometric visibility. The revival peaks are extremely narrowed, thus cooling of the cantilever mode is required to allow for their experimental detection.*

thermal state. Taking the trace over all cantilever states we find the off-diagonal terms of the photon density matrix, which are the same as in (15) but with an additional Gaussian integral which can easily be computed (in appendix A.5 we performed a similar computation where dissipation is also included). This yields the visibility

$$v(t) = e^{-\kappa^2(2\bar{n}+1)(1-\cos(\omega_c t))}. \tag{46}$$

Note that to see the explicit temperature dependence we can also write:

$$2\bar{n} + 1 = \coth(kT/2\hbar\omega_c) \tag{47}$$

The effect of finite temperatures is thus to narrow the visibility peaks. It occurs because the thermal density matrix represents an average over coherent states with different phases. This reflects the fact that the experiment requires averaging over many runs, and thus the quantum distinguishability is masked by the unknown random phase shifts.

One can see how the unkown initial state affects the data at the two detectors by looking at the detection probabilities, eqn. (26):

$$p(A) - p(B) = \cos\left(\theta - \tilde{\varphi}(t)\right) e^{-\kappa^2(1-cos\omega_c t)} \tag{48}$$

with $\tilde{\varphi}(t,\beta) = \kappa^2(\omega_c t - \sin\omega_c t) + 2\kappa \mathrm{Im}[\beta(1-e^{-i\omega_c t})]$. The experiment consists of many different runs. However, we have no knowledge about the actual initial state $|\,\beta\rangle$ of the cantilever since at finite temperatures the cantilever will have randomly some coherent amplitude β during every experimental run. So the initial state of the mirror can be different at each run, and hence the phase $\tilde{\varphi}(t,\beta)$ will be different in every run as well.

Therefore we have to average over all possible coherent cantilever states. Given a thermal Boltzman distribution we average over $e^{-|\beta|^2/\bar{n}}$. The result is

$$p(A) - p(B) = \cos\left(\theta - \varphi_0(t)\right) e^{-\kappa^2(1+2\bar{n})(1-cos\omega_c t)} \tag{49}$$

with $\varphi_0(t) = \kappa^2(\omega_c t - \sin\omega_c t)$. It shows that a lack of knowledge of the exact mirror state will effectively reduce the envelope. It coincides with the calculation of the visibility for finite temperatures, eqn. (46). The visibility is thus now only partly due to optomechanical entanglement, but mostly due to the uncertainty about the initial state of the mirror.

This is illustrated in figure 6 which shows that cantilever temperatures on the order of 1 mK will already make an experimental detection of the interferometric visibility extremely hard. For that reason it has been proposed to optically cool the center of mass mode of the cantilever to only a few quanta or even to the ground state [21].

However, another important aspect of finite cantilever temperatures has to be considered. Since the system can only be described in a mixed state, the interpretation of the interferometric visibility is altered. At finite cantilever temperatures the interferometric visibility becomes a bad measure for the non-classicality of the mirror. This can be easily seen by the the relation between the von Neumann entropy and the visibility, eqn. (39). It is valid at arbitrary temperatures, but at $T > 0$ the system is in a mixed state and the entropy is only an upper bound for entanglement [35]. One thus needs to analyze the non-classicality of the cantilever state by other means. In the next chapter we use the integrated negativity of the Wigner function [36] to quantify the non-classicality of the cantilever with respect to temperature.

We note though that after a full mechanical period the net phase shift from any initial state goes to zero and so full visibility should still return in a narrow window whose width scales like $\bar{n}^{-1/2}$. This leaves open the possibility for measuring quantum collapse mechanisms at higher temperatures if one assumes that the cantilever was in a superposition state. Provided that the opto-mechanical coupling strength κ is relatively well known (e.g., by independently measuring m, ω_c, L, etc.) and the instantaneous quantum state of the cantilever is regarded as some random coherent state (as should be the case for the weakly mechanically damped systems discussed here) it can be easily determined from our analysis in the previous sections when a superposition should have been created.

Thus a full return of visibility at higher temperatures can be used to strongly imply the existence of a quantum superposition when $\kappa \gtrsim 1/\sqrt{2}$, even though the superposition cannot be directly measured by the visibility loss at $t \sim \pi\omega_c$ (since it is mainly due to classical phase averaging over many experimental runs). Nevertheless, an unambiguous demonstration can be provided if the temperature is low enough such that the visibility loss due to quantum distinguishability is still resolvable.

4 Analysis in Phase Space: The Wigner Function of the Cantilever

To study transitions between the quantum and the classical regimes, it is often convenient to refer to quasi-probability distributions, with which quantum mechanics can be formulated in the common classical phase space. One such distribution was proposed in 1932 by Wigner [37] and can be obtained from the density matrix $\hat{\rho}$:

$$W(x,p) = \frac{1}{\pi\hbar}\int_{-\infty}^{+\infty} dy \langle x-y\,|\hat{\rho}|\,x+y\rangle e^{2ipy/\hbar}. \tag{50}$$

This is known as the Wigner-Weyl transformation which maps an operator onto a complex function in phase space. The Wigner function is thus a powerful tool for the study of transitions between quantum and classical regimes, since it describes quantum states in phase space that is common to classical mechanics. Due to Heisenberg's uncertainty principle, it is not an exact distribution function for both x and p (states will not be described by single points in phase space, but rather by a smeared distribution). However, one can obtain the probability distribution for either x or p by taking $\int dp\, W(x,p)$ or $\int dx\, W(x,p)$, respectively. In fact, although the Wigner function is obtained from a quantum mechanical density matrix, it can be interpreted as a classical probability distribution $P(q_i(t), p_i(t))$ in phase space in the regime $\hbar \to 0$. To see this, let us first look at the classical equations of motion: According to Liouville's theorem, the total time derivative of $P(q_i(t), p_i(t))$ vanishes along a phase space trajectory

$$\frac{dP}{dt} = \frac{\partial P}{\partial t} - \{H, P\} = 0 \tag{51}$$

where $\{\,,\}$ denotes the Poisson bracket. For a single particle with mass m in a potential $V(x)$, we thus find Liouville's equation

$$\Big(\frac{\partial}{\partial t} + \frac{p}{m}\frac{\partial}{\partial x} - \frac{dV(x)}{dx}\frac{\partial}{\partial p}\Big)\, P(x,p,t) = 0 \tag{52}$$

In quantum mechanics, the evolution equation for the Wigner function $W(x,p,t)$ can be obtained from the von Neumann equation, and reads [38]

$$\Big(\frac{\partial}{\partial t} + \frac{p}{m}\frac{\partial}{\partial x} - \frac{dV(x)}{dx}\frac{\partial}{\partial p}\Big)\, W(x,p,t) = \sum_{k=1}^{\infty} \frac{\hbar^{2k}(-1)^k}{4^k(2k+1)!}\frac{d^{2k+1}V(x)}{dx^{2k+1}}\frac{\partial^{2k+1}}{\partial p^{2k+1}} W(x,p,t) \tag{53}$$

It was found by Wigner himself in 1932 [37]. For $\hbar \to 0$, the right hand side goes to 0, as long as no derivatives blow up. In this classical limit, the Wigner function $W(x,p,t)$ thus evolves according to the same Liouville equation (52). Note, however, that the quantum nature of $W(x,p,t)$ is also contained in its initial conditions. In fact, in the special case of a harmonic potential, all non-classical behavior is encoded in the initial conditions of the Wigner function only since the right hand side of Eq. (53) is always 0. But for $\hbar \to 0$ also the initial conditions become classical and $W(x,p,t)$ can be fully identified with some classical probability density $P(x,p,t)$. In this sense, quantum and classical stochastic descriptions of a harmonic oscillator coincide.

On the other hand, the Wigner function can become negative for some quantum states, such as for energy eigenstates. It is therefore referred to as a quasi-probability distribution, since

a negative function in phase space has no classical analogue. Thus, if the Wigner function is negative, it can only refer to a quantum state. This allows for the possiblity to analyze and quantify the non-classicality of the cantilever using the Wigner function in phase space. In the following we will compute the cantilever's Wigner function after a photon state has been detected, and we will also use the Wigner function to set a lower bound on the non-classicality of the cantilever when it is at finite temperatures.

4.1 Wigner Function for a Pure Initial State

We start our analysis with the wavefunction of the bipartite photon- cantilever system, eqn. (8):

$$|\,\Psi(t)\rangle = \frac{1}{\sqrt{2}} e^{-i\omega_a t}\Big(|\,0,1\rangle \otimes |\,\Phi_0(t)\rangle + e^{i\varphi(t)}|\,1,0\rangle \otimes |\,\Phi_1(t)\rangle\Big) \tag{54}$$

where we have the following relations:

$$\begin{aligned} \Phi_0(t) &= \beta e^{-i\omega_c t} \\ \Phi_1(t) &= \beta e^{-i\omega_c t} + \kappa(1 - e^{-i\omega_c t}) \\ \varphi(t) &= \kappa^2\left(\omega_c t - \sin\omega_c t\right) + \kappa \mathrm{Im}[\beta(1 - e^{-i\omega_c t})] \end{aligned} \tag{55}$$

For later discussion it is convinient to split the phase factor $\varphi(t)$ into a part $\varphi_0(t)$ independent of the initial state and into a β - dependent part $\varphi_\beta(t)$:

$$\varphi(t) = \varphi_0(t) + \varphi_\beta(t) \tag{56}$$

with

$$\begin{aligned} \varphi_0(t) &= \kappa^2\left(\omega_c t - \sin\omega_c t\right) \\ \varphi_\beta(t) &= \kappa \mathrm{Im}[\beta(1 - e^{-i\omega_c t})] = -\mathrm{Im}[\Phi_0 \Phi_1^*] \end{aligned} \tag{57}$$

The density matrix of the system is given by (we omit the labelling of the photon state in arm B)

$$\begin{aligned} \hat{\rho}(t) &= \frac{1}{2}|\,0\rangle\langle 0\,| \otimes |\,\Phi_0\rangle\langle\Phi_0\,| + \frac{1}{2}|\,1\rangle\langle 1\,| \otimes |\,\Phi_1\rangle\langle\Phi_1\,| + \\ &+ \frac{1}{2}e^{-i\varphi}|\,0\rangle\langle 1\,| \otimes |\,\Phi_0\rangle\langle\Phi_1\,| + \frac{1}{2}e^{i\varphi}|\,1\rangle\langle 0\,| \otimes |\,\Phi_1\rangle\langle\Phi_0\,| \\ &= \hat{\rho}_{00} + \hat{\rho}_{11} + \hat{\rho}_{01} + \hat{\rho}_{10} \end{aligned} \tag{58}$$

We are interested in the Wigner function of the mirror, under the condition that we have measured a photon in a superposition state. This Wigner function can be obtained from the above density matrix after we perform a measurement on the photon part, i.e. we need to project the photon part onto $|\,+\rangle = \frac{1}{\sqrt{2}}(|\,0\rangle + e^{i\theta}|\,1\rangle)$, as discussed in section 3.6. The phase θ can be arbitary and determines in which basis the detector is measuring the photon, also the choice of projection onto $|\,+\rangle$ is arbitary, since $|\,-\rangle$ can be obtained by a π - phase shift. After the projection we need to renormalize the resulting mirrror state with the complex number $\mathcal{N}(\beta)$ which ensures that $\int d^2\alpha W(\alpha,\alpha^*) = 1$. This implies dividing out the photon detection probability, eqn. (24), from the projected state. Hence $|\mathcal{N}(\beta)|^2$ is equivalent to $|\mathcal{N}_+|^{-2}$ from our previous discussion, eqn. (22).

The resulting projected and renormalized cantilever density matrix reads:

$$\hat{\rho}_p(t) = \frac{1}{4}|\mathcal{N}(\beta)|^2\Big(|\,\Phi_0\rangle\langle\Phi_0\,| + |\,\Phi_1\rangle\langle\Phi_1\,| + e^{-i\varphi(t)+i\theta}|\,\Phi_0\rangle\langle\Phi_1\,| + e^{i\varphi(t)-i\theta}|\,\Phi_1\rangle\langle\Phi_0\,|\Big) \tag{59}$$

We now calculate the Wigner function for the projected mirror state via the characteristic function $\chi(\lambda,\lambda^*)$. The Wigner function is the Fourier transform of the characteristic function:

$$W(\alpha,\alpha^*) = \frac{1}{\pi^2}\int d^2\lambda\, e^{\lambda^*\alpha-\lambda\alpha^*}\chi(\lambda,\lambda^*) \tag{60}$$

and the characteristic function is obtained from the density matrix via

$$\chi(\lambda,\lambda^*) = \mathrm{Tr}\{\hat{\rho}(t)\, e^{\lambda\hat{c}^\dagger-\lambda^*\hat{c}}\} = \mathrm{Tr}\{\hat{\rho}(t)\, e^{\lambda\hat{c}^\dagger}e^{-\lambda^*\hat{c}}\}\, e^{-|\lambda|^2/2} \tag{61}$$

The relation to eqn. (50) is established through $\alpha = x + ip$.

For our projected state, eqn. (59), computation of the characteristic function can easily be performed, since the coherent states $|\,\Phi_n\rangle$ are eigenstates of the annihilation operator. Using the trace relation $\mathrm{Tr}\{|\,\alpha\rangle\langle\beta\,|\} = \langle\beta\,|\,\alpha\rangle$ the characteristic function is obtained as

$$\begin{aligned}\chi(\lambda,\lambda^*) = \frac{1}{4}|\mathcal{N}|^2\, e^{-|\lambda|^2/2}\Big(&e^{\lambda\Phi_0^*-\lambda^*\Phi_0} + e^{\lambda\Phi_1^*-\lambda^*\Phi_1} + \\ &+ e^{-i\varphi(t)+i\theta}\langle\Phi_1\,|\,\Phi_0\rangle\, e^{\lambda\Phi_1^*-\lambda^*\Phi_0} + e^{i\varphi(t)-i\theta}\langle\Phi_0\,|\,\Phi_1\rangle\, e^{\lambda\Phi_0^*-\lambda^*\Phi_1}\Big)\end{aligned} \tag{62}$$

We now compute the Wigner function from the Fourier transform of the characteristic function, using relation (60). To this end, we compute seperately the four parts corresponding to the diagonal and off-diagonal elements of the density matrix. The total Wigner function is simply the sum of those parts. We present here the computation of W_{01} (with the phase factor $e^{i\theta}$ factored out, since it only represents a choice of our projection), the other three parts are obtained in an equivalent manner. To perform the calculation, we obtain Gaussian integrals of the form $\int dx e^{-x^2/c} = \sqrt{c/\pi}$ when using $\lambda = a + ib$ in eqn. (60) :

$$\begin{aligned}W_{01} &= \frac{|\mathcal{N}|^2}{4\pi^2}\, e^{-i\varphi}\langle\Phi_1\,|\,\Phi_0\rangle\int d^2\lambda\, e^{\lambda\Phi_1^*-\lambda^*\Phi_0}\, e^{\lambda^*\alpha-\lambda\alpha^*}\, e^{-|\lambda|^2/2} \\ &= \frac{|\mathcal{N}|^2}{4\pi^2}\, e^{-i\varphi}\langle\Phi_1\,|\,\Phi_0\rangle\int da\, db\, e^{(a+ib)\Phi_1^*-(a-ib)\Phi_0+(a-ib)\alpha-(a+ib)\alpha^*}\, e^{-\frac{1}{2}(a^2+b^2)} \\ &= \frac{|\mathcal{N}|^2}{4\pi^2}\, e^{-i\varphi}\langle\Phi_1\,|\,\Phi_0\rangle\int da\, db\, e^{-\frac{1}{2}\left(a^2-2a\left(\Phi_1^*-\Phi_0+\alpha-\alpha^*\right)\right)}\, e^{-\frac{1}{2}\left(b^2-2ib\left(\Phi_1^*+\Phi_0-\alpha-\alpha^*\right)\right)} \\ &= \frac{|\mathcal{N}|^2}{4\pi^2}\, e^{-i\varphi}\langle\Phi_1\,|\,\Phi_0\rangle\int d\tilde{a}\, d\tilde{b}\, e^{-\frac{1}{2}(\tilde{a}^2+\tilde{b}^2)}\, e^{\frac{1}{2}\left(\Phi_1^*-\Phi_0+\alpha-\alpha^*\right)^2}\, e^{-\frac{1}{2}\left(\Phi_1^*+\Phi_0-\alpha-\alpha^*\right)^2} \\ &= \frac{|\mathcal{N}|^2}{2\pi}\, e^{-i\varphi}\langle\Phi_1\,|\,\Phi_0\rangle\, e^{\frac{1}{2}\left(-4\Phi_1^*\Phi_0-4\alpha\alpha^*+4\Phi_1^*\alpha+4\Phi_0\alpha^*\right)}\end{aligned} \tag{63}$$

Writing out the inner product of coherent states as given by eqn. (152) and rewriting the phase as in eqn. (57), and performing the same computation for the other three parts of the Wigner

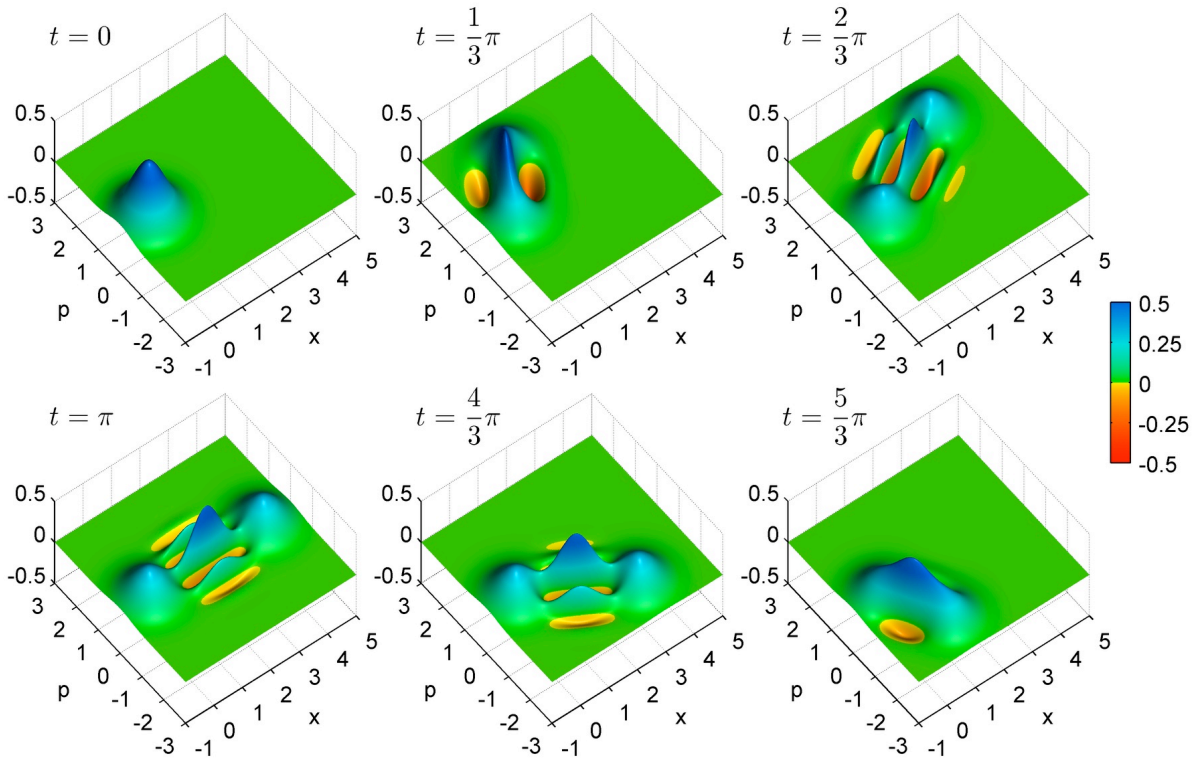

Figure 7: *The time evolution of the cantilever's projected Wigner function for $\beta = 0$, $\kappa = 2$ and $\hbar = \omega_c = m = 1$. When the photon enters the cavity, the Gaussian Wigner function is split into two maxima, with the second performing a periodic motion and returning to the original position after exactly a full mechanical rountrip. The two maxima represent the two possible cantilver states. The interference pattern inbetween shows that the two states are in a quantum superposition, the regions where the Wigner function is negative, shown in yellow and red, have no classical analogue.*

function, we get the final result for the total Wigner function:

$$\begin{aligned} W(\alpha,\alpha^*,\beta,t) &= W_{00} + W_{11} + e^{i\theta}W_{01} + e^{-i\theta}W_{10} \\ &= \frac{|\mathcal{N}|^2}{2\pi}\Big(\exp\left\{-2|\Phi_0|^2 - 2|\alpha|^2 + 2\alpha\Phi_0^* + 2\alpha^*\Phi_0\right\} \\ &\quad + \exp\left\{-2|\Phi_1|^2 - 2|\alpha|^2 + 2\alpha\Phi_1^* + 2\alpha^*\Phi_1\right\} \\ &\quad + \exp\left\{-i\varphi_0(t) + i\theta - \kappa^2(1-\cos\omega_c t) - \Phi_0\Phi_1^* - \Phi_0^*\Phi_1 - 2|\alpha|^2 + 2\alpha\Phi_1^* + 2\alpha^*\Phi_0\right\} \\ &\quad + \exp\left\{i\varphi_0(t) - i\theta - \kappa^2(1-\cos\omega_c t) - \Phi_0\Phi_1^* - \Phi_0^*\Phi_1 - 2|\alpha|^2 + 2\alpha\Phi_0^* + 2\alpha^*\Phi_1\right\}\Big) \end{aligned} \tag{64}$$

where $\Phi_n(t) = \beta e^{-i\omega_c t} + n\kappa(1 - e^{-i\omega_c t})$ and $\varphi_0(t) = \kappa^2(\omega_c t - sin(\omega_c t))$ as in eqns. (55) and (57), and the normalization factor is $|\mathcal{N}|^2 = |\mathcal{N}_+|^{-2}$ as in eqn. (22).

The Wigner function is characterized by two spatially separated Gaussians, given by the first two exponentials in eqn. (64), and by an interference pattern between those two, characterized by the last two exponentials. The time-dependence of the amplitudes $\Phi_1(t)$ and $\Phi_0(t)$ also

determines the time evolution of the Wigner function: After each full mechanical roundtrip the two Gaussians in the Wigner function overlap and no interference pattern occurs. On the other hand, at half a mechanical roundtrip the cantilever is maximally displaced and the Wigner function at that time is characterized by two maximally seperated Gaussians with a strong interference inbetween. This is illustrated in figure 7. It shows the quantum nature of the experiment, since in a purely classical experiment no interference between the two phase-space maxima would occur and the Wigner function would represent merely a statistical probability of finding the cantilever in either state.

The computation of the Wigner function in this section was performed for an initial pure cantilever state. However, the only effect of the initial state β is on the location and on the size of the Wigner function in phase space. The qualitative time-dependent effects are not altered if we change β.

4.2 Wigner Function for a Thermal Initial State

We now proceed with the case when the cantilever is initially in a mixed state, $\hat{\rho}_{th}$, due to finite temperature, and compute the corresponding Wigner function $\bar{W}(\alpha, \alpha^*, \bar{n}, t)$. As expressed in eqn. (45), we obtain the time evolved, temperature dependent density matrix by integrating the density matrix for the pure state over all possible initial coherent states β with a Gaussian weight of width $\bar{n} = 1/(e^{\hbar\omega_c/kT} - 1)$. From eqns. (60) and (61) we see that to obtain the corresponding Wigner function it is sufficient to simply perform the same procedure on the Wigner function for an initially pure state, eqn. (64). Note though that the factor $|\mathcal{N}|^2$ has to be excluded from the integral, since it represents only the proper renormalization of the state after a photon has been detected. For a thermal initial state, photon detection probabilities will be different and hence in that case a different renormalization factor is required, which is given by $|\bar{\mathcal{N}}(\bar{n})|^2 = \frac{1}{\pi\bar{n}} \int d^2\beta\, e^{-|\beta|^2/\bar{n}} |\mathcal{N}(\beta)|^2$.

For the calculations it is convenient to seperate the β - dependent part of the cantilever state from the rest, given by $\zeta(t)$:

$$\zeta(t) = \kappa(1 - e^{-i\omega_c t}) \tag{65}$$

such that we have

$$\begin{aligned} \Phi_0(t) &= \beta e^{-i\omega_c t} \\ \Phi_1(t) &= \Phi_0(t) + \zeta(t) \\ \frac{1}{2}|\zeta(t)|^2 &= \kappa^2(1 - \cos\omega_c t) \end{aligned} \tag{66}$$

We can now compute the cantilever's Wigner function corresponding to an initial thermal state. In terms of $\bar{n}$ and with the new renormalization factor $|\bar{\mathcal{N}}(\bar{n})|^2$ it is given by

$$\bar{W}(\alpha, \alpha^*, \bar{n}, t) = \frac{1}{\pi\bar{n}} \int d^2\beta\, e^{-|\beta|^2/\bar{n}} \frac{|\bar{\mathcal{N}}(\bar{n})|^2}{|\mathcal{N}(\beta)|^2} W(\alpha, \alpha^*, \beta, t) \tag{67}$$

The renormalization can easily be computed and is found to be

$$|\bar{\mathcal{N}}(\bar{n})|^2 = \frac{1}{\pi\bar{n}} \int d^2\beta |\mathcal{N}(\beta)|^2 = \frac{2}{1 + \cos(\varphi_0)\, e^{-\kappa^2(1+2\bar{n})(1-\cos\omega_c t)}} \tag{68}$$

The calculation for $\bar{W}_{01}$, corresponding to W_{01} from eqn. (63), can be performed by using

$$\frac{1}{\pi}\int d^2\beta\, e^{-a|\beta|^2+b\beta+c\beta^*} = \frac{1}{a}\, e^{\,b\,c/a} \tag{69}$$

for arbitary a, b and c. This relation can easily be checked by writing β in terms of its real and imaginary parts and performing the Gaussian integrals.

With the above relation and the definitions (66) for the amplitudes and (57) for the phase we obtain:

$$\begin{aligned}
\bar{W}_{01} &= \frac{|\bar{\mathcal{N}}|^2}{2\pi^2\bar{n}}\, e^{-i\varphi_0-\frac{1}{2}|\zeta|^2}\int d^2\beta\, e^{-|\beta|^2/\bar{n}}\, e^{-\Phi_0\Phi_1^*-\Phi_0^*\Phi_1-2|\alpha|^2+2\alpha\Phi_1^*+2\alpha^*\Phi_0} \\
&= \frac{|\bar{\mathcal{N}}|^2}{2\pi^2\bar{n}}\, e^{-i\varphi_0-\frac{1}{2}|\zeta|^2}\int d^2\beta\, e^{-|\beta|^2/\bar{n}}\, e^{-2|\beta|^2-\beta^*\zeta e^{i\omega_c t}-\beta\zeta^* e^{-i\omega_c t}} e^{-2|\alpha|^2+2\alpha\beta^* e^{i\omega_c t}+2\alpha^*\beta e^{-i\omega_c t}+2\alpha\zeta^*} \\
&= \frac{|\bar{\mathcal{N}}|^2}{2\pi^2\bar{n}}\, e^{-i\varphi_0-\frac{1}{2}|\zeta|^2}\int d^2\beta\, e^{-|\beta|^2(1+2\bar{n})/\bar{n}}\, e^{\beta e^{-i\omega_c t}(2\alpha^*-\zeta^*)+\beta^* e^{i\omega_c t}(2\alpha-\zeta)}\, e^{-2|\alpha|^2+2\alpha\zeta^*} \\
&= \frac{|\bar{\mathcal{N}}|^2}{2\pi(1+2\bar{n})}\, e^{-i\varphi_0-\frac{1}{2}|\zeta|^2}\, e^{-2|\alpha|^2+2\alpha\zeta^*}\, e^{\frac{\bar{n}}{(1+2\bar{n})}(4|\alpha|^2+|\zeta|^2-2\alpha\zeta^*-2\alpha^*\zeta)} \\
&= \frac{|\bar{\mathcal{N}}|^2}{2\pi(1+2\bar{n})}\, e^{-i\varphi_0}\, e^{-\frac{1}{(1+2\bar{n})}(2|\alpha|^2+\frac{1}{2}|\zeta|^2-2(\bar{n}+1)\alpha\zeta^*+2\bar{n}\alpha^*\zeta)}
\end{aligned} \tag{70}$$

Performing the same calculation for the other three parts of the Wigner fucntion we obtain the final result:

$$\begin{aligned}
\bar{W}(\alpha,\alpha^*,\bar{n},t) &= \bar{W}_{00}+\bar{W}_{11}+e^{i\theta}\bar{W}_{01}+e^{-i\theta}\bar{W}_{10} \\
&= \frac{|\bar{\mathcal{N}}(\bar{n})|^2}{2\pi(1+2\bar{n})}\left(\exp\left\{-\frac{1}{1+2\bar{n}}2|\alpha|^2\right\}\right. \\
&\quad + \exp\left\{-\frac{1}{1+2\bar{n}}\left(2|\alpha|^2+2|\zeta|^2-2\alpha\zeta^*-2\alpha^*\zeta\right)\right\} \\
&\quad + \exp\left\{-i\varphi_0+i\theta-\frac{1}{1+2\bar{n}}\left(2|\alpha|^2+\frac{1}{2}|\zeta|^2-2(\bar{n}+1)\alpha\zeta^*+2\bar{n}\alpha^*\zeta\right)\right\} \\
&\quad \left. + \exp\left\{i\varphi_0-i\theta-\frac{1}{1+2\bar{n}}\left(2|\alpha|^2+\frac{1}{2}|\zeta|^2+2\bar{n}\alpha\zeta^*-2(\bar{n}+1)\alpha^*\zeta\right)\right\}\right)
\end{aligned} \tag{71}$$

with $\zeta(t) = \kappa(1-e^{-i\omega_c t})$, $\frac{1}{2}|\zeta(t)|^2 = \kappa^2(1-\cos\omega_c t)$, $\varphi_0(t) = \kappa^2(\omega_c t - sin(\omega_c t))$ and $\bar{n} = 1/(e^{\hbar\omega_c/kT}-1)$.

From the above result we see that the effect of finite temperatures is to widen the Gaussian maxima and at the same time to suppress the interference terms between them. Thermal averaging thus results in a Wigner function that is spread out over all phase space and is highly washed out, since all possible cantilever coherent states and the corresponding quantum interferences are averaged over. This can be seen in figure 8.

It has been argued by Bernád et al. [39] that at high temperatures, the Wigner function becomes completely independent of $\hbar$ and thus no quantum effects will be observable, since the Wigner function will be equivalent to a classical phase space probability distribution. Indeed, in the high temperature limit $kT >> \hbar\omega_c$, the factor $\kappa^2\bar{n}$ becomes independent of $\hbar$ if we plug

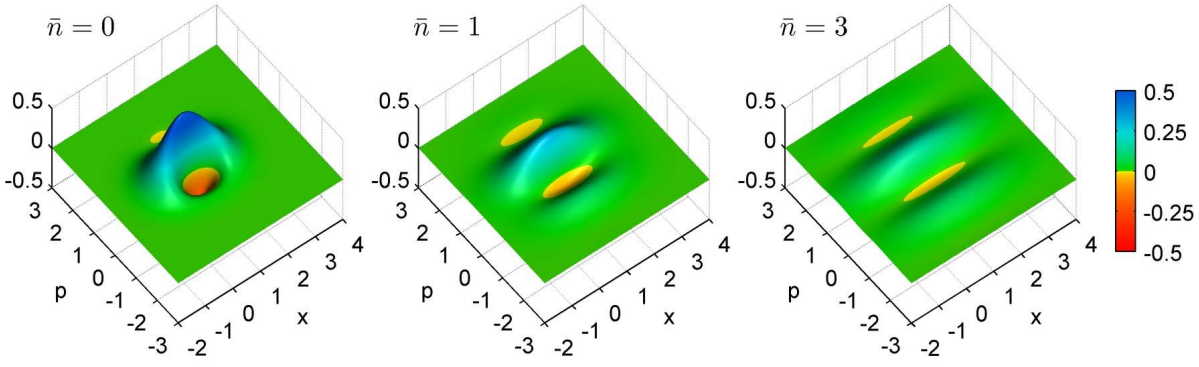

Figure 8: *The effect of finite temperatures on the cantilever's projected Wigner function, at time* $t = \pi$ *for* $\kappa = 1/\sqrt{2}$ *(*$\hbar = \omega_c = m = 1$*). The peaks and the negative regions of the Wigner function can be seen to quickly wash out with increasing thermal phonon occupations.*

in the definition for the optomechanical coupling, eqn. (2), and expand $\bar{n} \approx kT/\hbar\omega_c$. However, from the above calculation we see that apart from factors $\kappa^2\bar{n}$ the averaged Wigner function also contains other combinations of κ and $\bar{n}$ in its interference terms. Thus, in the high temperature limit the thermally averaged Wigner function (71) is still a function of $\hbar$. It remains a quantum quantity even in this limit.

4.3 Negativity in Phase Space as a Measure of Non-Classicality

We have shown that the Wigner function cannot be considered to be completely classical even in the thermal case. However, we have already noted in the end of section 3.10 that interpreting and quantifying non-classical effects unambigiously at higher temperatures poses a challenge. For pure states we were able to use the relation between visibility and entropy to quantify the entanglement between photon and cantilever. But determining entanglement between mixed states is a very difficult challenge and still an important open problem in quantum information science. Although in some related work entanglement at finite temperatures was considered [16, 14, 13, 12], we follow here a different route and use the negativity of the thermally averaged Wigner function as a lower bound for the non-classicality of the cantilever.

As we have noted, if a Wigner function is negative it cannot have any classical analogue. It is thus convenient to quantify the total negativity of the Wigner function [36]:

$$N = \int dx \int dp \Big(|W(x,p)| - W(x,p) \Big) = \int dx \int dp \, |W(x,p)| - 1. \tag{72}$$

For our case, as long as part of the Wigner function is negative, the cantilever is clearly in a non-classical superposition state. Thus we use the negativity to put a bound on the tolerable temperatures for the interpretation of the cantilever state to be unambiguously non-classical. Figure 9 shows the numerical computation of the negativity at $t = \pi/\omega_c$ for different values of κ and $\bar{n}$.

The negativity of the Wigner function at half a mechanical round trip decreases rapidly with $\bar{n}$ and is also dependent on κ . In practice, this implies that $\bar{n}$ must of order 1 for $\kappa \approx 1$ if we want to unambiguously proof a quantum superposition. If the temperature is higher, statistical

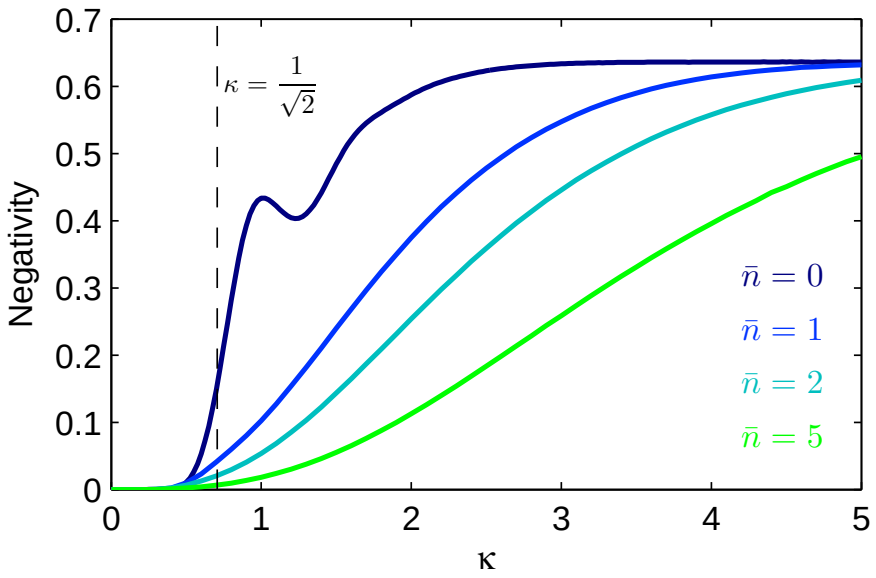

Figure 9: *Negativity of the projected cantilever state as a function of coupling constant κ for several different mean phonon numbers, $\bar{n}$. At higher temperatures, the negativity is strongly reduced, showing that for $\kappa \approx 1/\sqrt{2}$ cooling close to the ground state would be neccessary for an unambiguous non-classical interpretation of the experimental outcome. For higher κ larger initial temperatures would be tolerable. The oscillations present when $\bar{n} = 0$ are due to a phase shift in the interference terms when it overlaps with the two maxima of the states.*

averaging over many experimental runs will mask the quantum effects. Note that somewhat higher values of $\bar{n}$ are tolerable for higher κ, but increasing the optomechanical coupling is a very difficult experimental challenge.

With the negativity of the Wigner function we have obtained a quantification of the non-classicality of the experimental outcome. It serves as a lower bound, since a quantum superposition is expected to be present even if the cantilever is not cooled to the ground state. But since we cannot distinguish statistical averaging from the quantum effects, we have to rely on the above results in order to make the claim of a quantum superposition of the cantilever to be unambiguous.

5 Decoherence

In the preceeding discussions we have assumed that the system is fully decoupled from any external effects. In practice, the experimental setup will inevitably interact with its environment. The environmental states will entangle with the states of the cantilever and will thus obtain information on the system. In this way, a monitoring of the cantilever states takes place and destroys quantum superpositions. It is not necessary that the environmental states are being read out, the information storage in the environment is sufficient. This is known as decoherence, and poses an experimental challenge for all investigations of quantum effects at large scales [40, 41, 42, 43, 44]. Here we are concerned about the desctruction of quantum coherence in the cantilever states due to its coupling to other degrees of freedom. We will discuss how decoherence of the cantilever can be described and will estimate the effect of different physical environments on the quantum superposition.

When considering a closed system comprising both the system and the entire environment with which it interacts (the so-called bath if it is in a thermal equilibrium state), one can apply the Hamiltonian formulation and study the unitary time evolution. Such a description applies to the full system including all degrees of freedom of the bath and all internal correlations. However, it is practically impossible to keep track of the bath, and we are only interested in the few degrees of freedom of the system under investigation, the reduced system. We would thus like to find effective time evolution equations for our reduced system which incorporate the effects of the environment without keeping track of the environment itself. We are led to an open quantum system description in which the bath is integrated out. Such a reduced system is described via its reduced density matrix, which is obtained from the full density matrix including all degrees of freedom by tracing out the bath states. The time evolution of the reduced density matrix is governed by a differential equation, called the master equation.

Obtaining a master equation that describes the time evolution of a system including the effect of an external bath can be done in different ways [45, 46, 47, 48, 49, 50]. One possibility is to start from a phenomenological Hamiltonian of the full system, which includes the bath and all interactions, and subsequently integrate out all states of the bath. With some approximations it is possible to derive a master equation for the reduced system in this way. Another approach is to take the general mathematical form of a master equation for an open quantum system and choose the specific terms on physical grounds. In the next chapters, we will briefly outline those two approaches and use them to find the decoherence timescale for the cantilever when coupled to the environment.

5.1 Timescales in an Open Quantum System

For the study of open quantum systems it is of ample importance to indentify the timescales involved. The validity of master equations that describe an open quantum system usually depends on a particular seperation between those timescales, which enables the use of certain approximations. The three main timescales for open quantum systems are the following [47, 51]: The dissipation timescale $\tau_{diss} = 1/\gamma$ is a characteristic timescale for the open system to reach equilibrium, where γ is the dissipation rate. τ_{sys} is a typical system timescale on which the free system evolves, in our case it is approximately an oscillation period $2\pi/\omega_c$. The typical timescale of internal bath correlations is given by τ_{bath}, which governs the lifetime of "memory effects" in the bath. We expect it to be on the order of $\hbar/kT_b$, where T_b is the temperature of the bath

In a very well isolated system the interaction with the bath is weak and thus the dissipation time is relatively large. However, even for very slow thermalization with the environment quantum superpositions in the system can be destroyed rapidly, since the environment effectively measures the state of the system. This loss of quantum coherence happens on the decoherence timescale τ_{dec} which can be much smaller than τ_{diss} in most cases. Our goal is to find τ_{dec} for the experiment at hand for different environmental influences and to investigate the validity of the various approximations used.

The specifications of the experiment are the following: The cantilever's frequency is on the order of $\omega_c = 2\pi \times 1\text{kHz}$. Such a kHz silicon nano-oscillator can currently be fabricated with a Q-factor of ca. $Q = 10^5$, which gives us the dissipation rate $\gamma = \omega_c/Q \sim 0.1\text{Hz}$. The bath can be cooled down to about $T_b = 1mK$, or even lower. Thus the characteristic timescales in our experiment are the following:

$$\begin{aligned} \tau_{diss} &\sim 10\, s \\ \tau_{sys} &\sim 10^{-3} s \\ \tau_{bath} &\sim 10^{-8} s \end{aligned} \tag{73}$$

Hence the experiment takes place in the regime

$$\tau_{bath} \ll \tau_{sys} \ll \tau_{diss} \tag{74}$$

Such a seperation of timescales allows us to use Markovian master equations to describe the influence of a bosonic bath on our system. In the following, we present a general mathematical structure of Markovian master equations.

5.2 The Lindblad Form of a Master Equation

The time evolution of a density matrix $\hat{\rho}_{SB}(t)$ describing a closed system of the bath and the actual setup is given by a unitary operator $\hat{U}(t)$. As we said before, such a unitary evolution is not possible for an open system which consists of only a few degrees of freedom. Instead, the time evolution of a reduced density matrix describing an open system, $\hat{\rho}(t)$, is governed by a so-called dynamical map $\mathcal{V}(t)$:

$$\hat{\rho}(t) = \mathcal{V}(t)\hat{\rho}(0) \tag{75}$$

The difference to a unitary evolution is schematically represented in figure 10. Such a dynamical map has to be a completely positive, trace preserving quantum operation in order to allow for the correct physical interpretation of $\hat{\rho}(t)$ as the density matrix. If, additionally, we assume that our reduced system can be described in a Markovian regime where memory effects of the environment are neglected (i.e. $\tau_{bath} \ll \tau_{sys}$), the dynamical map has also the semigroup property $\mathcal{V}(t_1)\mathcal{V}(t_2) = \mathcal{V}(t_1 + t_2)$ [51]. Such a semigroup can usually be generated by a linear map $\mathcal{L}$ [52]:

$$\mathcal{V} = e^{\mathcal{L}t}$$

which yields the general master equation for the reduced density matrix of the system :

$$\frac{d\hat{\rho}}{dt} = \mathcal{L}\hat{\rho} \tag{76}$$

$\mathcal{L}$ is a superoperator (an operator whose action on other operators yields an operator) which generalizes a Liouville operator from classical mechanics. Linblad has shown that the most

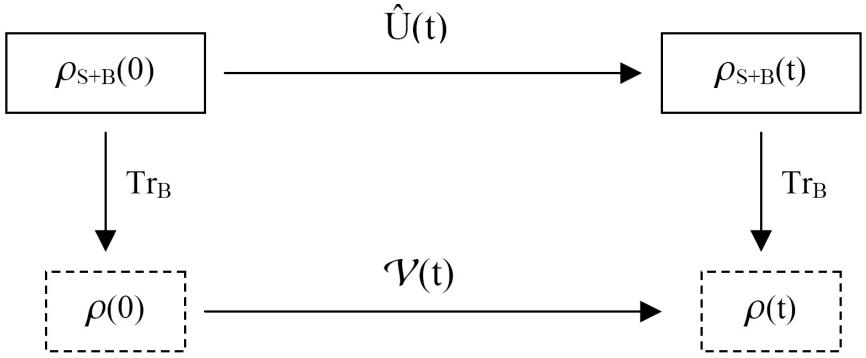

Figure 10: *The action of a dynamical map $\mathcal{V}(t)$ on the reduced density matrix $\hat{\rho}(0)$. The unitary evolution $\hat{U}(t)$ acts on the total system $\hat{\rho}_{S+B}$.*

general form of such a Markovian master equation describing the time evolution of a reduced system is given by [53] :

$$\frac{d\hat{\rho}}{dt} = -\frac{i}{\hbar}[\hat{H}, \hat{\rho}] + \sum_j (\hat{L}_j \hat{\rho} \hat{L}_j^\dagger - \frac{1}{2}\hat{L}_j^\dagger \hat{L}_j \hat{\rho} - \frac{1}{2}\hat{\rho}\hat{L}_j^\dagger \hat{L}_j) \tag{77}$$

Here, $\hat{H}$ is the Hamiltonian (with some possible renormalization of the frequency due to the interaction with the bath) and the first term represents the unitary part of the evolution. $\hat{L}_j$ are so-called jump operators which incorporate the influence of the bath on the system. They have to be chosen when trying to model an open system, or derived from a phenomenological interaction Hamiltonian. The proof by Lindblad for eqn. (77) assumes that the operators $\hat{L}_j$ and the Hamiltonian are bound operators, but in physical systems they are usually not. His theorem was extended to unbound operators by Holevo [54]. Interestingly, all physical master equations are of the Lindblad form (77) or can be brought into the form by slight modifications, even those obtained from phenomenologial and microscopic models [55, 56, 57, 51]. Thus we assume that a realistic master equation should be related to the above form.

We can understand the various terms in the Lindblad equation in the following way: When a jump takes place, the term proportional to $\hat{L}_j \hat{\rho} \hat{L}_j^\dagger$ changes the state of the system into a new state which is goverened by the interaction to the bath. The other terms, $-\frac{1}{2}\hat{L}_j^\dagger \hat{L}_j \hat{\rho} - \frac{1}{2}\hat{\rho}\hat{L}_j^\dagger \hat{L}_j$, are important for the case when no jump takes place. Without a jump we gain some information on the state of the system, since the probability to find the system in its original state is higher. Thus those terms incorporate a proper probability renormalization of the system state in the case when no jump takes place.

It has been common practice when dealing with decoherence phenomena in quantum optics to start with the Lindblad equation (77) and use appropriately chosen jump operators to model an interaction with the environment [58]. We shall adapt this approach but will also justify our choices for the jump operators and relate the resulting master equations to those obtained from microscopic, or rather phenomenological, models.

5.3 Effect of Dissipation on Quantum Coherence

Any dissipative effects in the system will lead inevitably to decoherence. In this section we calculate in detail the effect of damping of the cantilever and compute the decoherence time. The damping occurs in our case by coupling of the fundamental cantilever mode to other modes and also to the bulk which it is attached to. All these modes we consider as the bath. Here we assume that it is effectively at zero temperature, so that it can only absorb phonons from the cantilever. Therefore we investigate a dissipative process only which doesn't include thermal fluctuations. The advantage is that the problem can be solved exactly for the system at hand.

We start our discussion by using our system Hamiltonian

$$\hat{H} = \hbar\omega_a(\hat{a}^\dagger\hat{a} + \hat{b}^\dagger\hat{b}) + \hbar\omega_c\,\hat{c}^\dagger\hat{c} - \kappa\,\hbar\omega_c\,\hat{a}^\dagger\hat{a}(\hat{c} + \hat{c}^\dagger) \tag{78}$$

which we insert into the Linblad equation (77) and choose the only jump operator to be

$$\hat{L} = \sqrt{\gamma}\,\hat{c} \tag{79}$$

The operator $\hat{c}$ annihilates a phonon in the cantilever, which happens at the rate γ. This phonon dissipates into the bath. There is also no back-action from the bath, so no phonon can be created in the cantilever. Thus the interaction with the bath causes only an amplitude damping of the cantilever's oscillation. The resulting master equation reads

$$\frac{d\hat{\rho}(t)}{dt} = -\frac{i}{\hbar}[\hat{H}, \hat{\rho}] + \frac{\gamma}{2}\left(2\,\hat{c}\,\hat{\rho}\,\hat{c}^\dagger - \hat{c}^\dagger\hat{c}\,\hat{\rho} - \hat{\rho}\,\hat{c}^\dagger\hat{c}\right) \tag{80}$$

Concerning the validity of this master equation we note that it can be derived from a specific interaction Hamiltonian that couples the bath to the system, which we will show in our discussion of finite temperature baths, section 5.4. Thus our choice for the jump operator indeed yields a physically justified master equation for a dissipative oscillator.

The master equation (80) can be solved exactly for the states of the full photon-cantilever system. The solutions to the Hamiltonian part and to the dissipative part of the equation are known and are given in terms of coherent states. Therefore, we can construct the full solution by combining the two separate solutions in a proper way. The details of the calculations are found in appendix A.5.

Here we quote the final result for the interferometric visibility, when the cantilever is initially in a thermal state with mean phonon number $\bar{n}$:

$$v(\gamma, \bar{n}, t) = \exp\left\{-D(\gamma, t) - \frac{\kappa^2\omega_c^2}{2\left(\omega_c^2 + \frac{\gamma^2}{4}\right)}(1 + 2\bar{n})\left(1 + e^{-\gamma t} - 2e^{-\frac{\gamma}{2}t}\cos\omega_c t\right)\right\} \tag{81}$$

with $D(\gamma, t)$ given by

$$D(\gamma, t) = \frac{\kappa^2\omega_c^2}{2\left(\omega_c^2 + \frac{\gamma^2}{4}\right)}\left\{\gamma t + 1 - e^{-\gamma t} + \frac{\gamma^2\left(e^{-\frac{\gamma}{2}t}\cos\omega_c t - 1\right) - 2\gamma\omega_c\,e^{-\frac{\gamma}{2}t}\sin\omega_c t}{\omega_c^2 + \frac{\gamma^2}{4}}\right\} \tag{82}$$

The term $D(\gamma, t)$ is responsible for the decoherence of the cantilever, and it thus reduces the interferometric visibility. If the cantilever superposition has completely decohered, no interference visibility would be possible since the bath has effectively measured the system. The

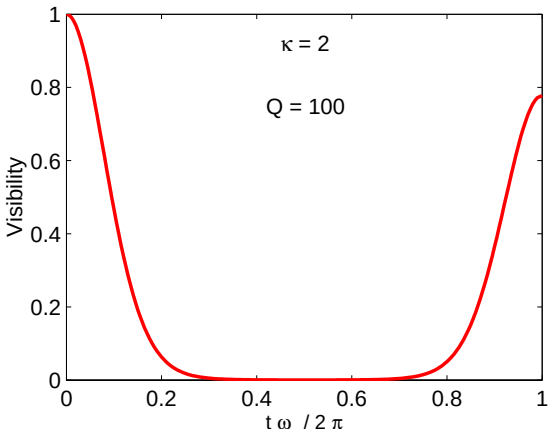

Figure 11: *Interferometric visibility in the presence of strong mechanical damping, according to eqn.* (84) *with* $\gamma = \omega_c/Q$ *. The experimental goal is to achieve much higher values of* Q*.*

second term in the above equation for the visibility (81) stems from the overlap between the two possible coherent states of the cantilever. The γ - dependence there is due to the damping of the states. Note that the visibility reduces in the limit $\gamma \to 0$ to the correct non-dissipative result, eqn. (46).

We emphasize that the thermal averaging which we performed here is due to the finite phonon occupation number in the cantilever, whereas the bath temperature is still zero. Thus we implicitly assume a seperation of temperatures: the finite initial temperature of the cantilever and the zero temperature of the bath. Those two temperatures can indeed be seperated by optical Stokes and anti-Stokes processes acting on the cantilever's center of mass mode, such as in optical cooling [7, 8, 9].

In practice, one will be interested in reducing the interaction with the bath as much as possible. We have noted in section 5.1 that the cantilever can be expected to have a damping rate on the order of $\gamma = 0.1$Hz. The first visibility revival peak will be after $t = 2\pi/\omega_c = 1$ms. Thus we are in the regime

$$\gamma << \omega_c \,, \qquad \gamma t << 1 \tag{83}$$

and we can expand the equation for the interferometric visibility, eqn. (81). To first order in the approximation we get

$$v(\gamma, \bar{n}, t) \approx \exp\left\{-\kappa^2\left(\gamma t - \frac{\gamma}{\omega_c}\sin\omega_c t\right) - \kappa^2\left(1+2\bar{n}\right)\left(1-\frac{1}{2}\gamma t\right)\left(1-\cos\omega_c t\right)\right\} \tag{84}$$

After a full mechanical period, $t = 2\pi/\omega_c$, the second term vanishes. But rather than having a complete revival of the interferometric visibility, we see that in the damped case the visibility has decohered to

$$v(\gamma, \bar{n}, t = 2\pi/\omega_c) \approx e^{-\kappa^2 2\pi\gamma/\omega_c} \tag{85}$$

Therefore, decoherence takes place in the weak coupling limit at a rate

$$\tau_{dec}^{-1} = \kappa^2\gamma \tag{86}$$

which is close to the dissipation rate γ. This is not surprising, since the only way the environment can gain information on the state of the system is via dissipation. Therefore, the state can only

significantly decohere once a phonon has leaked out which happens after the time (for $\kappa \sim 1$)

$$\tau_{dec}^{(\gamma)} = 10s \tag{87}$$

Since the experiment takes place on the order of ms, decoherence due to dissipation will not pose a significant problem.

In terms of the spatial seperation of the two superposed states, given in eqn. (12), the decoherence rate can be written as

$$\tau_{dec}^{-1} = \frac{\gamma\, m\, \omega_c}{8\hbar}(\Delta x)^2 \tag{88}$$

Thus we have found the decoherence rate of the cantilever due to dissipation into a zero temperature bath by solving exactly a model for damping. The solutions generalize our previous results for the states of the system to include dissipation. The resulting decoherence is governed by the dissipation rate, and it is independent of the initial temperature of the cantilever. Also, in our case decoherence only depends on the spatial seperation of the states in question, but not on the exact details of the driving by the photon. These results will be helpful in our subsequent discussion of decoherence at finite bath temperatures.

5.4 Bosonic Bath in the Born-Markov Approximation

At finite temperatures, we expect the decoherence process to be accelerated while the dissipation should remain basically the same as calculated in the previous section. This is due to the fact that thermal fluctuations will allow the bath to obtain information on the system more rapidly, but there is no extra energy transfer which could lead to more dissipation. Thus, what we expect is that the decoherence factor $D(\gamma, t)$ from the previous section (eqn. (82)) will have to be modified to include finite temperature effects of the bath.

Naively, we can anticipate that the decoherence factor might have to be modified in the following way: $D \to \bar{N} D$, where $\bar{N}$ is the average thermal occupation number of bath phonons at resonance with the cantilever. Thermal phonons in the bath should accelerate the decoherence process since they are responsible for thermal fluctuations, and indeed we will show from studies of a master equation that the above estimate holds well.

Instead of choosing specific jump operators we are interested in deriving a master equation from a phenomenological interaction model which yields us the proper coefficients. Here we will briefly outline the approximations used in the derivations and state the result in the most general form. We note that the same result can be derived in many ways as can be found in the literature on quantum optics and open quantum systems [49, 59, 60, 51, 61]. We will mostly follow the route used for quantum optical setups.

The usual assumption, which holds very well in our case (see section 5.1), is a memoryless bath so that the interaction at one time is independent of the interaction at a later time. That is to say, the correlations in the bath are very short-lived. This is called the *Markovian approximation* and allows us to derive a master equation for the open system. A second assumption that is invoked is a weak coupling between the bath and the system. It allows to treat the evolution of the full system perturbatively and truncate it after the second order in the interaction, which is the usual *Born approximation*.

To be more specific, let us consider the density matrix $\hat{\rho}_{SB}(t)$ describing the states of the system and the bath. The evolution is goverend by a Hamiltonian of the general form

$$\hat{H} = \hat{H}_S + \hat{H}_B + \hat{H}_{int} \tag{89}$$

with the system, the bath and the interaction Hamiltonians, respectively. In the interaction picture we can therefore write the evolution of the full density matrix as

$$\frac{d\hat{\rho}_{SB}(t)}{dt} = -\frac{i}{\hbar}[\hat{H}_{int}(t), \hat{\rho}_{SB}(t)] \tag{90}$$

By formal integration and insertion of the result back into the above equation we can write it as

$$\frac{d\hat{\rho}_{SB}(t)}{dt} = -\frac{i}{\hbar}[\hat{H}_{int}(t), \hat{\rho}_{SB}(0)] - \frac{1}{\hbar^2}\int_0^t ds[\hat{H}_{int}(t), [\hat{H}_{int}(s), \hat{\rho}_{SB}(s)]] \tag{91}$$

This is still an exact result and we have not invoked any approximations.

We are interested in a master equation for the density matrix of the system alone, with the bath degrees of freedom traced out:

$$\hat{\rho}(t) = \mathrm{Tr}_B[\hat{\rho}_{SB}(t)] \tag{92}$$

We now perform the trace in (91) and use the assumption that the system and the bath are initially uncorrelated, i.e. $\hat{\rho}_{SB}(0) = \hat{\rho}(0) \otimes \hat{\rho}_B(0)$. This yields

$$\frac{d\hat{\rho}(t)}{dt} = -\frac{i}{\hbar}\mathrm{Tr}_B\left\{[\hat{H}_{int}(t), \hat{\rho}(0) \otimes \hat{\rho}_B(0)]\right\} - \frac{1}{\hbar^2}\mathrm{Tr}_B\left\{\int_0^t ds[\hat{H}_{int}(t), [\hat{H}_{int}(s), \hat{\rho}_{SB}(s)]]\right\} \tag{93}$$

This is still a formal integro-differential equation. However, we can use the Born and the Markov approximations to obtain the general form of a time-local master equation. For a large bath, the bath states will remain unchanged in time whereas the system density matrix will evolve. Any correlations between those two will be on the order of the interaction $\hat{H}_{int}$. The Born approximation thus allows us to replace $\hat{\rho}_{SB}(s)$ in the above expression by $\hat{\rho}(s) \otimes \hat{\rho}_B(0)$. However, since this quantity appears in the integral over all past times, the final density matrix will depend on all previous states of the system. This happens because the interaction allows the reservoir to obtain and store information on the system. In the Markovian approximation we neglect this dependence and set $\hat{\rho}(s) \approx \hat{\rho}(t)$. This can be done if the time correlations between the bath operators which are coupled to the system (i.e. appear in $\hat{H}_{int}$) are delta peaked, so that we get an additional $\delta(t-s)$ when computing terms like $\mathrm{Tr}_B[\rho_B \hat{d}_j^\dagger(t)\hat{d}_j(s)]$. In fact, the entire influence of the bath on the system enters through such correlation functions alone [62].

With the Born-Markov approximation we can now write the master equation for the system's density matrix in the most general form:

$$\frac{d\hat{\rho}(t)}{dt} = -\frac{i}{\hbar}\mathrm{Tr}_B\left\{[\hat{H}_{int}(t), \hat{\rho}(0) \otimes \hat{\rho}_B(0)]\right\} - \frac{1}{\hbar^2}\mathrm{Tr}_B\left\{\int_0^t ds[\hat{H}_{int}(t), [\hat{H}_{int}(s), \hat{\rho}(t) \otimes \hat{\rho}_B(0)]]\right\} \tag{94}$$

To be more specific, one needs a model for the interaction between system and the bath, so that the above integral can be computed.

The usual bath model assumes that the bath consists of infinitely many harmonic oscillators, which couple linearly to the system under investigation. For a finite temperature bath, one assumes that it is initially in a thermal equilibrium state and that it will not be significantly altered by the interaction due to its vast size. Thus the bath will have a thermal density matrix with a mean thermal phonon number (taken at resonance with the cantilever) $\bar{N} =$

$1/(e^{\hbar\omega_c/kT_b}-1)$, where T_b is the bath temperature. The interaction Hamiltonian is taken to be of the form

$$\hat{H}_{int} = (\hat{c}+\hat{c}^\dagger)\sum_j \hbar\lambda_j\,(\hat{d}_j+\hat{d}_j^\dagger) \tag{95}$$

where $\hat{c}$ acts on the center of mass mode of the cantilever, $\hat{d}_j$ are bosonic bath operators, and λ_j are coupling coefficients between the bath modes j and the cantilever. This interaction Hamiltonian assumes a linear coupling between the position operator of the cantilever and the position operators of the bath modes, thus representing a force acting on the cantilever. One can easily generalize the interaction to include linear coupling between momentum operators as well.

In the so-called rotating frame approximation ("RWA") the terms $\hat{c}\hat{d}$ and $\hat{c}^\dagger\hat{d}^\dagger$ are neglected, since they are not energy conserving on short timescales. This is common practice in quantum optical systems and is valid when the frequency of the system is much larger than the damping rate, which holds for a weak coupling regime [48]. In the RWA, the interaction Hamiltonian (95) becomes

$$\hat{H}_{int} = \sum_j \hbar\lambda_j\,(\hat{c}\,\hat{d}_j^\dagger + \hat{c}^\dagger\,\hat{d}_j) \tag{96}$$

Such an interaction Hamiltonian together with a thermal bath density matrix can be used in eqn. (94) to derive a proper master equation. One then encounters bath correlation functions of the form $\mathrm{Tr}_B[\rho_B\hat{d}_j^\dagger(t)\hat{d}_j(s)]$, as we have mentioned before. These can be computed when invoking a Markovian approximation, such that they become proportional to $\delta(t-s)$ [49, 59, 60]. One also needs to make an assumption on the various coupling constants λ_j. The usual procedure is to take a so-called "Ohmic bath" in which all bath modes act effectively as a Langevin damping force on the system that is proportional to the system's velocity.

Here we quote the resulting Markovian master equation, first obtained by Agarwal [63] and later, using path integral techniques by Caldeira and Leggett [46]:

$$\frac{d\hat{\rho}}{dt} = -\frac{i}{\hbar}[\hat{H}_{ren},\hat{\rho}] - i\frac{\gamma}{\hbar}[\hat{x},\{\hat{p},\hat{\rho}\}] - \frac{D(T_b)}{\hbar^2}[\hat{x},[\hat{x},\hat{\rho}]] \tag{97}$$

where $\{\,,\}$ is the anti-commutator, $\hat{H}_{ren}$ is the system Hamiltonian with a slightly renormalized frequency and $\hat{x}$ and $\hat{p}$ are the position and momentum operators of the system, respectively. The coefficient γ is the damping coefficient as we used in the previous section, whereas $D(T_b)$ is a diffusion coefficient given by

$$D(T_b) = m\gamma\hbar\omega_c\coth\frac{\hbar\omega_c}{2kT_b} \tag{98}$$

We will show in the next section that it is a generalization of the decoherence factor (82) which includes the effects of finite bath temperatures.

We note that with the RWA, the above master equation can also be written in the form common in quantum optical literature [49, 59, 60]:

$$\frac{d\hat{\rho}}{dt} = -\frac{i}{\hbar}[\hat{H},\hat{\rho}] + \frac{\gamma}{2}\Big\{(\bar{N}+1)(2\hat{c}\hat{\rho}\hat{c}^\dagger - \hat{c}^\dagger\hat{c}\hat{\rho} - \hat{\rho}\hat{c}^\dagger\hat{c}) + \bar{N}(2\hat{c}^\dagger\hat{\rho}\hat{c} - \hat{c}\hat{c}^\dagger\hat{\rho} - \hat{\rho}\hat{c}\hat{c}^\dagger)\Big\} \tag{99}$$

For $\bar{N}=0$, i.e. for a zero temperature bath, the above master equation reduces to the one we used in the previous section, eqn. (80).

5.5 Decoherence Induced by Thermal Fluctuations

When discussing decoherence due to dissipation, we have found in eqn. (88) that in our system the decoherence rate depends on the spatial seperation of the two superposed states, Δx. The details of how this superposition state is created, in our case by the photon pressure in the Hamiltonian evolution, can be neglected and we can simply assume that a superposition state is already given. This assumption helps us to quickly obtain an estimate for the decoherence rate at finite temperatures, without explicitly solving for the states of the system. The result will be slightly higher than the actual rate since Δx is the maximal displacement which in reality is only present at every half mechanical period.

Note that the dissipative term $-i\frac{\gamma}{\hbar}[\hat{x},\{\hat{p},\hat{\rho}\}]$ in (97) is independent of $\hbar$, whereas the diffusion term $-\frac{D(T_b)}{\hbar^2}[\hat{x},[\hat{x},\hat{\rho}]]$ in the high temperature limit scales like $\hbar^{-1}$. Therefore, we can safely assume that the diffusion term will dominate over the damping term when considering a relatively large object, and we are left with

$$\frac{d\hat{\rho}}{dt} = -\frac{D(T_b)}{\hbar^2}[\hat{x},[\hat{x},\hat{\rho}]] \tag{100}$$

We can easily evaluate this differential equation in the position representation with $\rho(x,x',t) = \langle x\,|\hat{\rho}(t)|\,x'\rangle$:

$$\frac{d\rho(x,x',t)}{dt} = -\frac{D(T_b)}{\hbar^2}(x-x')^2\rho(x,x',t) \tag{101}$$

Here, x and x' refer to the positions of the two superposed states in question, thus we have $(x-x')^2 = (\Delta x)^2$. The solution to the above equation is

$$\rho(x,x',t) = \rho_0\, e^{-\frac{D(T_b)}{\hbar^2}(\Delta x)^2 t} \tag{102}$$

Thus off-diagonal terms in the position representation decay with a rate

$$\tau_{dec}^{-1} = \frac{D(T_b)(\Delta x)^2}{\hbar^2} \tag{103}$$

This is the decoherence rate due to a finite temperature bath and is a generalization of our previous result (88). Note that taking the limit $T_b \to 0$ for the above decoherence rate indeed gives $\tau_{dec}^{-1} = \gamma m\omega_c(\Delta x)^2/\hbar$. It is equivalent to what we found in the previous section in eqn.(88), up to a numerical factor of order unity which can be absorbed in the damping term γ.

For the high temperature limit $kT_b \gg \hbar\omega_c$ we find the decoherence rate in terms of the system parameters (using eqn. (12)) to be

$$\tau_{dec}^{-1} = \frac{2\gamma m k T_b(\Delta x)^2}{\hbar^2} = \frac{16\,kT_b\,\kappa^2}{\hbar\,Q} \tag{104}$$

with $Q = \omega_c/\gamma$. This result is an order of magnitude esgtimate of the decoherence time due to thermal fluctuations. As we have expected, it is indeed approximately the result (88) of the previous section multiplied by $\bar{N}$ in the high temperature limit.

For the system parameters $\kappa \sim 1/\sqrt{2}$, $Q \sim 10^5$ and $T_b \sim 1$mK we thus expect the cantilever superposition to decohere after a time

$$\tau_{dec}^{(T_b)} = 0.1ms \tag{105}$$

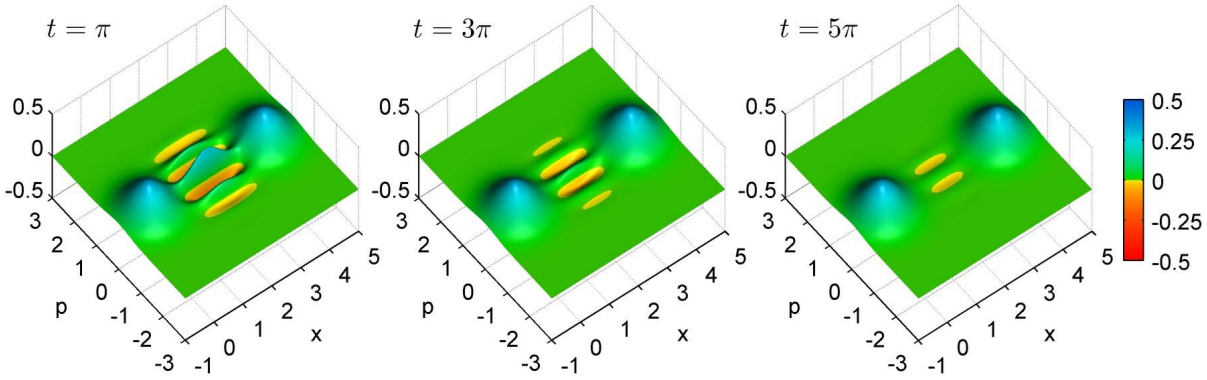

Figure 12: *Wigner function of the system in the presence of environmentally induced decoherence. The interference terms are suppressed according to eqn.* (102)*. The parameters are chosen as* $\kappa = 2$ *and* $T_b/Q = 10^{-10}K$ *(*$\hbar = \omega_c = m = 1$*). In the ideal case, experimentally realizing a Q-factor of* 10^5 *and a bath temperature of* $10\mu K$ *could be possible with a combination of forced helium cooling and adiabatic demagnetization [64].*

This indicates that decoherence due to a thermal bath can be a serious obstacle to measuring an interferometric revival. The expriment takes place on a timescale of 1ms, thus reducing thermal decoherence by increasing the mechanical Q-factor and reducing the bath temperature T_b as much as possible is required. The bath considered here is a very generic bosonic bath, which in the realistic device includes the bulk to which the cantilever is attached as well as other modes of the cantilever.

We have performed an approximate analysis of the decoherence timescale, as it was first introduced by Zurek [42, 65, 66]. An exact open quantum system analysis of the experimental setup based on eqn. (97) has been performed by Bassi et al. [67] and Bernád et al. [39]. The former authors neglect the term proportional to $\hat{p}$ in eqn. (97) and solve the resulting recoilless equation for the density matrix projected onto the off-diagonal photon states. The latter authors find the solution of the full master equation for such a density matrix. To obtain an analytic solution, they use a characteristic function similiar to the one we used in eqn. (61) to map the master equation (97) onto a first order Fokker-Planck type equation in phase space, which can be solved by the method of characteristics or by a Gaussian Ansatz. To remain within the scope of this thesis, we will not present the calculational details but simply state their results: the decoherence rate of the revival peaks in those papers is remarkably close to our estimate, both predicting a longer coherence time by only a factor of 8/3. The slower decoherence rate in the exact treatment confirms the assumption that here we have found an upper bound to the decoherence rate, since the cantilever was taken to be initially in a maximally seperated superposition state. Thus the exact value of τ_{dec} is indeed slightly larger than in eqn. (105), but the order of magnitude of decoherence is well captured in our estimate.

5.6 Modelling the Scattering of Particles

We will now discuss the effect of scattering on the quantum coherence of the cantilever. We assume that the free evolution of the cantilever is disturbed by scattering from the surrounding environment, which could be an external bath of molecules or photons. In our case the mirror

on the cantilever will be "localized" due to a continuous monitoring from the scattered particles, and thus the cantilever's quantum coherence will be lost. Here, we discuss the effect of a general scattering environment on quantum coherence and investigate in the next sections the scattering of photons and molecules in particuliar.

Instead of deriving a master equation from a microscopic model, we use a shortcut by taking the Linblad form of the master equation (77) and choosing the jump operators as proposed by Alicki [68] to be

$$\hat{L}_q = \sqrt{\gamma_{\mathbf{q}}}\, e^{i\mathbf{q}\cdot\hat{\mathbf{x}}/\hbar} \tag{106}$$

This choice can be justified the following way: when acting on the particle's momentum eigenstates, it will change them according to

$$e^{i\mathbf{q}\cdot\hat{\mathbf{x}}/\hbar}|\,\mathbf{p}\rangle\langle\mathbf{p}\,|\,e^{-i\mathbf{q}\cdot\hat{\mathbf{x}}/\hbar} = |\,\mathbf{p}+\mathbf{q}\rangle\langle\mathbf{p}+\mathbf{q}\,| \tag{107}$$

Hence each "jump" corresponds to a scattering event which changes the particle's momentum from $\mathbf{p}$ to $\mathbf{p}+\mathbf{q}$. The momentum of the scattered, usually much lighter particle of the environment thus changes from $\mathbf{q_i}$ to $\mathbf{q_f}$ with $\mathbf{q} = \mathbf{q_i} - \mathbf{q_f}$. This is represented in figure 13

The pre-factor $\gamma_{\mathbf{q}}$ has to be related to physical quantities of the system. It is a rate at which the jumps take place, thus we interpret it as the mean number of collisions in the system. This can be written as the flux of incoming particles, times the differential cross section of the scattering center, averaged over all outgoing angles. We thus write

$$\gamma_{\mathbf{q}} = \int \frac{d\Omega_f}{4\pi}\, nv(q_i)\frac{d\sigma}{d\Omega}(\mathbf{q_i},\mathbf{q_f}) \tag{108}$$

where n is the number density and $v(q_i)$ the velocity of incoming bath particles. Note that for elastic scattering we have $q_i = q_f$. The sum in eq. (77) is replaced by the integral over all angles and momenta with the weight $\nu(q)$, where $\nu(q)dq$ is the fraction of bath particles with momentum magnitude in the interval $[q, q+dq]$. We thus obtain the general form of the master eqation for elastic scattering (omitting the unitary evolution):

$$\frac{d\hat{\rho}}{dt} = -\int dq\,\nu(q)nv(q)\int \frac{d\Omega\, d\Omega_f}{4\pi}\frac{d\sigma}{d\Omega}(\mathbf{q_i},\mathbf{q_f})\big(\hat{\rho} - e^{i(\mathbf{q}_i-\mathbf{q}_f)\cdot\hat{\mathbf{x}}/\hbar}\hat{\rho}\, e^{-i(\mathbf{q}_i-\mathbf{q}_f)\cdot\hat{\mathbf{x}}/\hbar}\big) \tag{109}$$

Although we have only qualitatively derived the above master equation by using appropriate jump operators, a microscopic derivation using scattering matrix theory is also possible. This was done by Joos and Zeh [69] in the limit of $xq/\hbar \ll 1$ and by Gallis and Flemming [70] in the general case. A careful analysis was performed by Hornberger and Sipe [71] yielding exactly the master equation (109).

We now apply the above master equation to our system under investigation. We want to obtain an order of magnitude estimate for the decoherence time due to scattering. In such an estimate we can ignore the internal dynamics of our system and just analyze the change of the density matrix according to (109). In the position representation it reads

$$\frac{d\rho(x,x',t)}{dt} = -\int dq\,\nu(q)nv(q)\int \frac{d\Omega\, d\Omega_f}{4\pi}\frac{d\sigma}{d\Omega}(\mathbf{q_i},\mathbf{q_f})\big(1 - e^{i(\mathbf{q}_i-\mathbf{q}_f)\cdot(\mathbf{x}-\mathbf{x}')/\hbar}\big)\rho(x,x',t) \tag{110}$$

Here, $\mathbf{x}$ and $\mathbf{x}'$ correspond to the different possible positions of the mirror. Since in our system the spatial superposition is small compared to typical wavelengths of the surrounding particles,

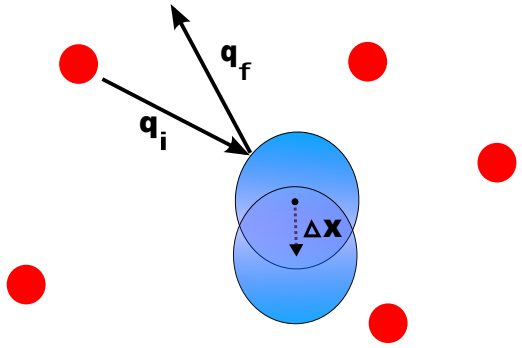

Figure 13: *A gas consisting of light particles that scatter elastically from a larger particle, which is in a spatial quantum superposition.*

we have $q\Delta x/\hbar \ll 1$ and can expand the exponential in (110) which yields

$$\begin{aligned}\frac{d\rho(x,x',t)}{dt} &\approx -\frac{1}{2}\int dq\,\nu(q)nv(q)\int \frac{d\Omega\,d\Omega_f}{4\pi\hbar^2}\frac{d\sigma}{d\Omega}(\mathbf{q_i},\mathbf{q_f})\big((\mathbf{q}_i-\mathbf{q}_f)\cdot(\mathbf{x}-\mathbf{x}')\big)^2\rho(x,x',t)\\ &= -\frac{(\Delta x)^2}{\hbar^2}\int dq\,\nu(q)nv(q)q^2\sigma_{eff}(q)\rho(x,x',t)\end{aligned} \tag{111}$$

We have used the fact that the linear term averages to zero and have included all angular integrals in the effective cross-section

$$\sigma_{eff}(q) = \frac{1}{2}\int \frac{d\Omega\,d\Omega'}{4\pi}\frac{d\sigma}{d\Omega}(\mathbf{q},\mathbf{q}')(\cos\theta-\cos\theta')^2 \tag{112}$$

If the surrounding particles scatter isotropically, we simply get $\sigma_{eff}(q) = \frac{1}{3}\sigma(q)$.

With the above result, we find the time evolution of the density matrix to be

$$\rho(t) = \rho_0 e^{-\Lambda(\Delta x)^2 t} \tag{113}$$

with

$$\Lambda = \frac{1}{\hbar^2}\int dq\,\nu(q)nv(q)q^2\sigma_{eff}(q) \tag{114}$$

which is the so-called localization rate for a scattering environment.

We have left the specifications of the environment open. Let us now apply the above formula to find the localization rates for the case of surrounding molecules and for a surrounding photon field.

5.7 Decoherence due to Scattering of Photons

Although the experimental setup can easily be shielded from electromagnetic radiation, it is still instructional to consider the effect of photon scattering on the quantum coherence of our mirror.

The photon field can be characterized by Planck's distribution law for black body radiation. We know that the density of modes with momenta in the interval $[q, q+dq]$ is given by $q^2dq/\hbar^3\pi^2$. The mean number of photons with momentum q and with two polarization modes is bose

distributed, $2(e^{qc/k_BT}-1)^{-1}$. Thus the density of occupied momentum modes, $u(q)$, is the product of those two, given by

$$u(q) = \frac{q^2}{\pi^2\hbar^3}\frac{2}{e^{qc/k_BT}-1} \tag{115}$$

and the probability to find photons with a momentm magnitude in the interval $[q, q+dq]$ becomes

$$\nu(q)dq = \frac{u(q)dq}{u_{tot}} \tag{116}$$

where $u_{tot}(q) = \int dq u(q)$.

The photon density that enters expression (114) is obtained by integrating the mean number of photons per mode over all momentum space:

$$n = \int \frac{d^3q}{(2\pi\hbar)^3}\frac{2}{e^{qc/k_BT}-1} \tag{117}$$

After using equations (117) and (116) in the expression for the localization, (114), we are left with integrals of the form

$$\int_0^\infty \frac{x^{n-1}dx}{e^x-1} = \zeta(n)\Gamma(n) \tag{118}$$

where $\zeta(n)$ is the Riemann Zeta function and $\Gamma(n)$ is the Gamma function. With $x = qc/k_BT$ this yields $u_{tot} = 4/\pi^2 \cdot (k_BT/\hbar c)^3\zeta(3)$ and $n = 2/\pi^2 \cdot (k_BT/\hbar c)^3\zeta(3)$ Thus the localization rate from photon scattering becomes

$$\Lambda^{(Ph)} = \frac{c}{2\hbar^2}\int dq\, u(q)q^2\sigma_{eff}(q) \tag{119}$$

The effective scattering cross-section σ_{eff} can vary depending on the wavelength of the incoming light. We use the general form $\sigma_{eff} = \tilde{\sigma}(q/\hbar)^p$ in which the value of p determines the type of scattering. With this and the expressions (115) and (118) we obtain the general result for localization due to black-body radiation:

$$\Lambda^{(Ph)} = \frac{2\,\tilde{\sigma}c}{\pi^2}\zeta(5+p)\,\Gamma(5+p)\left(\frac{k_BT}{\hbar c}\right)^{5+p} \tag{120}$$

The differential cross-section depends on the wavelength of the incoming light, λ. If it is much larger than the extension of our object, $\lambda \gg a$, then light is scattered mostly by Rayleigh scattering. In this case the differential cross-section is given by

$$\frac{d\sigma}{d\Omega} = \frac{1}{2}\left(\frac{q}{\hbar}\right)^4 a^6\left(1+\cos^2(\theta)\right) \tag{121}$$

We obtain σ_{eff} from expression (112):

$$\sigma_{eff} \approx \pi a^6\left(\frac{q}{\hbar}\right)^4 \tag{122}$$

Thus we have $p = 4$ and $\tilde{\sigma} = \pi a^6$ in eq. (120) and the localization rate becomes

$$\Lambda^{(Ph_-)} = \frac{2}{\pi}a^6 c\,8!\,\zeta(9)\left(\frac{k_BT}{\hbar c}\right)^9 \tag{123}$$

With $\zeta(9) \approx 1.002$ the localization rate as a function of temperature (in K) and object size (in meters) reads

$$\Lambda^{(Ph_-)} = 4 \cdot 10^{36} \, [T/K]^9 \, [a/m]^6 \; m^{-2} s^{-1} \tag{124}$$

We have thus found an expression for the effect of Rayleigh scattering of photons on the quantum coherence of our object. This result was first obtained by Joos and Zeh in 1985 [69]. We see that the result is highly dependent on the temperature of the photon emitter and the size of the object under investigation.

The localization rate allows us to calculate the decoherence time for our particular setup. From eq. (113) we see that

$$\tau_{dec} = \frac{1}{\Lambda (\Delta x)^2} \tag{125}$$

The spatial separation of the two superposed mirror states for $\kappa \approx 1$ is $(\Delta x)^2 = 10^{-25} m^2$, and the size of the mirror is $a = 10 \mu m$. We thus obtain

$$\tau_{dec}^{(Ph_-)} = 2 \cdot 10^{18} \, [T/K]^{-9} \, s = \begin{cases} 10^{18} s & T = 1K \\ 10^{-4} s & T = 300K \end{cases} \tag{126}$$

For a low temperature radiation field the decoherence effect is extremely weak. However, radiation from an object at room temperature can have a significant influence on the quantum superposition of the mirror. Since a typical experimental run will last about 1ms, thermal radiation from objects in the laboratory can be enough to destroy the quantum coherence of the setup. Thus shielding from radiation is neccessary, although required independently by the cooling mechanism anyway.

It is important to note that we have considered Rayleigh scattering, which is valid for $\lambda \gg a$. Since $a \approx 10 \mu m$, this type of scattering occurs only for wavelengths which are greater than the infrared. Thus, from Wien's law, only a small fraction of emitted photons from black bodies with temperatures larger than $300K$ will undergo Rayleigh scattering.

Now let us consider the opposite case, in which the wavelength of the radiation is smaller than the object size, $\lambda < a$. This type of scattering will be valid for a black body emitter at temperatures $T > 300K$. In this case the geometric cross-section of the object becomes important and we have

$$\sigma_{eff} \approx \frac{1}{3} \pi a^2 \tag{127}$$

Hence for the case of high frequency radiation the coefficients in eq. (120) are $p = 0$ and $\tilde{\sigma} = \pi a^2 / 3$. The localization rate becomes

$$\begin{aligned} \Lambda^{(Ph_+)} &= \frac{2}{3\pi} a^2 c \, 4! \, \zeta(5) \Big(\frac{k_B T}{\hbar c} \Big)^5 \\ &= 2 \cdot 10^{22} \, [T/K]^5 \, [a/m]^2 \; m^{-2} s^{-1} \end{aligned} \tag{128}$$

where we used $\zeta(5) \approx 1.037$. Note the completely different dependence on temperature and size compared to the result for Rayleigh scattering, eq. (124).

The decoherence timescale we again obtain by using eq. (125), the size of the mirror, $a = 10 \mu m$, and the superposition distance $(\Delta x)^2 = 10^{-25} m^2$. The result is

$$\tau_{dec}^{(Ph_+)} = 4 \cdot 10^{12} \, [T/K]^{-5} \, s = \begin{cases} 1s & T = 300K \\ 1ms & T = 1300K \end{cases} \tag{129}$$

We can see that for room temperature Rayleigh scattering will have a larger effect, even when taking into account that less particles are emitted at the required low frequencies. But for higher temperatures the above decoherence time will be valid, and hot objects close to the experiment will emit thermal radiation that can easily destroy the quantum coherence of the mirror.

5.8 Decoherence due to Scattering of Surrounding Molecules

In the previous section we have described the effect of a photon gas on the quantum coherence of the mirror. As we have noted, the setup can be shielded from incoming radiation and thus the majority of scattering events will be due to the surrounding molecules. To describe this process we again use the formalism developed in section 5.6.

The vacuum surrounding the mirror mostly consists of Helium atoms that originate from the dilution refrigerator. We can estimate the localization rate due to the Helium by using the general formula, eqn. (114), with the geometric cross section $\sigma = \pi a^2$, the average thermal velocity of the atoms, $v_{th} = \sqrt{8k_BT/\pi m_{He}}$, and the density of Helium particles, n. This yields

$$\Lambda^{(He)} = \frac{1}{3}\frac{\pi a^2 n}{\hbar^2}\sqrt{\frac{8k_BT}{\pi m_{He}}}\int dq\nu(q)q^2 \tag{130}$$

As in [68], we can interpret the integral as the typical average squared momentum of the surrounding particles, $\int dq\nu(q)q^2 =< q^2 >= v_{th}^2 m_{He}^2$, and get

$$\Lambda^{(He)} = \frac{a^2 n}{3\sqrt{\pi}\hbar^2}\sqrt{(8k_BT)^3 m_{He}} \tag{131}$$

Using the ideal gas law, we can write the particle density in terms of pressure and temperature as $n = p/kT$. With the atomic mass of Helium, $m_{He} = 10^{-26}kg$, we get the localization rate

$$\Lambda^{(He)} = 2\cdot 10^{44}\,[T/K]^{1/2}\,[p/Pa]\,[a/m]^2\ m^{-2}s^{-1} \tag{132}$$

For $(\Delta x)^2 = 10^{-25}m^2$ and with the mirror size $a = 10\mu m$, the decoherence time for the superposition becomes

$$\tau_{dec}^{(He)} = 10^{-9}\cdot[p/\mathrm{Pa}]^{-1}\,[T/\mathrm{K}]^{-1/2}\,s = \begin{cases} 3s & T = 1\,\mathrm{mK}\,, \quad p = 10^{-8}\,\mathrm{Pa} \\ 1ms & T = 10\,\mathrm{mK}\,, \quad p = 10^{-5}\,\mathrm{Pa} \end{cases} \tag{133}$$

The first timescale, computed for ideal parameters, is much larger than the oscillator period $2\pi/\omega_c \approx 10^{-3}s$. Thus decoherence due to scattering of the environment will not affect the experiment in a significant way if those parameters are reached. However, for a less ideal vacuum or for higher temperatures decoherence due to scattered Helium particles will have a strong effect.

The analysis presented here yields only a qualitative result for the decoherence time. It does not take into account the system geometry with the mirror attached to a cantilever that oscillates in only one direction. The pressure gradient inside the setup and the internal dynamics of the system coupled to the single photon are also neglected. Thus we have obtained only a rough estimate of the expected decoherence time. However, the estimate captures well the order of magnitude of the effect of Helium on the coherence of our setup. It shows that decoherence due to elastic scattering will be negligible compared to decoherence due to the thermal coupling of the cantilever with other phonon modes, computed in (105). It also shows that a higher pressure inside the shielded setup can be tolerable, up to $p \approx 10^{-5}Pa$.

6 Towards Testing a Gravitationally Induced Wavefunction Collapse

In this last section we address the ultimate goal of the experiment, to test a possible gravitationally induced collapse of a quantum wavefunction as discussed in section 2. If a gravitationally induced wavefunction collapse takes place, no signature of a quantum superposition should be observable after a characteristic time τ_{col}. In practice this means that in our experiment no visibility revival peak would be observable, since the cantilever becomes completely classical and thus stores perfectly the which-path-information of the photon. Thus one can probe the collapse by observing the visibility revival peak if the duration of the experiment is on the order of τ_{col}. Any quantum decoherence effects as discussed in the previous sections will also reduce the visibility and one will have to seperate those two similar effects which are of fundamentally different origin. Therefore it is neccessary to reduce the "background" of an environmentally induced decoherence such that a possible collapse would be observable. It will be a significant challenge to extract the correct interpretation from the data, and it will be of ample importance to understand all possible decoherence sources.

It was suggested by Penrose [22] that a collapse will take place on the timescale of

$$\tau_{col} \sim \frac{\hbar}{\Delta E} \tag{134}$$

where ΔE is the gravitational self energy of the system and is given by

$$\Delta E = G \int d^3x \int d^3y \, \frac{(\rho(\mathbf{x}) - \rho'(\mathbf{x}))(\rho(\mathbf{y}) - \rho'(\mathbf{y}))}{|\mathbf{x} - \mathbf{y}|} \tag{135}$$

The primed and unprimed mass densities refer to the two superposed states. This estimate comes about from considering the different gravitational forces due to the two superposed states acting on a test particle.

Here we are interested in giving an estimate of τ_{col} for the experiment at hand. From eqn. (135) we see that the proposed collapse time depends on the mass density of the object in superposition. However, it is not known what the exact mass distribution of matter on a quantum level is. We will therefore estimate the collapse time for different possible choices of the mass distribution.

Let us first assume that the mass is evenly distributed within the object. When the distance Δx by which the cantilever is being displaced is smaller than the thickness of the mirror, a, parts of the two superposed masses overlap. It is for our purposes sufficient to simply estimate the gravitational self energy:

$$\Delta E = \frac{1}{2}\frac{G}{a}\left(\frac{m\Delta x}{a}\right)^2 \tag{136}$$

which is just the Newtonian gravitational energy for the non-overlapping pieces of mass $m\Delta x/a$. This result can be deduced by simple dimensional analysis but can also be obtained from solving equation (135) explicitly [72]. The displacement of the mirror is due to the photon pressure and is given in terms of the optomechanical coupling constant κ in eqn. (12). Thus the Penrose timescale for gravitational collapse becomes

$$\tau_{col} \approx \frac{a^3\omega_c}{Gm\kappa^2} \tag{137}$$

For $a = 10\mu$m, $\omega_c = 2\pi \times 1$kHz, $m = 10^{-12}$kg and $\kappa = 1$ we get the collapse time

$$\tau_{col} \approx 10^{11} s \tag{138}$$

Thus, if this estimate was correct, the collapse would never be experimentally observable in this setup.

However, we note that the assumption for an evenly distributed mass cannot be realistic. The mass is concentrated in the nuclei of matter, and we thus should use a granular density distribution for a better estimate of the collapse timescale. Thus we calculate more rigorously the gravitational self energy for a collection of tiny spheres, which represent the mass constituents of the cantilever. We assume that the superposition size is larger than the diameter of the spheres, and that their mass distribution is homogeneous.

For the calculations, note that we can write the gravitational self energy (135) also in terms of the gravitational potential Φ:

$$\Phi(\mathbf{y}) = -G \int d^3x \frac{\rho(\mathbf{x})}{|\mathbf{x}-\mathbf{y}|} \tag{139}$$

For a solid sphere of radius R and mass m_0 the potential can easily be found by Gauss' law and reads

$$\Phi(\mathbf{x}) = \begin{cases} -\frac{Gm_0}{r} & , \quad r > R \\ -\frac{Gm_0}{2R}\left(3 - \frac{r^2}{R^2}\right) & , \quad r \leq R \end{cases} \tag{140}$$

Thus for a sphere with a homogeneous mass density $\rho = 3M/4\pi R^3$ we get

$$\begin{aligned} \Delta E_{\rho\rho} &= G \int d^3x \int d^3y \, \frac{\rho(\mathbf{x})\rho(\mathbf{y})}{|\mathbf{x}-\mathbf{y}|} = -\int d^3y \, \rho(\mathbf{y})\Phi(\mathbf{y}) \\ &= 4\pi\rho \int_0^R dr \, r^2 \frac{Gm_0}{2R}\left(3 - \frac{r^2}{R^2}\right) \\ &= \frac{8\pi}{5} G m_0 \rho R^2 \\ &= \frac{6}{5}\frac{Gm_0^2}{R} \end{aligned} \tag{141}$$

whereas for the other integral we get (for $\Delta x \gg R$):

$$\begin{aligned} \Delta E_{\rho\rho'} &= G \int d^3x \int d^3y \, \frac{\rho(\mathbf{x})\rho'(\mathbf{y})}{|\mathbf{x}-\mathbf{y}|} = -\int d^3y \, \rho'(\mathbf{y})\Phi(\mathbf{y}) \\ &\approx \frac{Gm_0^2}{\Delta x} \end{aligned} \tag{142}$$

Thus the total gravitational self energy for a sphere in a superposition becomes

$$\Delta E = \frac{2Gm_0^2}{R}\left(\frac{6}{5} - \frac{R}{\Delta x}\right) \quad , \qquad \text{for} \quad \Delta x \gg R \tag{143}$$

Having found the gravitational self energy for a single sphere in superposition, we can sum up all such spheres in our cantilever (corresponding to the number of atoms, N), assuming that the distance d between the nuclei is much larger than the suerposition size such that the

gravitational interaction energy to all neighbouring spheres will be less than the contribution from the superposed sphere. We therefore obtain the final result

$$\Delta E = \frac{2Gmm_0}{R}\left(\frac{6}{5} - \frac{R}{\Delta x}\right) \tag{144}$$

with $m = 10^{-12}$kg being the mass of the cantilever and $m_0 = 4.7 \times 10^{-26}$kg the mass of a single silicon nucleus (the cantilever is made of silicon).

We are now left with choosing a reasonable value of R. One could take the size of an atomic nucleus, $R = 10^{-15}$m, which yields the timescale

$$\tau_{col} \approx 10 \text{ ms} \tag{145}$$

However, it is also plausible to take a "smeared" distribution due to quantum fluctuations, and assume R to be on the size of the ground state wavepacket of the cantilever, $R = 10^{-13}m$. This yields

$$\tau_{col} \approx 1 \text{ s} \tag{146}$$

Even some other value of R might be reasonable, when estimating quantum fluctuations or even considering gluons. The results are therefore highly ambiguous, since they depend on the exact details of the mass distribution on a quantum level. This is an additional uncertainly, apart from the vague prediction given by (134). It is interesting to note though that the experiment at hand is already close to probing the regime given by the estimate in eqn. (145). Any experimental advancement in the future will allow to probe a whole range of regimes in which a gravitationally induced collapse can take place. However, to pursue an exact theoretical prediction is currently not feasible.

7 Summary and Outlook

The prospect of probing quantum mechanics in an entirely new regime, testing its limits and investigating possible effects of quantum gravitational nature were the motivation for this theoretical study of a highly promising experiment.

We have first outlined the idea for a possible gravitationally induced collapse of the wavefunction, which is a candidate for explaining the quantum-classical transition. We also presented a thorough analysis of the proposed setup, in which a single photon is put into a superpositon in an interferometer. In only one arm the photon is coupled through the photon pressure to a tiny cantilever. This cantilever is displaced, and observing the quantum interference of the photon when the two photon states from the two arms are combined provides a way of probing a quantum superposition state of the cantilever. We discussed in detail the states of the photon, the cantilever and the entanglement between those two, showing that observing the interferometric visibility when the cantilever is cooled to the ground state amounts to measuring the optomechanical entanglement. A reduction and a subsequent revival of the interferometric visibility thus corresponds to a periodic entanglement in the system which results in the cantilever to be in a superposition state.

For finite cantilever temperatures we showed that the interpretation of the interferometric visibility becomes more difficult. A reduction induced by entanglement is masked by a statistical phase averaging. To get an idea of the tolerable temperatures, such that one can convincingly infer a quantum effect of the cantilever from the interferometric data, we used a Wigner function analysis in phase space. By quantifying the non-classicality of the cantilever using the negativity of the Wigner function we showed that an unambiguous demonstration of a quantum superposition requires the cantilever to be close to its ground state. We also showed that higher cantilever temperatures can be tolerable if the optomechanical coupling can be increased. Further research on quantifying non-classicality in mixed states could provide a higher bound on the tolerable temperatures. One could think of using a different way to quantify non-classicality, such as using an entanglement measure for mixed states [73] or computing the quantum discord [74] for the system at hand. These are current research topics in quantum information science and future new insights might provide a better way of understanding quantum and classical correlations in the system.

We also discussed the effect of the environment on the outcome of the experiment, and computed the decoherence times for different possible influences of the bath. First, we completely solved the dynamical evolution of the system when it is dissipatively coupled to a zero temperature bath, generalizing the previous results to an amplitude damped system. We showed that pure dissipation yields a decoherence of the superposition with a timescale on the order of the damping rate. It is independent of the details of the creation of the superposition and also independent of the initial temperature of the cantilever. This result allowed us to generalize the decoherence timescale to include thermal fluctuations when the cantilever is coupled to a finite temperature bath (such as the bulk to which the cantilever is attached or to other cantilever modes). The resulting decoherence time is close to what an exact solution of a finite temperature master eqaution yields [39], with the difference being a numerical factor of order 1. We then also calculated the effect of a scattering environment and computed the dependence of the decoherence time on the system paramters. We showed that for a reasonable vacuum the decoherence rate due to Helium molecules in the setup can be neglected in comparison to decoherence due to thermal fluctuations within the bulk and the cantilever. We have thus covered any possible influence of an interaction with bosonic particles. However, it is still an

open question how a fermionic environment would influence the coherence of the sueprposition. This might be important when taking into account the defects within the amorphous silicon cantilever, and is a current research topic in the study of mechanical stability, open quantum systems and nanoelectromechanical systems [75, 76].

Finally, we have presented an outlook of testing a gravitationally induced collapse with the current setup. The vague estimate of the collapse timescale and the ambiguity in choosing a realistic mass distribution for matter don't allow for a precise prediction of the collapse timescale, and the possible results can vary by many orders of magnitude. However, we showed that the current experiment is close to a regime in which some models predict a collapse. It could also shed light on other proposals for a wavefunction collapse [77] and the nature of the quantum-classical transition [65, 78]. The experiment therefore serves as a first realistic attempt to start probing the border line between quantum mechanics, classical physics and gravity in an optomechanical setup.

A Appendices

A.1 Review of Coherent States

We briefly review coherent states and their properties, which are tantamount for the discussion of the experiment at hand. Coherent states most closely resembe a classical harmonic oscillator in accordance with the uncertainty principle and are also eigenstates of the annihilation operator, $\hat{c}$. Let us denote a coherent state by $|\,\alpha\rangle$. As stated above, they have the property:

$$\hat{c}|\,\alpha\rangle = \alpha|\,\alpha\rangle \tag{147}$$

We can also write a coherent state in terms of a displacement of the vacuum state:

$$|\,\alpha\rangle = \hat{D}(\alpha)|\,0\rangle = e^{\hat{c}^\dagger\alpha - \hat{c}\alpha^*}|\,0\rangle = e^{-\frac{|\alpha|^2}{2}}\sum_{n=0}^{\infty}\frac{\alpha^n}{\sqrt{n!}}|\,n\rangle \tag{148}$$

where $\hat{D}(\alpha)$ is the displacement operator. With the BCH-expansion (see eqn. (162)) we can also easily derive the following relation for the product of two displacement operators:

$$\hat{D}(\alpha)\hat{D}(\beta) = e^{i\,\mathrm{Im}[\alpha\beta^*]}\hat{D}(\alpha+\beta) \tag{149}$$

Coherent states are not orthogonal states. The inner product of two coherent states is a finite number given by

$$\begin{aligned}\langle\alpha\,|\,\beta\rangle &= e^{-\frac{|\alpha|^2+|\beta|^2}{2}}\sum_{n=0}^{\infty}\sum_{k=0}^{\infty}\frac{(\alpha^*)^k\beta^n}{\sqrt{n!k!}}\langle k\,|\,n\rangle \\ &= e^{-\frac{|\alpha|^2+|\beta|^2}{2}}\sum_{n=0}^{\infty}\frac{(\alpha^*\beta)^n}{n!} \\ &= e^{-\frac{1}{2}(|\alpha|^2+|\beta|^2-2\alpha^*\beta)}\end{aligned} \tag{150}$$

Note that

$$|\alpha-\beta|^2 = |\alpha|^2+|\beta|^2-\alpha^*\beta-\alpha\beta^* = |\alpha|^2+|\beta|^2-2\alpha^*\beta+2i\mathrm{Im}[\alpha^*\beta] \tag{151}$$

Thus we can write the inner product between two coherent states as

$$\langle\alpha\,|\,\beta\rangle = e^{-(|\alpha|^2+|\beta|^2)/2}\,e^{\alpha^*\beta} = e^{-|\alpha-\beta|^2/2}e^{i\mathrm{Im}[\alpha^*\beta]} \tag{152}$$

We can see that although the coherent states are not orthogonal, their inner product tends to 0 as the distance between two coherent states increases.

Coherent states also comprise a complete basis with the completeness relation

$$\frac{1}{\pi}\int d^2\alpha|\,\alpha\rangle\langle\alpha\,| = 1 \tag{153}$$

which can easily be checked by expressing them in terms of the usual Fock states, eqn. (148). In this way, any arbitary state can be expressed in terms of coherent states. The non-orthogonality of coherent states makes them over-complete such that the representation is not unique.

A.2 Optomechanical Coupling κ

We follow Pace et al. [79] to derive the linear optomechanical constant κ in terms of the system parameters.

A single mode light field in a cavity is described by $\hat{H} = \hbar\omega_a \hat{a}^\dagger \hat{a}$. Resonance in the cavity implies that the light field frequency can only have the values

$$\omega_a = \frac{n}{2}\omega_0 \tag{154}$$

where n is a positive integer and $\omega_0 = 2\pi c/L$ is the cavity frequency, with the total cavity length L. However, the moving mirror due to the photon pressure changes the cavity length, and the fundamental cavity frequency is reduced. If the mirror has moved by x, the Hamiltonian becomes

$$\hat{H} = \hbar\frac{n}{2}\frac{2\pi c}{L+x}\hat{a}^\dagger \hat{a} \tag{155}$$

Writing the Hamiltonian in terms of the original frequency ω_0 and expanding in the small parameter x/L we get:

$$\begin{aligned} \hat{H} &= \hbar\frac{n}{2}\omega_0\frac{L}{L+x}\hat{a}^\dagger \hat{a} \\ &\approx \hbar\omega_a(1-\frac{x}{L})\hat{a}^\dagger \hat{a} \\ &= \hbar\omega_a \hat{a}^\dagger \hat{a} - \hbar\frac{\omega_a}{L}\hat{a}^\dagger \hat{a}x \end{aligned} \tag{156}$$

We now quantize the position of the mirror: $x \to \hat{x} = \sqrt{\hbar/2m\omega_c}(\hat{c}+\hat{c}^\dagger)$ which yields

$$\hat{H} = \hbar\omega_a \hat{a}^\dagger \hat{a} - \hbar\omega_c\frac{\omega_a}{\omega_c L}\sqrt{\frac{\hbar}{2m\omega_c}}(\hat{c}+\hat{c}^\dagger)\hat{a}^\dagger \hat{a} \tag{157}$$

and hence the linear and dimensionless optomechanical coupling κ is given by

$$\kappa = \frac{\omega_a}{\omega_c}\frac{1}{L}\sqrt{\frac{\hbar}{2m\omega_c}} \tag{158}$$

such that

$$\hat{H} = \hbar\omega_a \hat{a}^\dagger \hat{a} - \hbar\omega_c \kappa \hat{a}^\dagger \hat{a}(\hat{c}+\hat{c}^\dagger) \tag{159}$$

In this derivation we have assumed that there is only one significant cavity mode and that the mirror displacement x is small compared to the cavity length L. The mirror displacement is also slow compared to the roundtrip time of the photon in the cavity, since we have not taken into account the Doppler-scattering of the photon into other cavity modes. This adiabatic approximation is valid when the wavelength of the photon is much larger than the mirror displacement x.

A.3 Unitary Evolution Operator

We would like to cast the time evolution operator in the form (3). This is done in several steps. With the Hamiltonian (1) the time evolution is given by (ignoring the phase factor $e^{-i\omega_a \hat{b}^\dagger \hat{b}t}$ for the photon in arm B):

$$\hat{U} = e^{-i\omega_a \hat{a}^\dagger \hat{a}} e^{-i\omega_c \hat{c}^\dagger \hat{c} + i\kappa\omega_c \hat{a}^\dagger \hat{a}(\hat{c}+\hat{c}^\dagger)} \tag{160}$$

We now make use of the unitary transformation operator as proposed in [80]:

$$\hat{S} = e^{\kappa \hat{a}^\dagger \hat{a}(\hat{c}-\hat{c}^\dagger)} \tag{161}$$

Its action on the system operators can be easily found with the help of the well-known Baker-Cambell-Hausdorff relation

$$e^{\hat{A}}\hat{B}e^{-\hat{A}} = \hat{B} + [\hat{A},\hat{B}] + \frac{1}{2}[\hat{A},[\hat{A},\hat{B}]] + \frac{1}{3}[\hat{A},[\hat{A},[\hat{A},\hat{B}]]] + ... \tag{162}$$

Here we use $\hat{A} = \kappa\hat{a}^\dagger\hat{a}(\hat{c}-\hat{c}^\dagger)$ and $\hat{B} = \hat{c}$ or $\hat{B} = \hat{c}^\dagger$. Note that $[\kappa\hat{a}^\dagger\hat{a}(\hat{c}-\hat{c}^\dagger),\hat{c}] = [\kappa\hat{a}^\dagger\hat{a}(\hat{c}-\hat{c}^\dagger),\hat{c}^\dagger] = \kappa\hat{a}^\dagger\hat{a}$ and all other nested commutators in (162) vanish. Thus:

$$\begin{aligned} \hat{S}\hat{c}\hat{S}^\dagger &= \hat{c} + \kappa\hat{a}^\dagger\hat{a} \\ \hat{S}\hat{c}^\dagger\hat{S}^\dagger &= \hat{c}^\dagger + \kappa\hat{a}^\dagger\hat{a} \end{aligned} \tag{163}$$

and $\hat{a}^\dagger\hat{a}$ remains unchanged. We now write

$$\begin{aligned} \hat{U} &= \hat{S}^\dagger\hat{S}e^{-i\omega_a\hat{a}^\dagger\hat{a}t}e^{-i\omega_c\hat{c}^\dagger\hat{c}t+i\kappa\omega_c\hat{a}^\dagger\hat{a}(\hat{c}+\hat{c}^\dagger)t}\hat{S}^\dagger\hat{S} \\ &= \hat{S}^\dagger e^{-i\omega_a\hat{a}^\dagger\hat{a}t}e^{-i\omega_c t(\hat{c}^\dagger+\kappa\hat{a}^\dagger\hat{a})(\hat{c}+\kappa\hat{a}^\dagger\hat{a})+i\kappa\omega_c t\hat{a}^\dagger\hat{a}(\hat{c}+\hat{c}^\dagger+2\kappa\hat{a}^\dagger\hat{a})}\hat{S} \\ &= e^{-i\omega_a\hat{a}^\dagger\hat{a}t}e^{i\kappa^2\omega_c(\hat{a}^\dagger\hat{a})^2 t}\hat{S}^\dagger e^{-i\omega_c\hat{c}^\dagger\hat{c}t}\hat{S} \end{aligned} \tag{164}$$

The next step is to switch the last two terms in the above expression. Using again the BCH-relation (162) with $\hat{A} = -i\omega_c\hat{c}^\dagger\hat{c}t$ and $\hat{B} = \hat{c} - \hat{c}^\dagger$ we get:

$$e^{-i\omega_c t\hat{c}^\dagger\hat{c}}(\hat{c}-\hat{c}^\dagger)e^{i\omega_c t\hat{c}^\dagger\hat{c}} = \hat{c}e^{i\omega_c t} - \hat{c}^\dagger e^{-i\omega_c t} \tag{165}$$

and hence

$$e^{-i\omega_c\hat{c}^\dagger\hat{c}t}\hat{S} = e^{-\kappa\hat{a}^\dagger\hat{a}(\hat{c}e^{i\omega_c t}-\hat{c}^\dagger e^{-i\omega_c t})}e^{-i\omega_c\hat{c}^\dagger\hat{c}t} \tag{166}$$

Finally, we combine the above exponentials with $\hat{S}^\dagger$ by using the BCH formula once more and obtain the final result

$$\hat{U} = e^{-i\omega_a\hat{a}^\dagger\hat{a}t}e^{i\kappa^2(\hat{a}^\dagger\hat{a})^2(\omega_c t-\sin(\omega_c t))}e^{\kappa\hat{a}^\dagger\hat{a}[\hat{c}^\dagger(1-e^{i\omega_c t})-\hat{c}(1-e^{-i\omega_c t})]}e^{-i\omega_c\hat{c}^\dagger\hat{c}t} \tag{167}$$

A.4 Photon States at the Output Ports

We calculate the quantum states of the photon in the output ports A and B. The setup is schematically shown in figure 14. For clarity, the cavities in both arms are not drawn and the single beam splitter through which the photon passes once from the front and once from the back side is represented by two different beam splitters B_1 and B_2. Note that the setup as represented here is equivalent to a Mach-Zehnder interferometer with one moving mirror. The evolution operators $\hat{U}_A$ and $\hat{U}_B$ give the evolution of the state in arm A or arm B only.

The states of the output light fields can be found if the input states are given in terms of creation operators acting on a vacuum state. These operators are then expressed in terms of the creation operators of the output field, taking into account the actions of the optical elements in the setup.

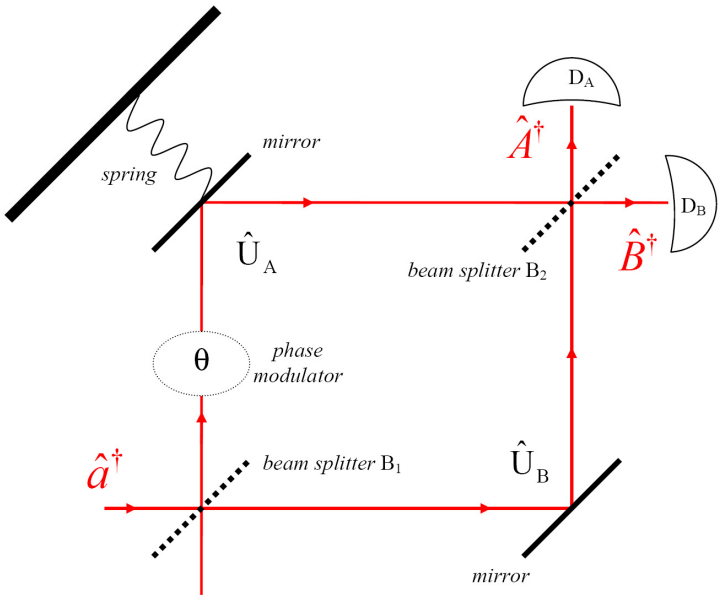

Figure 14: *Schematic drawing of the setup. The input photon, characterized by* $\hat{a}^\dagger$*, is split between the two arms. In one of the arms the photon passes a phase modulator and is entangled with the mirror. In the other arm, the photon is simply reflected. The pulse is then recombined and a photon state is measured by detectors A and B, represented by* $\hat{A}^\dagger$ *and* $\hat{B}^\dagger$*, respectively.*

Let us first look at the action of a beam splitter on an incoming light field. Two input modes, described by the operators $\hat{a}$ and $\hat{b}$, are transformed through transmission and reflection into the outgoing field modes $\hat{A}$ and $\hat{B}$. This action is described by the unitary matrix [38]

$$S = \begin{pmatrix} t & r \\ r & t \end{pmatrix} \tag{168}$$

with t and r being the transmission and the reflection coefficients, respectively. For a lossless 50-50 beam splitter, the coefficients can be written as $t = ir = i/\sqrt{2}$ (we use a different convention than in [38]). Thus the two output field operators $\hat{A}$ and $\hat{B}$ are given in terms of the two input operators $\hat{a}$ and $\hat{b}$ as

$$\begin{pmatrix} \hat{A} \\ \hat{B} \end{pmatrix} = S \begin{pmatrix} \hat{a} \\ \hat{b} \end{pmatrix} \tag{169}$$

The inversion of the symmetric and unitary matrix S simply yields the same relation just with the operators replaced by their hermitian conjugates. We thus find that a single beam splitter yields

$$\begin{aligned} \hat{a}^\dagger &= t\hat{A}^\dagger + r\hat{B}^\dagger \\ \hat{b}^\dagger &= r\hat{A}^\dagger + t\hat{B}^\dagger \end{aligned} \tag{170}$$

These relations allow us to write the input state in terms of the output states. If only one beam enters the beam splitter, we still have to include the vacuum state of the second input mode to have a consistent description.

The action of a phase modulator in one of the arms can be simply described by

$$\Theta = \begin{pmatrix} e^{-i\theta} & 0 \\ 0 & 1 \end{pmatrix} \tag{171}$$

In our setup we also need to include the evolution of the mirror on the cantilever, since it becomes entangled with the photon state. We describe the unitary evolution of the total system by

$$U = \begin{pmatrix} e^{-i\hat{H}_A t/\hbar} & 0 \\ 0 & e^{-i\hat{H}_B t/\hbar} \end{pmatrix} = \begin{pmatrix} \hat{U}_A & 0 \\ 0 & \hat{U}_B \end{pmatrix} \tag{172}$$

with $\hat{H}_A = \hbar\omega_a \hat{a}^\dagger \hat{a} + \hbar\omega_c \hat{c}^\dagger \hat{c} - \hbar\omega_c \kappa \hat{a}^\dagger \hat{a}(\hat{c} + \hat{c}^\dagger)$ and $\hat{H}_B = \hbar\omega_a \hat{b}^\dagger \hat{b} + \hbar\omega_c \hat{c}^\dagger \hat{c}$ being the time evolution operators in arms A and B, respectively.

We now have all elements in the setup as illustrated in figure 14. The input modes in terms of the detector modes can now be written as

$$\begin{aligned} \begin{pmatrix} \hat{a}^\dagger \\ \hat{b}^\dagger \end{pmatrix} &= S_1 \Theta U S_2 \begin{pmatrix} \hat{A}^\dagger \\ \hat{B}^\dagger \end{pmatrix} \\ &= \begin{pmatrix} t & r \\ r & t \end{pmatrix} \begin{pmatrix} e^{-i\theta} & 0 \\ 0 & 1 \end{pmatrix} \begin{pmatrix} \hat{U}_A & 0 \\ 0 & \hat{U}_B \end{pmatrix} \begin{pmatrix} r & t \\ t & r \end{pmatrix} \begin{pmatrix} \hat{A}^\dagger \\ \hat{B}^\dagger \end{pmatrix} \\ &= r^2 \begin{pmatrix} i(\hat{U}_B + e^{-i\theta}\hat{U}_A) & \hat{U}_B - e^{-i\theta}\hat{U}_A \\ \hat{U}_B - ie^{-i\theta}\hat{U}_A & i(\hat{U}_B + e^{-i\theta}\hat{U}_A) \end{pmatrix} \begin{pmatrix} \hat{A}^\dagger \\ \hat{B}^\dagger \end{pmatrix} \end{aligned} \tag{173}$$

Here we used $t = ir$ and interchanged the transmission and reflection in the last beam splitter to take into account that both beam splitters are actually the same but with the photon entering from two different sides. We use $r = 1\sqrt{2}$ and the initial input state

$$|\, in\rangle = \hat{a}^\dagger |\, 0,0\rangle_{ab} |\, \beta\rangle_c \tag{174}$$

The input mode $\hat{a}^\dagger$ becomes

$$\hat{a}^\dagger = \frac{1}{2} i\hat{A}^\dagger \left(\hat{U}_B + e^{-i\theta}\hat{U}_A\right) + \frac{1}{2}\hat{B}^\dagger \left(\hat{U}_B - e^{-i\theta}\hat{U}_A\right) \tag{175}$$

Using this relation in the input field equation (174) we get the full output state of the combined photon-cantilever system at the detectors:

$$|\, out\rangle = |\, 1\rangle_{D_A} i\frac{1}{2} e^{-i\omega_a t} \left(|\, \Phi_0\rangle_c + e^{i\varphi(t) - i\theta} |\, \Phi_1\rangle_c\right) + |\, 1\rangle_{D_B} \frac{1}{2} e^{-i\omega_a t} \left(|\, \Phi_0\rangle_c - e^{i\varphi(t) - i\theta} |\, \Phi_1\rangle_c\right) \tag{176}$$

Comparison with eq. (18) indeed shows that up to a phase i between the two detectors (which can be neglected, since it is an overall phase of the cantilever wavefunction) the detector states $|\, 1\rangle_{D_A}$ and $|\, 1\rangle_{D_B}$ are given in terms of the photon states as in eq. (17), i.e.

$$\begin{aligned} |\, 1\rangle_{D_A} &= |\, +\rangle = \frac{1}{\sqrt{2}} \left(|\, 0,1\rangle + e^{i\theta} |\, 1,0\rangle\right) \\ |\, 1\rangle_{D_B} &= |\, -\rangle = \frac{1}{\sqrt{2}} \left(|\, 0,1\rangle - e^{i\theta} |\, 1,0\rangle\right) \end{aligned} \tag{177}$$

A.5 Exact Solution of the Master Eqation Describing a Dissipative Cantilever

We will present here an exact solution to the master equation used in section 5.3:

$$\frac{d\hat{\rho}(t)}{dt} = -\frac{i}{\hbar}[\hat{H}, \hat{\rho}] + \frac{\gamma}{2}\left(2\,\hat{c}\,\hat{\rho}\,\hat{c}^\dagger - \hat{c}^\dagger\hat{c}\,\hat{\rho} - \hat{\rho}\,\hat{c}^\dagger\hat{c}\right) \tag{178}$$

First, we split the above differential equation into two parts:

$$\begin{aligned}\frac{d\hat{\rho}^{(1)}}{dt} &= -\frac{i}{\hbar}[\hat{H}, \hat{\rho}] \\ \frac{d\hat{\rho}^{(2)}}{dt} &= \frac{\gamma}{2}\left(2\,\hat{c}\,\hat{\rho}\,\hat{c}^\dagger - \hat{c}^\dagger\hat{c}\,\hat{\rho} - \hat{\rho}\,\hat{c}^\dagger\hat{c}\right)\end{aligned} \tag{179}$$

For an initial state $\hat{\rho}^{(1)}(0)$ the solution for the unitary part is, as found in section 3.3:

$$\hat{\rho}^{(1)} = \hat{U}(t)\hat{\rho}^{(1)}(0)\hat{U}^\dagger(t) \tag{180}$$

with $\hat{U}(t)$ given by (5).

The solution to the dissipative part (which acts only on the cantilever) is for initial cantilever coherent states $\hat{\rho}^{(2)}(0) = |\,\alpha\rangle\langle\beta\,|$ known to be [81]:

$$\hat{\rho}^{(2)} = \langle\beta\,|\,\alpha\rangle^{1-e^{-\gamma t}}|\,\alpha\,e^{-\gamma t/2}\rangle\langle\beta\,e^{-\gamma t/2}\,| \tag{181}$$

We now make an Ansatz for the solution of the full master equation, (80). We can safely assume that any photon number state entering the cavity will not be altered, since the dissipative part acts only on the cantilever. Also, the photon pressure drives the cantilever into a coherent state, as we have seen previously. This will depend on the amount of photons in the cavity. The damping terms also result in coherent states, thus we know that the time evolved cantilever state will be some coherent state depending on the photon number state in the cavity. Our Ansatz is then given by

$$\hat{\rho}(t) = \sum_{n,m}\rho_{nm}(t)|\,n\rangle\langle m\,| \otimes |\,\Phi_n(\gamma,t)\rangle\langle\Phi_m(\gamma,t)\,| \tag{182}$$

Our goal is to find the cantilever state amplitudes $\Phi_n(\gamma,t)$ and the coefficients $\rho_{nm}(t)$. Of course, in our case we have only a single photon in the cavity, thus n and m can take on the values 0 or 1. However, we can keep the discussion general for now.

The above Ansatz has the advantage that we can treat each element $\rho_{nm}(t)|\,n\rangle\langle m\,| \otimes |\,\Phi_n(\gamma,t)\rangle\langle\Phi_m(\gamma,t)\,|$ seperately and perfom the sum over all matrix elements of the density matrix later, since they do not depend on each other. We will now calculate the exact state and the coefficients by applying the unitary evolution (180) and the non-unitary evolution (181) in turns for small timesteps Δt. Such a method has been used by Bose et al. [19], but in our treatment we correct some errors found in their result and include the effect of finite cantilever temperatures.

First, let us consider the effect of an infinitesimal unitary evolution (5) on a system state (omitting the phase $e^{-i\omega_a t}$ resulting from the photon in arm A and which gets cancelled in the density matrix by the photon being in arm B):

$$\begin{aligned}\hat{U}(\Delta t)|\,n\rangle|\,\beta\rangle &= e^{i\kappa^2 n^2(\omega_c\Delta t - \sin\omega_c\Delta t)}e^{i\kappa n\mathrm{Im}[\beta(1-e^{-i\omega_c\Delta t})]}|\,n\rangle|\,\beta e^{-i\omega_c\Delta t} + \kappa n(1-e^{-i\omega_c\Delta t})\rangle \\ &\approx e^{i\kappa n\mathrm{Im}[\beta i\omega_c\Delta t)]}|\,n\rangle|\,\beta(1-i\omega_c\Delta t) + \kappa n i\omega_c\Delta t)\rangle \\ &\approx \Big(1 + i\kappa n\omega_c\Delta t\,\mathrm{Im}[i\beta]\Big)|\,n\rangle|\,\beta(1-i\omega_c\Delta t) + \kappa n i\omega_c\Delta t)\rangle\end{aligned} \tag{183}$$

With the Ansatz (182) we find from (180) the unitary infinitesimal increment of the density matrix:

$$\begin{aligned}\hat{\rho}^{(1)}_{nm}(t+\Delta t) = \rho^{(1)}_{nm}(t)\Big(1 + i\kappa\omega_c\Delta t\,\mathrm{Im}\left[i\left(n\Phi_n(\gamma,t) - m\Phi_m(\gamma,t)\right)\right]\Big)\,|\,n\rangle\langle m\,|\otimes \\ \otimes\,|\,\Phi_n(\gamma,t)(1-i\omega_c\Delta t) + \kappa n i\omega_c\Delta t)\rangle\langle\Phi_m(\gamma,t)(1-i\omega_c\Delta t) + \kappa m i\omega_c\Delta t)\,|\end{aligned} \tag{184}$$

Similarly, we find the infinitesimal non-unitary evolution from (181):

$$\begin{aligned}\hat{\rho}^{(2)}_{nm}(t+\Delta t) = \rho^{(2)}_{nm}(t)\Big(1 - \frac{\gamma}{2}\left(|\Phi_n(\gamma,t) - \Phi_m(\gamma,t)|^2 - 2i\mathrm{Im}[\Phi_n(\gamma,t)\Phi^*_m(\gamma,t)]\right)\Delta t\Big)\times \\ \times\,|\,n\rangle\langle m\,|\otimes|\,(1-\frac{1}{2}\gamma\Delta t)\Phi_n(\gamma,t)\rangle\langle(1-\frac{1}{2}\gamma\Delta t)\Phi_m(\gamma,t)\,|\end{aligned} \tag{185}$$

We are now able to construct differential equations for the coherent state amplitudes $\Phi_n(\gamma,t)$ and for the coefficients $\rho_{nm}(t)$.

For the amplitudes, we add the contributions for $\Phi^{(1)}_n(\gamma,t+\Delta t)$ and for $\Phi^{(2)}_n(\gamma,t+\Delta t)$ from the above equations (184) and (185), and use $\Phi^{(1)}_n(\gamma,t) = \Phi^{(2)}_n(\gamma,t) = \Phi_n(\gamma,t)$. Taylor expanding and setting $d\Phi_n(\gamma,t) = d\Phi^{(1)}_n(\gamma,t) + d\Phi^{(2)}_n(\gamma,t)$ we get

$$\frac{d\Phi_n(\gamma,t)}{dt} = -(i\omega_c + \frac{\gamma}{2})\Phi_n(\gamma,t) + i\kappa\omega_c n \tag{186}$$

We can easily solve this linear differential equation by the method of inhomogeneous parameters and obtain for an initial coherent state $|\,\beta\rangle$ the coherent state amplitude at time t:

$$\Phi_n(\gamma,t) = \frac{i\kappa\omega_c n}{i\omega_c + \frac{\gamma}{2}}\left(1 - e^{-(i\omega_c+\gamma/2)t}\right) + \beta e^{-(i\omega_c+\gamma/2)t} \tag{187}$$

This is a direct generalization of the states in (9) for a damped oscillator and reduces to the previous result for $\gamma \to 0$. It shows that the amplitudes of the cantilever oscillations are damped by the rate γ.

We now proceed to calculate the coefficients $\rho_{nm}(t)$. As for the state amplitudes, we construct a differential equation by summing up the contributions from (184) and (185). This yields

$$\frac{d\rho_{nm}(t)}{dt} = \rho_{nm}(t)\left(i\kappa\omega_c\,\mathrm{Im}\left[i\left(n\Phi_n - m\Phi_m\right)\right] - \frac{\gamma}{2}\left(|\Phi_n - \Phi_m|^2 - 2i\mathrm{Im}[\Phi_n\Phi^*_m]\right)\right) \tag{188}$$

which can easily be solved. The result is

$$\rho_{nm}(t) = \rho_{nm}(0)e^{i\kappa\omega_c\int_0^t dt'\,\mathrm{Im}[i(n\Phi_n - m\Phi_m)]}e^{-\frac{\gamma}{2}\int_0^t dt'\left(|\Phi_n-\Phi_m|^2 - 2i\mathrm{Im}[\Phi_n\Phi^*_m]\right)} \tag{189}$$

with $\Phi_n(\gamma,t')$ given by (187). We have therefore found the full solution of the master equation (80) describing a dissipative cantilever in our setup.

To be more explicit, we can compute the integrals in the above expression for the case $n = 1, m = 0$ which corresponds to our setup where we have only a single photon in the cavity.

For the integral resulting from the unitary evolution we have:

$$
\begin{aligned}
& i\kappa \int_0^t dt' \omega_c \,\mathrm{Im}[i\Phi_1(\gamma,t')] = \\
& = i\kappa \mathrm{Im}\left[\frac{i\kappa\omega_c^2}{\omega_c^2+\frac{\gamma^2}{4}}\left(\omega_c+i\frac{\gamma}{2}\right)\left(t+\frac{e^{-(i\omega_c+\gamma/2)t}-1}{i\omega_c+\frac{\gamma}{2}}\right)+\frac{i\omega_c\beta}{i\omega_c+\frac{\gamma}{2}}\left(1-e^{-(i\omega_c+\gamma/2)t}\right)\right] \\
& = \frac{i\kappa^2\omega_c^2}{\omega_c^2+\frac{\gamma^2}{4}}\left\{\omega_c t+\frac{\mathrm{Im}\left[\left(\frac{\gamma^2}{4}-\omega_c^2-i\gamma\omega_c\right)\left(1-e^{-(i\omega_c+\gamma/2)t}\right)\right]}{\omega_c^2+\frac{\gamma^2}{4}}\right\}+ \\
& \quad + i\,\mathrm{Im}\left[\frac{\beta\kappa\omega_c}{\omega_c^2+\frac{\gamma^2}{4}}\left(\omega_c+i\frac{\gamma}{2}\right)\left(1-e^{-(i\omega_c+\gamma/2)t}\right)\right] \\
& = \frac{i\kappa^2\omega_c^2}{\omega_c^2+\frac{\gamma^2}{4}}\left\{\omega_c t-\frac{1}{\omega_c^2+\frac{\gamma^2}{4}}\left[\left(\omega_c^2-\frac{\gamma^2}{4}\right)e^{-\frac{\gamma}{2}t}\sin\omega_c t+\gamma\omega_c\left(e^{-\frac{\gamma}{2}t}\cos\omega_c t-1\right)\right]\right\}+ \\
& \quad + i\,\mathrm{Im}\left[\frac{\beta\kappa\omega_c}{\omega_c^2+\frac{\gamma^2}{4}}\left(\omega_c+i\frac{\gamma}{2}\right)\left(1-e^{-(i\omega_c+\gamma/2)t}\right)\right]
\end{aligned}
\tag{190}
$$

For the dissipative parts we get

$$
\begin{aligned}
& -\frac{\gamma}{2}\int_0^t dt'\left(|\Phi_1(\gamma,t')-\Phi_0(\gamma,t')|^2\right) = \\
& = -\frac{\gamma}{2}\int_0^t dt'\left|\frac{i\kappa\omega_c}{i\omega_c+\frac{\gamma}{2}}\left(1-e^{-(i\omega_c+\gamma/2)t'}\right)\right|^2 \\
& = -\frac{\gamma}{2}\int_0^t dt'\frac{\kappa^2\omega_c^2}{\omega_c^2+\frac{\gamma^2}{4}}\left(1+e^{-\gamma t'}-2e^{-\frac{\gamma}{2}t'}\cos\omega_c t'\right) \\
& = -\frac{\kappa^2\omega_c^2}{2\left(\omega_c^2+\frac{\gamma^2}{4}\right)}\left\{\gamma t+1-e^{-\gamma t}+\frac{\gamma^2\left(e^{-\frac{\gamma}{2}t}\cos\omega_c t-1\right)-2\gamma\omega_c\, e^{-\frac{\gamma}{2}t}\sin\omega_c t}{\omega_c^2+\frac{\gamma^2}{4}}\right\}
\end{aligned}
\tag{191}
$$

and

$$
\begin{aligned}
& i\gamma\int_0^t dt'\,\mathrm{Im}[\Phi_1(\gamma,t')\Phi_0^*(\gamma,t')] = \\
& = i\gamma\int_0^t dt'\,\mathrm{Im}\left[\frac{\beta^*\kappa\omega_c}{\omega_c^2+\frac{\gamma^2}{4}}\left(i\frac{\gamma}{2}+\omega_c\right)\left(e^{-(\frac{\gamma}{2}-i\omega_c)t'}-e^{-\gamma t'}\right)\right] \\
& = i\,\mathrm{Im}\left[\frac{\beta\kappa\omega_c}{\omega_c^2+\frac{\gamma^2}{4}}\left(\left(\omega_c-i\frac{\gamma}{2}\right)\left(1-e^{-\gamma t}\right)+i\gamma\left(1-e^{-(\frac{\gamma}{2}+i\omega_c)t}\right)\right)\right]
\end{aligned}
\tag{192}
$$

Combining the three integrals (190), (191) and (192) in (189) and plugging the result into (182) we get the final expression for the density matrix of the damped cantilever:

$$
\begin{aligned}
\hat{\rho}(\gamma,t) = & \frac{1}{2}|\,0\rangle\langle 0\,|\otimes|\,\Phi_0(\gamma,t)\rangle\langle\Phi_0(\gamma,t)\,|+\frac{1}{2}|\,1\rangle\langle 1\,|\otimes|\,\Phi_1(\gamma,t)\rangle\langle\Phi_1(\gamma,t)\,|+ \\
& + \frac{1}{2}\,e^{-D(\gamma,t)}e^{-i\varphi_0(\gamma,t)-i\varphi_\beta(\gamma,t)}|\,0\rangle\langle 1\,|\otimes|\,\Phi_0(\gamma,t)\rangle\langle\Phi_1(\gamma,t)\,|+ \\
& + \frac{1}{2}\,e^{-D(\gamma,t)}e^{i\varphi_0(\gamma,t)+i\varphi_\beta(\gamma,t)}|\,1\rangle\langle 0\,|\otimes|\,\Phi_1(\gamma,t)\rangle\langle\Phi_0(\gamma,t)\,|
\end{aligned}
\tag{193}
$$

with

$$\begin{aligned}
\Phi_n(\gamma,t) &= \frac{i\kappa\omega_c n}{i\omega_c+\frac{\gamma}{2}}\left(1-e^{-(i\omega_c+\gamma/2)t}\right)+\beta e^{-(i\omega_c+\gamma/2)t}\\
\varphi_0(\gamma,t) &= \frac{\kappa^2\omega_c^2}{\omega_c^2+\frac{\gamma^2}{4}}\left\{\omega_c t-\frac{1}{\omega_c^2+\frac{\gamma^2}{4}}\left[\left(\omega_c^2-\frac{\gamma^2}{4}\right)e^{-\frac{\gamma}{2}t}\sin\omega_c t+\gamma\omega_c\left(e^{-\frac{\gamma}{2}t}\cos\omega_c t-1\right)\right]\right\}\\
\varphi_\beta(\gamma,t) &= \mathrm{Im}\left[\frac{\beta\kappa\omega_c}{\omega_c^2+\frac{\gamma^2}{4}}\left(\left(\omega_c-i\frac{\gamma}{2}\right)\left(1-e^{-\gamma t}\right)+\left(\omega_c+i\frac{3\gamma}{2}\right)\left(1-e^{-(\frac{\gamma}{2}+i\omega_c)t}\right)\right)\right]\\
D(\gamma,t) &= \frac{\kappa^2\omega_c^2}{2\left(\omega_c^2+\frac{\gamma^2}{4}\right)}\left\{\gamma t+1-e^{-\gamma t}+\frac{\gamma^2\left(e^{-\frac{\gamma}{2}t}\cos\omega_c t-1\right)-2\gamma\omega_c\, e^{-\frac{\gamma}{2}t}\sin\omega_c t}{\omega_c^2+\frac{\gamma^2}{4}}\right\}
\end{aligned} \tag{194}$$

Note that the state amplitudes $\Phi_n(\gamma,t)$ and the phase factor $\varphi(\gamma,t)=\varphi_0(\gamma,t)+\varphi_\beta(\gamma,t)$ reduce to the undamped values (9) for $\gamma\to 0$. The damping factor $D(\gamma,t)$ reduces the off-diagonal elements of the density matrix and is thus responsible for decoherence due to dissipation. We see therefore that a dissipative cantilever causes decoherence even when the bath is effectively at zero temperature, as was the case in this model.

We now compute the effect of dissipation on the interferometric visibility, $v(\gamma,\bar{n},t)=2|\rho(\gamma,\bar{n},t)_{01}^{(Ph)}|$ for finite initial temperatures of the cantilever. Taking the trace over the cantilever states in (193) we get an extra factor for the off-diagonal elements due to the non-orthogonality of coherent states:

$$\begin{aligned}
\langle\Phi_0(\gamma,t)\,|\,\Phi_1(\gamma,t)\rangle &= \exp\left\{-\frac{1}{2}|\Phi_1(\gamma,t)-\Phi_0(\gamma,t)|^2+i\mathrm{Im}[\Phi_1(\gamma,t)\Phi_0^*(\gamma,t)]\right\}\\
&= \exp\left\{-\frac{\kappa^2\omega_c^2}{2\left(\omega_c^2+\frac{\gamma^2}{4}\right)}\left(1+e^{-\gamma t}-2e^{-\frac{\gamma}{2}t}\cos\omega_c t\right)+\right.\\
&\quad\left.+\,i\,\mathrm{Im}\left[\frac{\beta\kappa\omega_c}{\omega_c^2+\frac{\gamma^2}{4}}\left(\omega_c-i\frac{\gamma}{2}\right)\left(e^{-\gamma t}-e^{-(\frac{\gamma}{2}+i\omega_c)t}\right)\right]\right\}
\end{aligned} \tag{195}$$

Combining the β - dependent part with $\varphi_\beta(\gamma,t)$ we find the phase factor of $\rho(\gamma,\beta,t)_{01}^{(Ph)}$ to be $e^{i\mathrm{Im}[\beta\zeta(\gamma,t)]}$ with

$$\zeta(\gamma,t)=\frac{\kappa\omega_c}{\omega_c^2+\frac{\gamma^2}{4}}\left(2\omega_c+i\gamma\right)\left(1-e^{-(\frac{\gamma}{2}+i\omega_c)t}\right) \tag{196}$$

We can perform the thermal averaging as in the previous chapters by noting that

$$\frac{1}{\pi\bar{n}}\int d^2\beta\, e^{-|\beta|^2/\bar{n}}e^{i\mathrm{Im}[\beta\zeta(\gamma,t)]}=e^{\bar{n}|\zeta(\gamma,t)|^2/4} \tag{197}$$

Thus we get the final result for the interferometric visibility:

$$v(\gamma,\bar{n},t)=\exp\left\{-D(\gamma,t)-\frac{\kappa^2\omega_c^2}{2\left(\omega_c^2+\frac{\gamma^2}{4}\right)}\left(1+2\bar{n}\right)\left(1+e^{-\gamma t}-2e^{-\frac{\gamma}{2}t}\cos\omega_c t\right)\right\} \tag{198}$$

with $D(\gamma,t)$ given in (194) .

References

[1] E. Schrödinger. Die gegenwärtige Situation in der Quantenmechanik. *Naturwissenschaften*, 23:844–849, December 1935.

[2] A. J. Leggett. Topical Review: Testing the limits of quantum mechanics: motivation, state of play, prospects. *Journal of Physics Condensed Matter*, 14, April 2002.

[3] M. Arndt, O. Nairz, J. Vos-Andreae, C. Keller, G. van der Zouw, and A. Zeilinger. Wave-particle duality of C_{60} molecules. *Nature*, 401:680–682, October 1999.

[4] C. H. van der Wal, A. C. J. ter Haar, F. K. Wilhelm, R. N. Schouten, C. J. P. M. Harmans, T. P. Orlando, S. Lloyd, and J. E. Mooij. Quantum Superposition of Macroscopic Persistent-Current States. *Science*, 290:773–777, October 2000.

[5] J. R. Friedman, V. Patel, W. Chen, S. K. Tolpygo, and J. E. Lukens. Quantum superposition of distinct macroscopic states. *Nature*, 406:43–46, July 2000.

[6] J.-M. Courty, A. Heidmann, and M. Pinard. Quantum limits of cold damping with optomechanical coupling. *Eur. Phys. J. D*, 17:399–408, December 2001.

[7] I. Wilson-Rae, N. Nooshi, W. Zwerger, and T. J. Kippenberg. Theory of Ground State Cooling of a Mechanical Oscillator Using Dynamical Backaction. *Phys. Rev. Lett.*, 99(9):093901, August 2007.

[8] F. Marquardt, J. P. Chen, A. A. Clerk, and S. M. Girvin. Quantum Theory of Cavity-Assisted Sideband Cooling of Mechanical Motion. *Phys. Rev. Lett.*, 99(9):093902, August 2007.

[9] M. Bhattacharya and P. Meystre. Trapping and Cooling a Mirror to Its Quantum Mechanical Ground State. *Physical Review Letters*, 99(7):073601, August 2007.

[10] M. Bhattacharya, H. Uys, and P. Meystre. Optomechanical trapping and cooling of partially reflective mirrors. *Physical Review A*, 77(3):033819, March 2008.

[11] J. D. Thompson, B. M. Zwickl, A. M. Jayich, F. Marquardt, S. M. Girvin, and J. G. E. Harris. Strong dispersive coupling of a high-finesse cavity to a micromechanical membrane. *Nature*, 452:72–75, March 2008.

[12] S. Mancini, D. Vitali, V. Giovannetti, and P. Tombesi. Stationary entanglement between macroscopic mechanical oscillators. *Eur. Phys. J. D*, 22:417–422, March 2003.

[13] M. Pinard, A. Dantan, D. Vitali, O. Arcizet, T. Briant, and A. Heidmann. Entangling movable mirrors in a double cavity system. *Europhys. Lett.*, 72(5):747, November 2005.

[14] D. Vitali, S. Mancini, and P. Tombesi. Stationary entanglement between two movable mirrors in a classically driven Fabry Perot cavity. *Journal of Physics A Mathematical General*, 40:8055–8068, July 2007.

[15] D. Vitali, S. Gigan, A. Ferreira, H. R. Böhm, P. Tombesi, A. Guerreiro, V. Vedral, A. Zeilinger, and M. Aspelmeyer. Optomechanical Entanglement between a Movable Mirror and a Cavity Field. *Physical Review Letters*, 98(3):030405, January 2007.

[16] M. Paternostro, D. Vitali, S. Gigan, M. S. Kim, C. Brukner, J. Eisert, and M. Aspelmeyer. Creating and Probing Multipartite Macroscopic Entanglement with Light. *Physical Review Letters*, 99(25):250401, December 2007.

[17] V. Giovannetti, S. Mancini, and P. Tombesi. Radiation pressure induced Einstein-Podolsky-Rosen paradox. *Europhysics Letters*, 54:559–565, June 2001.

[18] J. Zhang, K. Peng, and S. L. Braunstein. Quantum-state transfer from light to macroscopic oscillators. *Physical Review A*, 68(1):013808, July 2003.

[19] S. Bose, K. Jacobs, and P. L. Knight. Preparation of nonclassical states in cavities with a moving mirror. *Phys. Rev. A*, 56:4175–4186, November 1997.

[20] S. Bose, K. Jacobs, and P. L. Knight. Scheme to probe the decoherence of a macroscopic object. *Phys. Rev. A*, 59:3204–3210, May 1999.

[21] W. Marshall, C. Simon, R. Penrose, and D. Bouwmeester. Towards Quantum Superpositions of a Mirror. *Phys. Rev. Lett.*, 91(13):130401, September 2003.

[22] R. Penrose, edited by A. Fokas et al. *Mathematical Physics 2000*. Imperial College, London, 2000.

[23] W. Marshall. Towards Quantum Superpositions of a Mirror. Doctoral Thesis, June 2004.

[24] D. Kleckner, I. Pikovski, E. Jeffrey, L. Ament, E. Eliel, J. van den Brink, and D. Bouwmeester. Creating and verifying a quantum superposition in a micro-optomechanical system. *New Journal of Physics*, 10(9):095020, September 2008.

[25] D. Kleckner and D. Bouwmeester. Sub-kelvin optical cooling of a micromechanical resonator. *Nature*, 444:75–78, November 2006.

[26] R. P. Feynman. *Lectures on gravitation*. Non-consecutive pag., Pasadena, Ca.: California Institute of Technology (CIT), 1971, 1971.

[27] F. Karolyhazy. Gravitation and quantum mechanics of macroscopic objects. *Nuovo Cimento A Serie*, 42:390–402, March 1966.

[28] L. Diósi. A universal master equation for the gravitational violation of quantum mechanics. *Physics Letters A*, 120:377–381, March 1987.

[29] L. Diósi. Models for universal reduction of macroscopic quantum fluctuations. *Physical Review A*, 40:1165–1174, August 1989.

[30] R. Penrose. Gravity and state vector reduction. In *Quantum Concepts in Space and Time*, pages 129–146, 1986.

[31] R. Penrose. On Gravity's role in Quantum State Reduction. *General Relativity and Gravitation*, 28:581–600, May 1996.

[32] C. K. Law. Interaction between a moving mirror and radiation pressure: A Hamiltonian formulation. *Phys. Rev. A*, 51:2537–2541, March 1995.

[33] W. H. Zurek, S. Habib, and J. P. Paz. Coherent states via decoherence. *Physical Review Letters*, 70:1187–1190, March 1993.

[34] J. J. Sakurai. *Modern quantum mechanics*. Reading, MA: Addison Wesley, edited by Tuan, San Fu, 1985.

[35] M. A. Nielsen and Chuang. *Quantum Computation and Quantum Information*. Cambridge University Press, 2000.

[36] A. Kenfack and K. Zyczkowski. Negativity of the Wigner function as an indicator of non-classicality. *Journal of Optics B: Quantum and Semiclassical Optics*, 6:396–404, October 2004.

[37] E. Wigner. On the Quantum Correction For Thermodynamic Equilibrium. *Physical Review*, 40:749–759, June 1932.

[38] W. P. Schleich. *Quantum Optics in Phase Space*. Wiley-VCH, April 2001.

[39] J. Zsolt Bernád, L. Diósi, and T. Geszti. Quest for quantum superpositions of a mirror: high and moderately low temperatures. *Physical Review Letters*, 97(25):250404, December 2006.

[40] W. H. Zurek. Reduction of the wavepacket: How long does it take? Technical report, 1984.

[41] R. F. O'Connell, C. M. Savage, and D. F. Walls. Decay of Quantum Coherence due to the Presence of a Heat Bath. *New York Academy Sciences Annals*, 480:267–274, December 1986.

[42] W. G. Unruh and W. H. Zurek. Reduction of a wave packet in quantum Brownian motion. *Physical Review D*, 40:1071–1094, August 1989.

[43] D. Guilini, E. Joos, C. Kiefer, J. Kupsch, I. O. Stamatescu, and H. D. Zeh. *Decoherence and the appearance of a classical world in quantum theory*. Springer-Verlag, 1996.

[44] M. Schlosshauer. Decoherence, the measurement problem, and interpretations of quantum mechanics. *Reviews of Modern Physics*, 76:1267–1305, February 2005.

[45] G. S. Agarwal. Master Equations in Phase-Space Formulation of Quantum Optics. *Physical Review*, 178:2025–2035, February 1969.

[46] A. O. Caldeira and A. J. Leggett. Path integral approach to quantum Brownian motion. *Physica A Statistical Mechanics and its Applications*, 121:587–616, September 1983.

[47] B. L. Hu, J. P. Paz, and Y. Zhang. Quantum Brownian motion in a general environment: Exact master equation with nonlocal dissipation and colored noise. *Physical Review D*, 45:2843–2861, April 1992.

[48] C. W. Gardiner. *Quantum noise*. Springer-Verlag, 1991.

[49] H. J. Carmichael. *Statistical Methods in Quantum Optics*. Springer-Verlag, 1999.

[50] K. Hornberger. Master Equation for a Quantum Particle in a Gas. *Physical Review Letters*, 97(6):060601, August 2006.

[51] H. P. Breuer and F. Petruccione. *The Theory of Open Quantum Systems*. Oxford University Press, 2002.

[52] R. Alicki and K. Lendi, editors. *Quantum Dynamical Semigroups and Applications*, volume 286 of *Lecture Notes in Physics, Berlin Springer Verlag*, 1987.

[53] G. Lindblad. On the generators of quantum dynamical semigroups. *Communications in Mathematical Physics*, 48:119–130, June 1976.

[54] A. S. Holevo. On the Structure of Covariant Dynamical Semigroups . *Journal of Functional Analysis*, 131(2):255–278, August 1995.

[55] B. Vacchini. Master-Equations for the Study of Decoherence. *International Journal of Theoretical Physics*, 44:1011–1021, July 2005.

[56] A. Isar, A. Sandulescu, and W. Scheid. Phase Space Representation for Open Quantum Systems Within the Lindblad Theory. *International Journal of Modern Physics B*, 10:2767–2779, 1996.

[57] L. Diósi. Calderia-Leggett master equation and medium temperatures. *Physica A Statistical Mechanics and its Applications*, 199:517–526, November 1993.

[58] J. Preskill. *Quantum Information and Computation*. Lecture Notes for Physics 229, California Institute of Technology, CA, USA, September 1998.

[59] D. F. Walls and G. J. Milburn. *Quantum Optics*. Springer-Verlag, 1994.

[60] M. Scully and M. S. Zubairy. *Quantum Optics*. Cambridge University Press, September 1997.

[61] J. Bosse. *Correlation Functions in Many-Particle Systems*. Notes on seminar held at Università Degli Studi Di Trento, Trento-Povo, Italy, April 1985.

[62] G. W. Ford, J. T. Lewis, and R. F. O'connell. Quantum Langevin equation. *Physcial Review A*, 37:4419–4428, June 1988.

[63] G. S. Agarwal. Brownian Motion of a Quantum Oscillator. *Physical Review A*, 4:739–747, August 1971.

[64] P. Strehlow, H. Nuzha, and E. Bork. Construction of a Nuclear Cooling Stage. *Journal of Low Temperature Physics*, 147:81–93, April 2007.

[65] W. H. Zurek. Decoherence and the transition from quantum to classical. *Physics Today*, 44:36–44, October 1991.

[66] W. H. Zurek. Decoherence, einselection, and the quantum origins of the classical. *Reviews of Modern Physics*, 75:715–775, May 2003.

[67] A. Bassi, E. Ippoliti, and S. L. Adler. Towards Quantum Superpositions of a Mirror: An Exact Open Systems Analysis. *Physical Review Letters*, 94(3):030401, January 2005.

[68] R. Alicki. Search for a border between classical and quantum worlds. *Physical Review A*, 65(3):034104, March 2002.

[69] E. Joos and H.D. Zeh. The emergence of classical properties through interaction with the environment. *Zeitschrift für Physik B Condensed Matter*, 59(2):223–243, June 1985.

[70] M. R. Gallis and G. N. Fleming. Environmental and spontaneous localization. *Physical Review A*, 42:38–48, July 1990.

[71] K. Hornberger and J. Sipe. Collisional decoherence reexamined. *Physical Review A*, 68(1):012105, July 2003.

[72] J. van Wezel. *Quantum Mechanics and The Big World*. Doctoral Thesis, Leiden University Press, The Netherlands, 2007.

[73] G. Vidal and R. F. Werner. Computable measure of entanglement. *Physical Review A*, 65(3):032314, March 2002.

[74] H. Ollivier and W. H. Zurek. Quantum Discord: A Measure of the Quantumness of Correlations. *Physical Review Letters*, 88(1):017901, January 2002.

[75] M. Schlosshauer, A. P. Hines, and G. J. Milburn. Decoherence and dissipation of a quantum harmonic oscillator coupled to two-level systems. *Physical Review A*, 77(2):022111, February 2008.

[76] M. Blencowe. *Private Correspondence*. 2008.

[77] G. C. Ghirardi, A. Rimini, and T. Weber. Unified dynamics for microscopic and macroscopic systems. *Physical Review D*, 34:470–491, July 1986.

[78] J. van Wezel, J. van den Brink, and J. Zaanen. An Intrinsic Limit to Quantum Coherence due to Spontaneous Symmetry Breaking. *Physical Review Letters*, 94(23):230401, June 2005.

[79] A. F. Pace, M. J. Collett, and D. F. Walls. Quantum limits in interferometric detection of gravitational radiation. *Physical Review A*, 47:3173–3189, April 1993.

[80] G. D. Mahan. *Many-Particle Physics*. Plenum Press, 1981.

[81] D. F. Walls and G. J. Milburn. Effect of dissipation on quantum coherence. *Physical Review A*, 31:2403–2408, April 1985.